AD-785 261

MODIFICATION AND CONTROL OF OXIDE STRUCTURES ON METALS AND ALLOYS

PHASE IV

WESTINGHOUSE ASTRONUCLEAR LABORATORY

PREPARED FOR

NAVAL AIR SYSTEMS COMMAND

MAY 1974

DISTRIBUTED BY:

NTIS

National Technical Information Service
U. S. DEPARTMENT OF COMMERCE

UNCLASSIFIED

Security Classification

AD-785-261

DOCUMENT CONTROL DATA - R&D

(Security classification of title, body of abstract and indexing annotation must be entered when the overall report is classified)

1. ORIGINATING ACTIVITY (Corporate author) Westinghouse Astronuclear Laboratory P. O. Box 10864 Pittsburgh, Pennsylvania 15236	2a. REPORT SECURITY CLASSIFICATION Unclassified 2b. GROUP Materials Science

3. REPORT TITLE

Modification and Control of Oxide Structures on Metals and Alloys: (Phase IV)

4. DESCRIPTIVE NOTES (Type of report and inclusive dates)

Final Technical Report - 2March 73 to 2 March 74

5. AUTHOR(S) (Last name, first name, initial)

Svedberg, Robert C.

6. REPORT DATE	7a. TOTAL NO. OF PAGES	7b. NO. OF REFS
May, 1974	161	8

8a. CONTRACT OR GRANT NO. N62269-73-C-0361 b. PROJECT NO. c. d.	9a. ORIGINATOR'S REPORT NUMBER(S) WANL-M-FR-74-003 9b. OTHER REPORT NO(S) (Any other numbers that may be assigned this report)

10. AVAILABILITY/LIMITATION NOTICES

Approved for public release; distribution unlimited.

11. SUPPLEMENTARY NOTES	12. SPONSORING MILITARY ACTIVITY

13. ABSTRACT

Nb-Co-Al and Nb-Fe-Al base alloys have been studied to determine the effects of composition both elemental and constituent (i.e., intermetallic alloy compounds used to make alloys) on the oxides formed during 1200°C oxidation in air. Alloys were formed by both pressing and sintering of intermetallic compounds and elemental powders and by arc melting alloy buttons from intermetallic compounds and elements in powder form. Oxidation kinetics have been measured, and the oxides formed have been examined by x-ray diffraction techniques. In addition, Y and Y_2O_3 additions were made to several alloys to evaluate the effects of rare earth additions on the oxide structure.

In addition to the oxidation kinetics and oxide structure correlation, metallographic techniques were used to evaluate the depth of penetration of oxygen into the various alloys. This study confirmed that rutile type oxides such as $NbAlO_4$, $NbFeO_4$, and $NbCrO_4$ are responsible for improved oxidation performance.

Parabolic rate constants between 0.042 to 0.47 $mg^2/cm^4/min$ were measured for these alloys, with overall metal consumption including the oxygen contaminated zone being 2.33 to 4.3 mils in 24 hours at 1200°C.

DD FORM 1 JAN 64 1473

UNCLASSIFIED

Security Classification

14. KEY WORDS	LINK A		LINK B		LINK C	
	ROLE	WT	ROLE	WT	ROLE	WT
Oxide						
Defect Structure						
Niobates						
Niobium Alloy Oxidation						

INSTRUCTIONS

1. **ORIGINATING ACTIVITY:** Enter the name and address of the contractor, subcontractor, grantee, Department of Defense activity or other organization *(corporate author)* issuing the report.

2a. **REPORT SECURITY CLASSIFICATION:** Enter the overall security classification of the report. Indicate whether "Restricted Data" is included. Marking is to be in accordance with appropriate security regulations.

2b. **GROUP:** Automatic downgrading is specified in DoD Directive 5200.10 and Armed Forces Industrial Manual. Enter the group number. Also, when applicable, show that optional markings have been used for Group 3 and Group 4 as authorized.

3. **REPORT TITLE:** Enter the complete report title in all capital letters. Titles in all cases should be unclassified. If a meaningful title cannot be selected without classification, show title classification in all capitals in parenthesis immediately following the title.

4. **DESCRIPTIVE NOTES:** If appropriate, enter the type of report, e.g., interim, progress, summary, annual, or final. Give the inclusive dates when a specific reporting period is covered.

5. **AUTHOR(S):** Enter the name(s) of author(s) as shown on or in the report. Enter last name, first name, middle initial. If military, show rank and branch of service. The name of the principal author is an absolute minimum requirement.

6. **REPORT DATE:** Enter the date of the report as day, month, year; or month, year. If more than one date appears on the report, use date of publication.

7a. **TOTAL NUMBER OF PAGES:** The total page count should follow normal pagination procedures, i.e., enter the number of pages containing information.

7b. **NUMBER OF REFERENCES:** Enter the total number of references cited in the report.

8a. **CONTRACT OR GRANT NUMBER:** If appropriate, enter the applicable number of the contract or grant under which the report was written.

8b, 8c, & 8d. **PROJECT NUMBER:** Enter the appropriate military department identification, such as project number, subproject number, system numbers, task number, etc.

9a. **ORIGINATOR'S REPORT NUMBER(S):** Enter the official report number by which the document will be identified and controlled by the originating activity. This number must be unique to this report.

9b. **OTHER REPORT NUMBER(S):** If the report has been assigned any other report numbers *(either by the originator or by the sponsor)*, also enter this number(s).

10. **AVAILABILITY/LIMITATION NOTICES:** Enter any limitations on further dissemination of the report, other than those imposed by security classification, using standard statements such as:

(1) "Qualified requesters may obtain copies of this report from DDC."

(2) "Foreign announcement and dissemination of this report by DDC is not authorized."

(3) "U. S. Government agencies may obtain copies of this report directly from DDC. Other qualified DDC users shall request through
____."

(4) "U. S. military agencies may obtain copies of this report directly from DDC. Other qualified users shall request through
____."

(5) "All distribution of this report is controlled. Qualified DDC users shall request through
____."

If the report has been furnished to the Office of Technical Services, Department of Commerce, for sale to the public, indicate this fact and enter the price, if known.

11. **SUPPLEMENTARY NOTES:** Use for additional explanatory notes.

12. **SPONSORING MILITARY ACTIVITY:** Enter the name of the departmental project office or laboratory sponsoring *(paying for)* the research and development. Include address.

13. **ABSTRACT:** Enter an abstract giving a brief and factual summary of the document indicative of the report, even though it may also appear elsewhere in the body of the technical report. If additional space is required, a continuation sheet shall be attached.

It is highly desirable that the abstract of classified reports be unclassified. Each paragraph of the abstract shall end with an indication of the military security classification of the information in the paragraph, represented as *(TS)*, *(S)*, *(C)*, or *(U)*.

There is no limitation on the length of the abstract. However, the suggested length is from 150 to 225 words.

14. **KEY WORDS:** Key words are technically meaningful terms or short phrases that characterize a report and may be used as index entries for cataloging the report. Key words must be selected so that no security classification is required. Identifiers, such as equipment model designation, trade name, military project code name, geographic location, may be used as key words but will be followed by an indication of technical context. The assignment of links, roles, and weights is optional.

FOREWORD

The work described herein was performed at the Astronuclear Laboratory of the Westinghouse Electric Corporation under Navy Contract N62269-73-C-0361. This work is a continuing effort started under Navy Contract N00019-70-C-0148 and continued under Contracts N00019-71-C-0089 and N00019-72-C-0132. Mr. I. Machlin of the Naval Air Systems Command served as Program Consultant. Program supervision at WANL was by Mr. R. W. Buckman, Jr., Manager, Materials Science.

The author wishes to acknowledge additional personnel contributing to this program. These are Messrs. S. S. Laciak for metallography, R. W. Conlin for x-ray diffraction studies, and R. P. Sprecace and F. L. Przywarty for alloy manufacture.

TABLE OF CONTENTS

LIST OF ILLUSTRATIONS

LIST OF ILLUSTRATIONS (Continued)

LIST OF ILLUSTRATIONS (Continued)

LIST OF ILLUSTRATIONS (Continued)

LIST OF TABLES

1.0 INTRODUCTION AND SUMMARY

Nb-Co-Al and Nb-Fe-Al base alloys have been studied to determine the effects of composition, both elemental and constituent (i.e., intermetallic alloy compounds used to make alloys) on the oxides formed during 1200°C oxidation in air. Alloys were formed by both pressing and sintering of intermetallic compounds and elemental powders and by arc melting alloy buttons from intermetallic compounds and elements in powder form. Oxidation kinetics have been measured, and the oxides formed have been examined by x-ray diffraction techniques. In addition, Y and Y_2O_3 additions were made to several alloys to evaluate the effects of rare earth additions on the oxide structure.

In addition to the oxidation kinetics and oxide structure correlation, metallographic techniques were used to evaluate the depth of penetration of oxygen into the various alloys. Hardness measurements for the various alloys are presented and oxygen diffusion through a Co_3O_4-Nb_2O_5 oxide has been measured. This study has confirmed the Phase III findings that a rutile-type oxide structure plus Al_2O_3 or an aluminate-spinel comprises the protective oxide on these alloys.

The overall program was initiated under Contract No. N00019-70-C-0148 and continued under Contracts Nos. N00019-71-C-0089 and N00019-72-C-0132 to investigate the feasibility of modifying oxide structures to enhance oxidation protection of elevated temperature structural materials[1-3].

The program has approached the problem of improving oxidation resistance by investigating various techniques designed to identify and then possibly modify the structure of the equilibrium oxides which are characteristic of the parent structural material and in this way attempt to improve oxidation resistance without either changing the structural and mechanical

properties of the substrate or adding additional components to the system. Two of the techniques which have been investigated thus far are, pre-oxidation treatments and modification of oxide defect structures by application of high pressures.

The chemical diffusion coefficient of oxygen through several mixed niobates was measured during Phases II and III. In addition, pre-oxidation effects and the oxidation of Nb alloys were studied. The oxide structures associated with improved oxidation performance of some niobium alloys and intermetallic compounds have been identified, and the alloy compositions required to support these structures are being investigated.

The Phase I[1] study has shown that high pressure high temperature exposure of Nb_2O_5 does produce a denser phase that maintains its characteristics after quenching to room temperature. However, it has not yet been possible to investigate the stability of the quenched phases nor the transport properties of the quenched phases. It has also been demonstrated that pre-exposure of alloy B-1 (Cb-15Ti-10W-10Ta-2Hf-3Al) in 20 torr oxygen at 650°C results in a decrease in the subsequent oxidation rate in air at 1040°C when compared to untreated B-1 alloys. This is the second method of pre-treatment shown to be effective in decreasing the rate of oxidation of the B-1 alloy. The first reported treatment involved an oxidation exposure at 2400°F in air for 1 hour which improved the oxidation during exposure to 2200°F air[2]. These experiments showed that changing the oxide structure is possible. The maximum potential of these various techniques has yet to be demonstrated.

Preliminary results from Phase II indicate that mixed oxides of Nb_2O_5-TiO_2 and Nb_2O_5-HfO_2 would not form protective oxide layers based on limiting the transport of oxygen through the scale and protecting the parent metal[2]. The NiO-Nb_2O_5 binary oxide exhibited no change in stoichiometry, i.e., no weight loss as a function of oxygen pressure until a partial pressure equivalent to that of the dissociation pressure of NiO is reached. At that point, a reduction reaction apparently begins, and large weight losses begin.

As a result of efforts during Phase III[3], the rutile structure family for oxide compounds of the type $Nb(B)O_4$ where B = Cr, Al, or Fe have been identified as the primary oxide phase in the scales formed on oxidation resistant Nb intermetallic compounds and Nb-Ti-Cr-Al, Nb-Fe-Al, Nb-Cr-Al-Co, and Nb-Cr-Al-Ni alloys. Along with this oxide, small amounts of either $(B)_2O_3$ where B = Cr, Al, or Fe or a $CoAl_2O_4$ spinel in cobalt containing alloys were detected. Oxygen transport rates through Nb_2O_3-Cr_2O_3, Nb_2O_5-TiO_2, Nb_2O_5 ZrO_2, and Nb_2O_5-Al_2O_3 were also determined using thermogravimetric techniques. Of the oxide compounds evaluated, only oxygen transport through Nb_2O_5-Cr_2O_3 was slow enough to warrant its classification as a protective scale. In addition to oxidation rate data, metallographic studies and electron microprobe studies were conducted on the Nb intermetallic compounds and alloys.

The present report includes (1) a continuation of the oxygen transport rate measurements in the binary niobate Nb_2O_5-Co_3O_4 and (2) the investigation of the oxidation kinetics and oxide structures formed on 37 different Nb based alloys containing Co-Fe-Al-Cr-Ni-Y, and/or Y_2O_3. The experimental results have been used to determine which alloys to scale up for mechanical property studies, based on the oxidation kinetics, the oxide structure formed, and the depth of substrate contamination which resulted during oxidation. These results indicate that both the Nb-Al-Fe and Nb-Co-Al alloys are oxidation resistant. The oxides on certain alloys become more protective as oxidation proceeds. In addition, the substrate contamination of these alloys by oxygen is very low. The protective oxide appears to be a rutile-type $NbAlO_4$ oxide. The Fe_2O_3 hemitite structure reported as forming on Nb-Fe-Al alloys has been shown to be located primarily at the oxide-gas interface by x-ray diffractometer studies. Additional work is required to determine whether the rate control is transport through the $NbAlO_4$ structure or some other layer between the oxide and metal, or, in fact, if the mechanical properties of the oxide are enhanced and the oxide has the ability to relieve internal stresses before the oxide spalls.

2.0 OXYGEN DIFFUSION THROUGH MIXED NIOBATES

The experimental techniques utilized and the sample preparation techniques employed have been explained previously[3]. The only change in the experimental technique was the method of acquiring the data. The output of the Cahn microbalance was recorded digitally on a Doric Digitrend 210, eliminating the need for reading the weight from a strip chart recorder. This technique also eliminates data loss due to overranging of the strip chart recorder and permitted unattended operation of the system.

2.1 EXPERIMENTAL RESULTS

Table 1 presents a summary of the experimental results for all of the oxygen diffusion experiments. Listed in Table 1 are the chemical diffusion coefficients, $\tilde{D}_L$, determined by measuring the slope of the line formed by plotting the quantity log (1 - M(t)/Q) vs time for $\tilde{D}t/l^2 \geq 0.15$ and the chemical diffusion coefficients D_p determined by measuring the slope of the line formed by plotting $(M(t)/A)^2$ vs time for $\tilde{D}t/l^2 \leq 0.25$. Also listed in Table 1 are the cumulative deviations from stoichiometry, the initial and final oxygen pressures between which each equilibration was made, and the time limitations for each model particular to each equilibration.

Tabular data is listed in Appendix B along with the computer plotted graphs for the various equilibrium conditions. The oxygen transport rates measured in the Co_3O_4-Nb_2O_5 oxide were lower than those measured in all but the Cr_2O_3-Nb_2O_5 system at 1175 and 850°C. However, at 1000°C the oxygen transport rate was found to be higher than any of the oxides previously measured. It is obvious that the dependence of the rate of diffusion of oxygen in all of these mixed niobates does not follow a simple temperature dependence which would be expected from a homogeneous single phase material. This lack of temperature dependence suggests strongly that the rate of diffusion of oxygen is being measured through several different phases at various combinations of oxygen partial pressure, degree of nonstòichiometry

Table 1. Chemical Diffusion Coefficients for Oxygen in the Binary Co-Nb-O Systems (Co_3O_4:Nb_2O_5 (0.67:1.00))

Run No.	D_L 10^{-7} cm^2/sec $\frac{Dt}{l^2} > 0.15$	$\tilde{D}_P$ 10^{-7} cm^2/sec $\frac{Dt}{l^2} < 0.25$	Total Deviation From Stoichiometry mg Oxygen	Initial Equil. Oxygen Pressure (atm.)	Final Equil. Oxygen Pressure (atm.)	$\log_{10}P$ (Final Equil.)	Temperature (°C)	Parabolic Model Upper Time Limit (min.)	Logarithmic Model Lower Time Limit (min.)
1	-	-	not meas.	.20	5.7×10^{-16}	-15.24	880	-	-
2	1.66, 0.78	.29, .407	65.51	5.7×10^{-16}	1.9×10^{-18}	-17.72	850	1882, 1203	177, 376
3	10.03	.29	45.45	.2	1.9×10^{-18}	-17.72	850	16.62	30
4	.578, .93	.538	111.96	1.9×10^{-18}	5.24×10^{-21}	-20.28	850	910	508, 316
5	-	-	1.14	.2	1.88×10^{-11}	-10.73	1000	-	-
6	15.79	4.75	61.94	1.88×10^{-11}	3.60×10^{-14}	-13.44	1000	103	19
7	7.35, 25.3, 36.0	2.02	40.8	.2	3.60×10^{-14}	-13.44	1000	242	40, 12, 8
8	8.4, 8.1	4.75	153.43	3.60×10^{-14}	8.48×10^{-17}	-16.07	1000	103	35, 36.3
9	1.27	3.24	38.22	.2	7.33×10^{-9}	- 8.13	1175	151	231
10	3.84	6.4	80.84	7.33×10^{-9}	1.98×10^{-11}	-10.70	1175	76	76.5
11	0.74, 0.611	0.361	137.23	1.98×10^{-11}	4.35×10^{-14}	-13.36	1175	1356	406, 480.6

and temperature. In fact, some of the plots of log (l-M(t)/Q) vs time give 2 and 3 distinct slopes indicating that the transport rate of oxygen is controlled by several different phases or substructures.

If one attempts to visualize the oxide formed on a niobium alloy, one finds an extremely low oxygen partial pressure at the oxide-metal interface and a large oxygen partial pressure at the oxide-gas interface. It is very possible that there are several different layers of oxide structures, sub-structures, and/or phases established by the oxygen partial pressure gradient and oxidation temperature. With an unknown number of oxide phases or substructures possible, which could depend upon oxygen partial pressure and temperature, it is very difficult to attempt to define a rate controlling phase or oxide structure.

More information is required on the equilibrium oxides and their structure-composition relationships for these complex systems before an understanding of their behavior can be developed. The behavior of the mixed niobate system observed during this transport study indicates the need for basic fundamental data about the equilibrium phase relationships in the alloy and oxides, the effects of oxygen partial pressure on these systems, and the relationship between the alloy composition and oxide composition.

3.0 OXIDATION BEHAVIOR OF EXPERIMENTAL NIOBIUM ALLOY

Thirty-seven Nb alloys from the systems Nb-Co-Al, Nb-Fe-Al, Nb-Cr, and Nb-Cr-Al were made by powder and arc melting techniques. Alloys were made from both elemental powders and pre-alloyed intermetallic powders. The alloys were oxidized in air at 1200°C for 7 to 24 hours during which time the oxidation kinetics were determined. X-ray diffraction techniques were then utilized to analyze the oxide structures formed on the alloys. The ultimate objectives of this study were; 1) the identification of oxide structures which provide a protective scale on niobium based alloys; 2) the correlation of these oxides with the alloy constitution and composition, and then 3) to design an alloy for further mechanical property evaluation.

3.1 ALLOY PREPARATION AND EXPERIMENTAL PROCEDURES

Alloys were fabricated from elemental powders and intermetallic compounds by pressing and sintering and arc melting. The compositions of the alloys investigated during this program are given in Table 2 as weight percent of the metal or intermetallic powder from which they were manufactured and in Table 3 as the weight percent of the elements in the alloy.

To manufacture the pressed and sintered alloys, the respective powders were blended with 120 drops of trichloroethane and 0.4 wt.% stearic acid for 1.5 hours in a polyethene container rotating at 4.5 rpm. The blended powders were pressed into 2.5 gram pellets in a 1/2 inch diameter opposed anvil die at 20,000 psig. After pressing, the pellets were stacked in an Al_2O_3 crucible on Al_2O_3 discs and sintered at about 2800°F for 6 hours in a 10^{-6} torr vacuum. Melting occurred on some of the discs. These alloys are designated with the B suffix.

The alloys were also prepared by arc melting 5 g buttons from the powder materials using a tungsten inert gas electrode on a copper chill in a controlled atmosphere weld box. The buttons were cut into two pieces, their surface area carefully measured, and then the samples were oxidized in a Stanton Thermal Balance System previously described[2,3]. Arc melted alloys are designated by the B & C suffix. After the samples were oxidized, the oxides

Table 2. Alloy Compositions Evaluated (Wt. % Components Mixed)

Alloy No.	Nb	$NbCr_2$	$NbAl_3$	Nb_2Al	$NbFe_2$	Al	Cr	Co	$NbCo_2$	Fe	NbNi	Y	Y_2O_3
1	65	35	-	-	-	-	-	-	-	-	-	-	-
2	70	-	-	30	-	-	-	-	-	-	-	-	-
3	35	35	-	30	-	-	-	-	-	-	-	-	-
4	70	-	30	-	-	-	-	-	-	-	-	-	-
5	66	25	-	-	-	-	9	-	-	-	-	-	-
6	76	-	-	20	-	4	-	-	-	-	-	-	-
7	62	15	10	-	-	4	9	-	-	-	-	-	-
8	50	50	-	-	-	-	-	-	-	-	-	-	-
9	25	75	-	-	-	-	-	-	-	-	-	-	-
10	65	25	-	-	-	-	10	-	-	-	-	-	-
11	50	-	25	-	25	-	-	-	-	-	-	-	-
12	50	40	-	-	-	-	10	-	-	-	-	-	-
13	65	-	25	-	-	-	-	10	-	-	-	-	-
14	60	-	-	-	30	10	-	-	-	-	-	-	-
15	60	-	-	-	-	10	-	-	-	30	-	-	-
16	60	-	25	-	-	-	-	-	-	15	-	-	-
17	70	-	-	-	-	15	-	15	-	-	-	-	-
18	60	-	20	-	-	-	-	-	20	-	-	-	-
19	70	-	-	-	-	10	-	-	20	-	-	-	-
20	70	-	15	-	-	-	-	-	15	-	-	-	-
21	70	-	-	15	-	-	-	-	15	-	-	-	-
22	60	10	15	-	-	-	-	-	15	-	-	-	-
23	60	-	15	-	-	-	-	-	15	-	10	-	-
24	60	-	30	-	-	-	-	-	10	-	-	-	-
25	60	-	10	-	-	-	-	-	30	-	-	-	-
26	63.7	-	24.5	-	-	-	-	9.8	-	-	-	1.96	-
27	63.7	-	24.5	-	-	-	-	9.8	-	-	-	-	1.96
28	58.8	-	-	-	29.4	9.8	-	-	-	-	-	1.96	-
29	58.8	-	-	-	29.4	9.8	-	-	-	-	-	-	1.96
30	54.9	-	-	-	-	9.8	18.6	14.7	-	-	-	1.96	-
31	54.9	-	-	-	-	9.8	18.6	14.7	-	-	-	-	1.96
32	68.6	-	-	-	-	14.7	-	14.7	-	-	-	1.96	-
33	68.6	-	-	-	-	14.7	-	14.7	-	-	-	-	1.96
34	58.8	9.8	14.7	-	-	-	-	-	14.7	-	-	1.96	-
35	58.8	9.8	14.7	-	-	-	-	-	14.7	-	-	-	1.96
36	58.8	-	29.4	-	-	-	-	-	9.8	-	-	1.96	-
37	58.8	-	29.4	-	-	-	-	-	9.8	-	-	-	1.96

Table 3. Alloy Compositions Evaluated (Wt. % Elements)

Alloy No.	Nb	Al	Co	Cr	Fe	Ni	Y	Y_2O_3
1	81.5	-	-	18.5	-	-	-	-
2	96.2	3.8	-	-	-	-	-	-
3	77.7	3.8	-	18.5	-	-	-	-
4	86.1	13.9	-	-	-	-	-	-
5	77.8	-	-	22.2	-	-	-	-
6	93.4	6.6	-	-	-	-	-	-
7	74.5	4.4	-	16.9	-	-	-	-
8	73.6	-	-	26.4	-	-	-	-
9	60.4	-	-	39.6	-	-	-	-
10	76.8	-	-	23.2	-	-	-	-
11	74.7	11.6	-	-	13.7	-	-	-
12	68.9	-	-	31.1	-	-	-	-
13	78.4	11.6	10	-	-	-	-	-
14	73.6	10.0	-	-	16.4	-	-	-
15	60	10	-	-	30	-	-	-
16	73.4	11.6	-	-	15	-	-	-
17	70	15	15	-	-	-	-	-
18	79.5	9.3	11.2	-	-	-	-	-
19	78.8	10	11.2	-	-	-	-	-
20	84.6	7	8.4	-	-	-	-	-
21	89.7	1.9	8.4	-	-	-	-	-
22	79.3	7	8.4	5.3	-	-	-	-
23	80.7	7	8.4	-	-	3.9	-	-
24	80.5	13.9	5.6	-	-	-	-	-
25	78.6	4.4	16.8	-	-	-	-	-
26	76.94	11.3	9.8	-	-	-	1.96	-
27	76.94	11.3	9.8	-	-	-	-	1.96
28	72.13	9.8	-	-	16.11	-	1.96	-
29	72.13	9.8	-	-	16.11	-	-	1.96
30	66	10	15	19	-	-	1.96	-
31	66	10	15	19	-	-	-	1.96
32	68.6	14.7	14.7	-	-	-	1.96	-
33	68.6	14.7	14.7	5.18	-	-	-	1.96
34	77.82	6.81	8.23	5.18	-	-	1.96	-
35	77.82	6.81	8.23	5.18	-	-	-	1.96
36	78.93	13.62	5.49	-	-	-	1.96	-
37	78.93	13.62	5.49	-	-	-	-	1.96

formed were analyzed by several x-ray diffraction techniques. Some of the oxides were sampled for powder diffraction analysis by scraping the oxide from the alloys or collecting spalled chips. For some analyses, oxide flakes were attached to the end of 0.1 mm glass fibers with Canadian Balsam. For others, the oxides were pulverized into a fine powder in an agate morter and attached to a 0.1 mm glass fiber using petroleum jelly. In all cases a 114.6 millimeter Debye-Scherrer camera was utilized for the powder analyses. The samples were exposed to either nickel filtered copper or iron filtered-cobalt radiation. The resultant films were compared to the 1971 ASTM diffusion index file for identification. To observe the oxides which formed on the metal substrate, nine of the alloy samples were ground before oxidation to provide a flat surface which, after oxidation, was subject to x-ray diffractometry analysis with the diffractometer trace being recorded on strip charts. This was an attempt to determine if any correlation between the alloy and oxide orientation could be detected and, also, to enable an x-ray analysis of the oxide as a function of distance from the substrate by grinding away the surface of the oxide and then taking an additional diffraction pattern of the oxide at different distances from the oxide metal interface. In addition, qualitative x-ray fluorescence analyses of some of the oxides were made using energy dispersive x-ray analysis (EDAX).

3.2 OXIDATION KINETIC MEASUREMENT RESULTS

Both the pressed and sintered alloys and the arc melted alloys were oxidized in air at 1200°C. The pressed and sintered alloys were oxidized primarily to obtain samples of the oxide scale for x-ray analysis. Because of the difficulty in obtaining a uniform degree of densification for the pressed and sintered alloys, it was not possible to obtain representative kinetic data because of the additional surface area which resulted from the porosity. However, alloys 10-A, 11-A, and 13-A exhibited a change in shape after sintering at 2800 $\pm$ 30°F indicating that the sintering temperature approached or slightly exceeded the melting point of these alloys.

Alloys 17-A, 18-A, and 19-A also exhibit extended sintering at a temperature of 2750 $\pm$ 30°F.

Because these alloys were densified and relatively nonporous, the oxidation kinetics for these alloys are shown in Figure 1. Also on the figure, the parabolic rate constant calculated from measuring the slope of the weight loss (mg/cm^2) vs the square root of time $\sqrt{t}$ are given. These are presented only for comparative purposes because of the uncertainties in surface area measurement due to undefined porosity. It was beyond the scope of this program to optimize sintering schedules for each alloy.

Figure 2 is a 75X photomicrograph of an alloy prepared by pressing and sintering which did not fully densify on sintering and shows the oxidation occurring at the pore surfaces. Some of these same alloys were also prepared by arc melting to determine if the oxide structure was dependent upon the constituents of the alloy. On the pressed and sintered alloys, the intermetallic compounds would be present as discrete particles. In the arc melted alloys, homogeneous mixing would occur.

The oxidation kinetics for the arc melted alloys are categorized into major alloy constituents for ease of explanation. The parabolic oxidation constants (k_p) are presented in Table 4 for the arc melted alloys. The parabolic oxidation constant was determined by calculating the slope of the weight gain/cm^2 (mg/cm^2) vs the square root of time $t^{1/2}$ using a computer program written to permit the selection of certain time intervals over which the parabolic rate constant could be measured. In Table 4 the parabolic rate constant is reported with the associated time interval over which it was measured. In Appendix A, the computer printout of the oxidation data is presented along with the plots of weight gain vs time for all of the alloys.

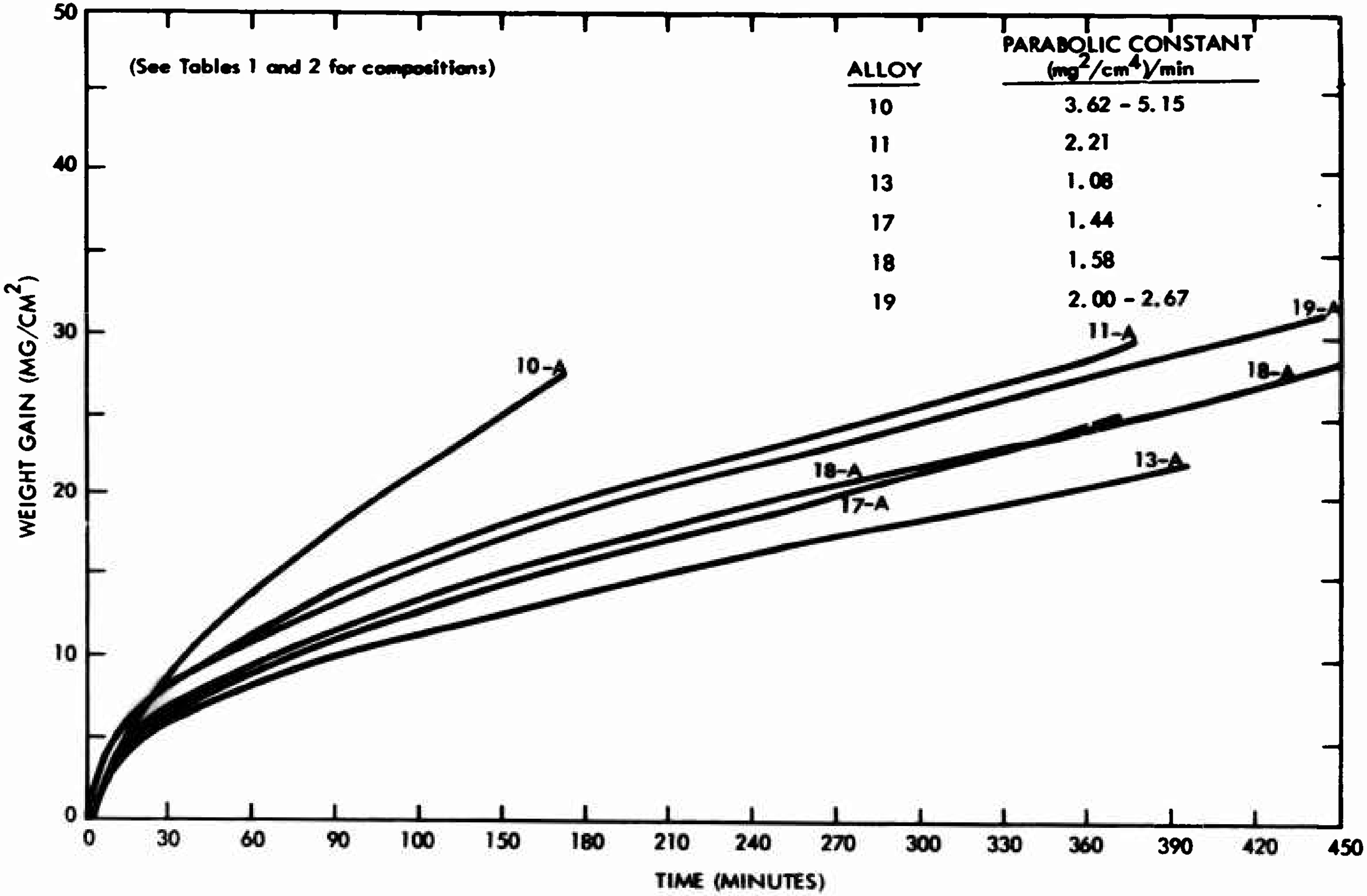

Figure 1. Weight Gain vs. Time in Air at 1200°C for Some of the Sintered Nb Based Alloys (A-Suffix)

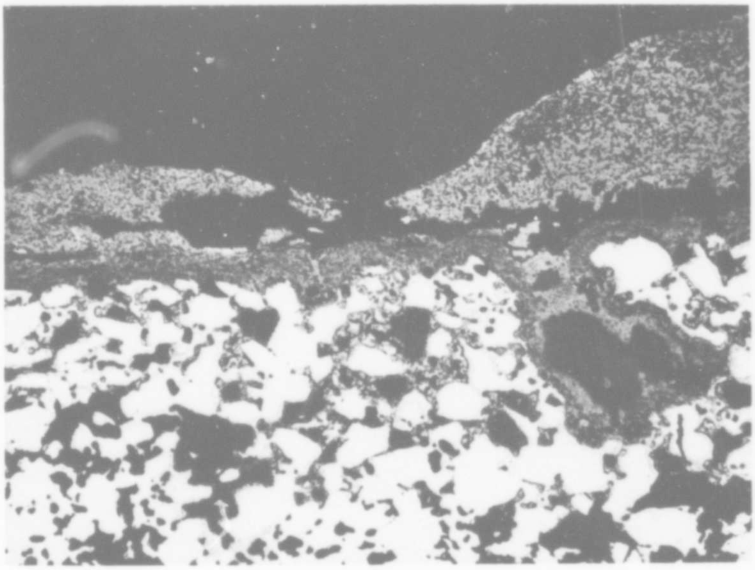

25066 75X

Figure 2. Alloy 15-A (60Nb-10Al-30Fe) Showing Oxidation at Pore Surfaces for a Typical Pressed and Sintered Alloy

Table 4. Parabolic Rate Constants for the Arc Melted Niobium Alloys at 1200°C

Alloy No.	Parabolic Rate Constant $(mg/cm^2)^2/min$	Oxidation Time (min)	Parabolic Rate Constant $(mg/cm^2)^2/min$	Oxidation Time (min)	Parabolic Rate Constant $(mg/cm^2)^2/min$	Oxidation Time (min)
Nb-Fe-Al Alloys						
11-B +	4.32	0 - 210	5.75	240 - 360	-	-
14-B	0.24	60 - 420	-	-	-	-
15-B	0.33	0 - 60	0.18	90 - 450	-	-
15-C	0.042	120 - 1400	-	-	-	-
16-B	0.29	30 - 150	0.24	180 - 420	-	-
16-C	0.17	1140 - 1530	-	-	-	-
28-B	0.68	90 - 390	-	-	-	-
29-B	0.88	50 - 420	-	-	-	-
Nb-Co-Al Alloys						
13-A	1.27	0 - 420	-	-	-	-
17-B	0.13	150 - 450	-	-	-	-
17-C	0.11	120 - 1100	0.15	1140 - 1410	-	-
18-B	0.57	0 - 420	-	-	-	-
18-C	0.76	0 - 600	1.17	630 - 990	1.69	1020 - 1200
19-B	0.54	0 - 420	-	-	-	-
19-C	0.47	0 - 990	0.59	1020 - 1260	0.59	1020 - 1260
20-A	0.72	0 - 240	1.1	240 - 390	-	-
21-A	0.307*	0 - 210	-	-	-	-
22-B	0.30	0 - 360	-	-	-	-
23-A	0.59	240 - 420	-	-	-	-
24-B	0.48	120 - 420	-	-	-	-
24-C	0.26	390 - 1410	-	-	-	-
25-A	0.084*	0 - 420	-	-	-	-
26-B	1.62	20 - 420	-	-	-	-
27-B	1.15	90 - 390	-	-	-	-
32-B	0.56	10 - 390	-	-	-	-
33-B	0.67	120 - 450	-	-	-	-
34-B	1.06	150 - 420	-	-	-	-
35-B	1.26	90 - 420	-	-	-	-
36-B	2.45	210 - 420	-	-	-	-
37-B	1.28	60 - 420	-	-	-	-
Nb-Cr-Al Alloys						
3-B	0.33*	0 - 360	-	-	-	-
7-B	7.17	120 - 390	-	-	-	-
Nb-Cr Alloy						
12-B	0.25	0 - 420	0.24	60 - 420	-	-
Nb-Cr-Al-Co Alloy						
31-B	.0921	90 - 420	-	-	-	-

* Denotes linear weight gain constant (no protective scale is formed).

\+ A denotes pressed and sintered alloy

B denotes arc melted alloy oxidized for 7 hours

C denotes arc melted alloy oxidized for 24 hours

3.2.1 Nb-Co-Al Alloys

Of the Nb-Co-Al alloys oxidized in air at 1200°C, alloys 17, 22, and 24 exhibited the best oxidation behavior as determined from the parabolic rate constant reported in Table 4. Table 5 gives the approximate values for the rate of metal consumption in 100 hours for several parabolic oxidation constants based on the assumption of a metal density of 8 gms/cc and rate of weight of metal consumed/weight gain of oxygen of 2. For these alloys, the metal consumption rate is between 2.5 to 6 mils/100 hours at 1200°C. This compares with the $NbAl_3$ intermetallic with a $k_p = 0.018\ (mg/cm^2)^2/min$ and a metal consumption rate ≈1 mil/100 hours. $NbAl_3$ is the most oxidation resistant Nb alloy or compound evaluated thus far in this program. For alloy 24, the parabolic rate constant decreases as the oxidation time increases. It decreased from 0.48 $(mg/cm^2)^2$/min for the 420 minutes of oxidation (7 hours) to 0.26 $(mg/cm^2)^2$/min for the 1410 minute (~24 hour) exposure. This indicates that as the oxide forms, it becomes more protective. This phenomenon was also shown for several Nb-Fe-Al alloys, which will be discussed in the next section.

Y_2O_3 + Y was added to several alloys to determine what effect these components would have on the oxidation behavior of the alloys. From Tables 2 and 3 it can be seen that alloys 26, 32, 34, and 36 are the Nb-Co-Al alloys 13, 17, 22, and 24 to which yttrium (Y) has been added while alloys 27, 33, 35, and 37 are Nb-Co-Al alloys 13, 17, 22, and 24 to which yttria (Y_2O_3) has been added. In all cases, the oxidation behavior was made worse by the addition of these components.

3.2.2 Metallography of the Oxide-Metal Interfaces (Nb-Co-Al Alloys)

In the refractory metals, the contamination of the metallic substrate by oxidants is a problem and must be analyzed as part of the overall oxidation behavior. Figures 3 thru 22 show the oxide metal interface of the Nb-Co-Al alloys in both the etched and unetched condition at 75 and 500X. Etching was done by using a 1:1:1 mixture of HNO_3:HF:H_2O.

Table 5. Correlation Between Metal Consumption in 100 Hours and the Parabolic Oxidation Constant

$k_p (mg/cm^2)^2/min$	mils/100 hr.
0.01	0.75
0.05	1.8
0.1	2.5
0.5	6
1.0	8
10.0	28
25.0	43

Oxide	$\frac{\text{Wt. of Metal Consumed}}{\text{Wt. of Oxygen Gained}}$
$NbFeO_4$	2.32
Nb_2O_5	2.32
$NbCrO_4$	2.26
$NbAlO_4$	1.87

Assumptions:

$$\frac{\text{Wt. of Metal Consumed}}{\text{Wt. of Oxygen Gained}} = 2.0$$

Metal Density = 8 g/cc

$$(\text{Wt. gain})^2 = k_p t$$

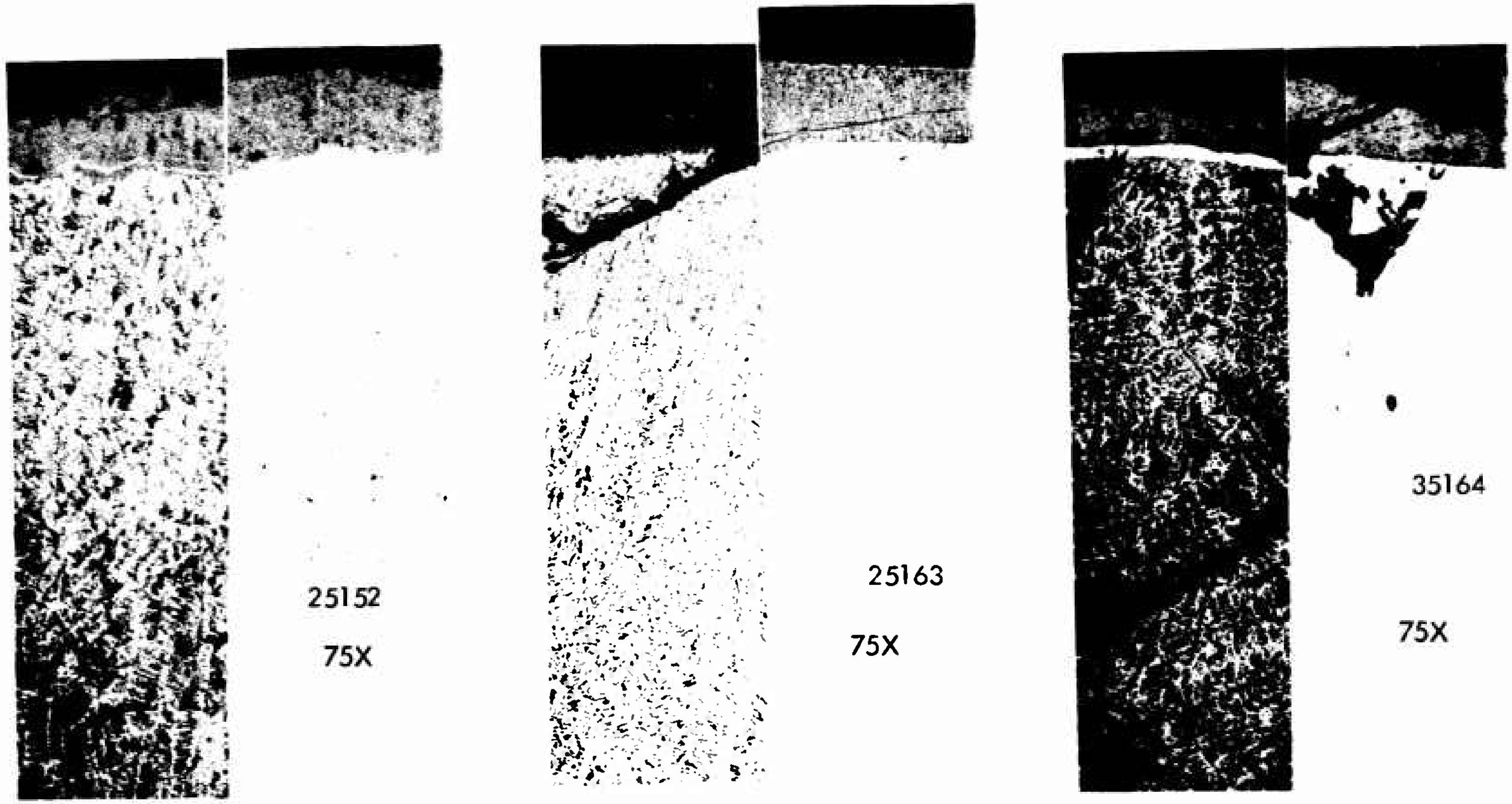

(ETCHED)
ALLOY 13
7 HOURS
1200°C
AIR

(ETCHED)
ALLOY 13 + Y
(ALLOY 26)
7 HOURS
1200°C
AIR

(ETCHED)
ALLOY 13 + Y_2O_3
(ALLOY 27)
7 HOURS
1200°C
AIR

Figure 3. Effects of Y and Y_2O_3 on the Microstructure and the Oxide Metal Interface of Alloy 13 (Nb-25$NbAl_3$-10Co) at 75X.

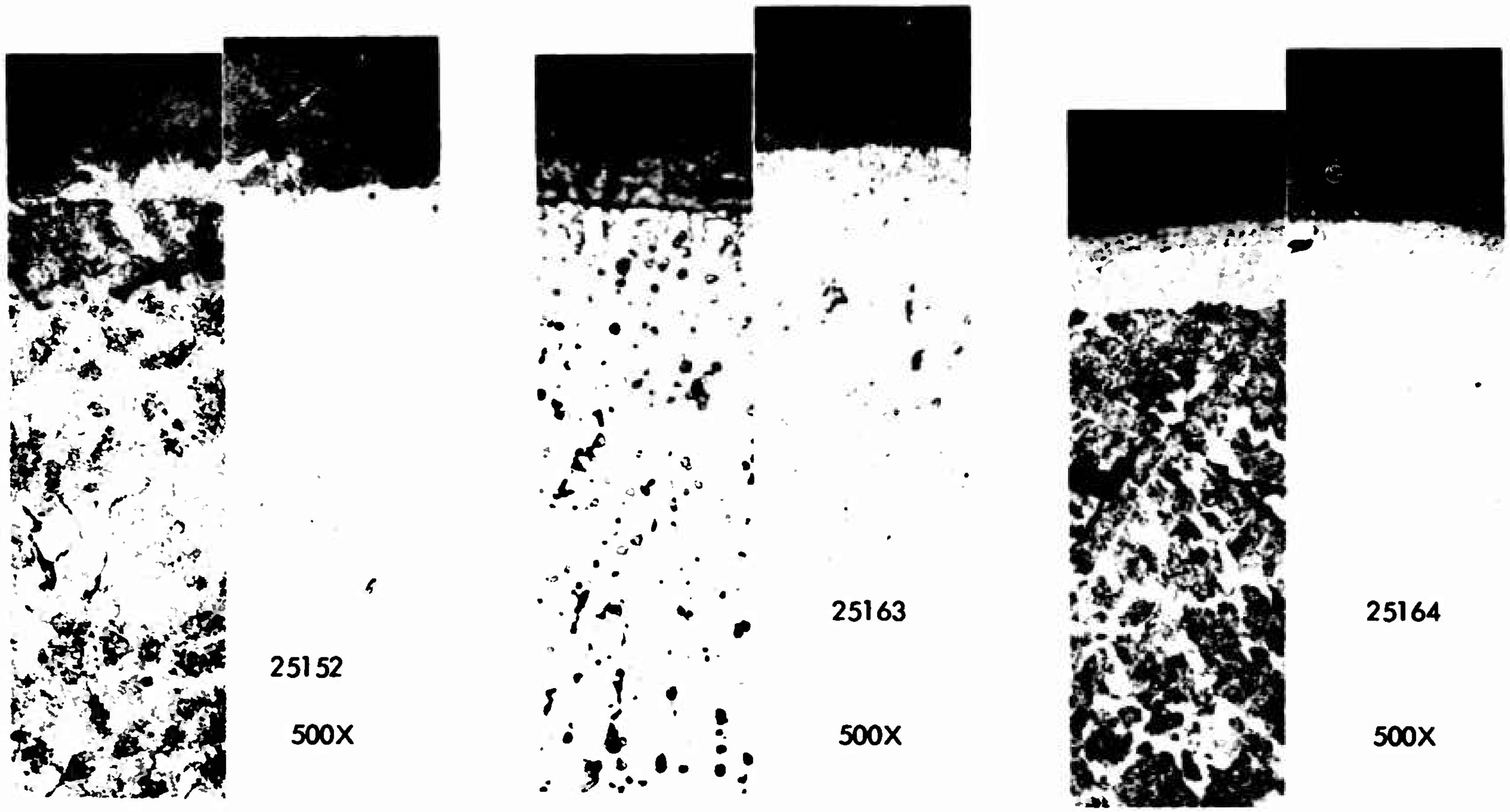

(ETCHED) (ETCHED) (ETCHED)

ALLOY 13 — 7 HOURS, 1200°C, AIR

ALLOY 13 + Y (ALLOY 26) — 7 HOURS, 1200°C, AIR

ALLOY 13 + Y_2O_3 (ALLOY 27) — 7 HOURS, 1200°C, AIR

Figure 4. Effects of Y and Y_2O_3 on the Microstructure and the Oxide Metal Interface of Alloy 13 (Nb-25$NbAl_3$-10Co) at 500X.

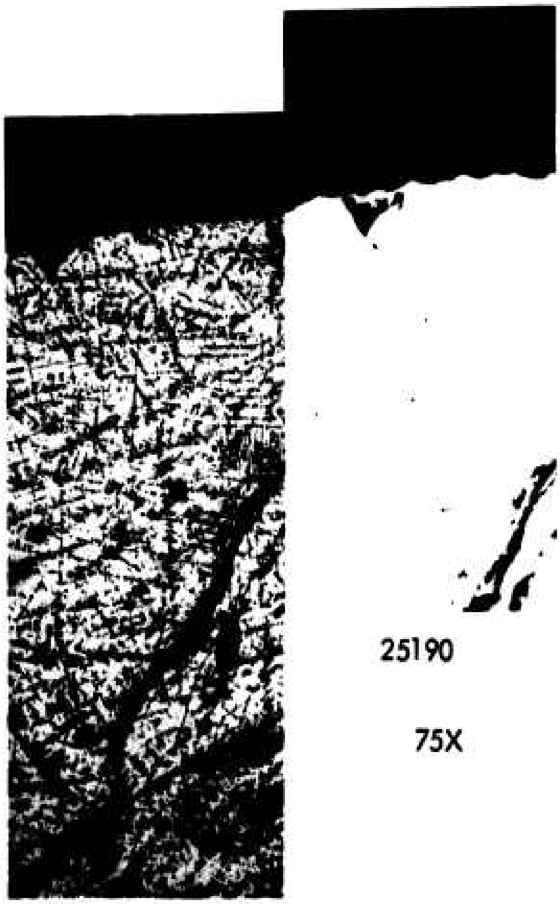

(ETCHED)

ALLOY 17-B
7 HOURS
1200°C
AIR

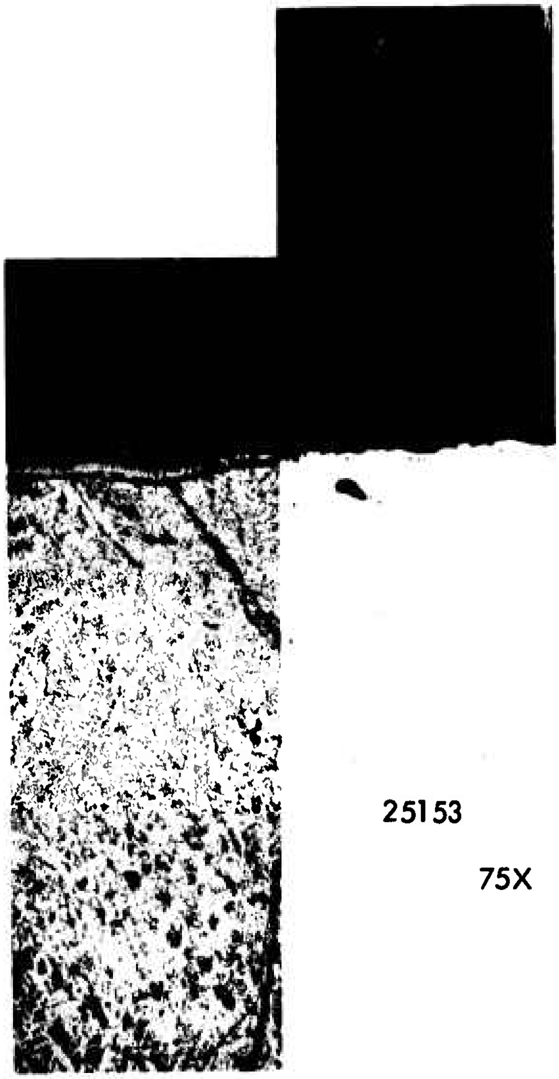

(ETCHED)

ALLOY 17-C
24 HOURS
1200°C
AIR

Figure 5. Effects of 7 Hour and 24 Hour Oxidation in Air at 1200°C on the Microstructure and Oxide-Metal Interface of Alloy 17 (Nb-15Al-15Co) at 75X.

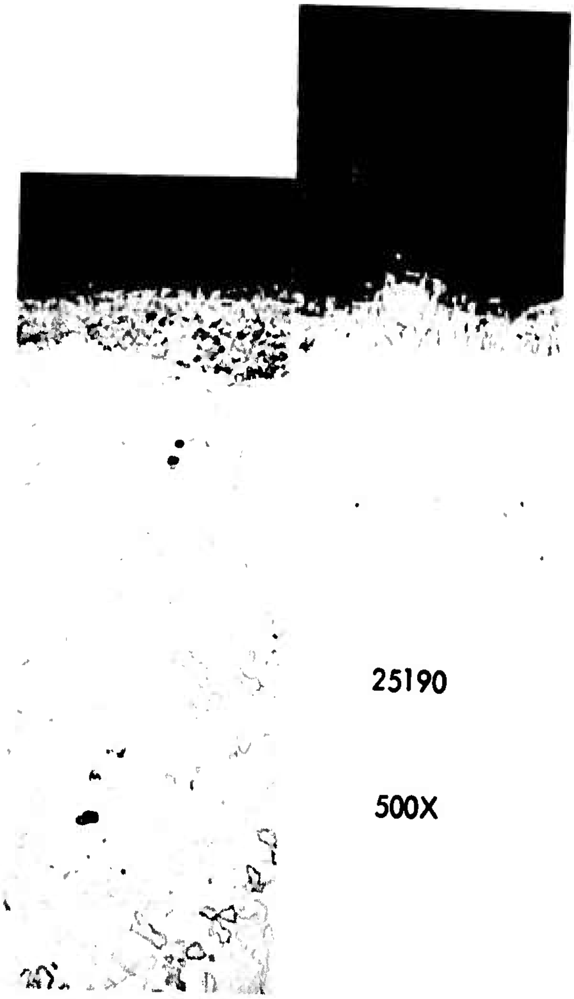

(ETCHED)

ALLOY 17-B

7 HOURS
1200°C
AIR

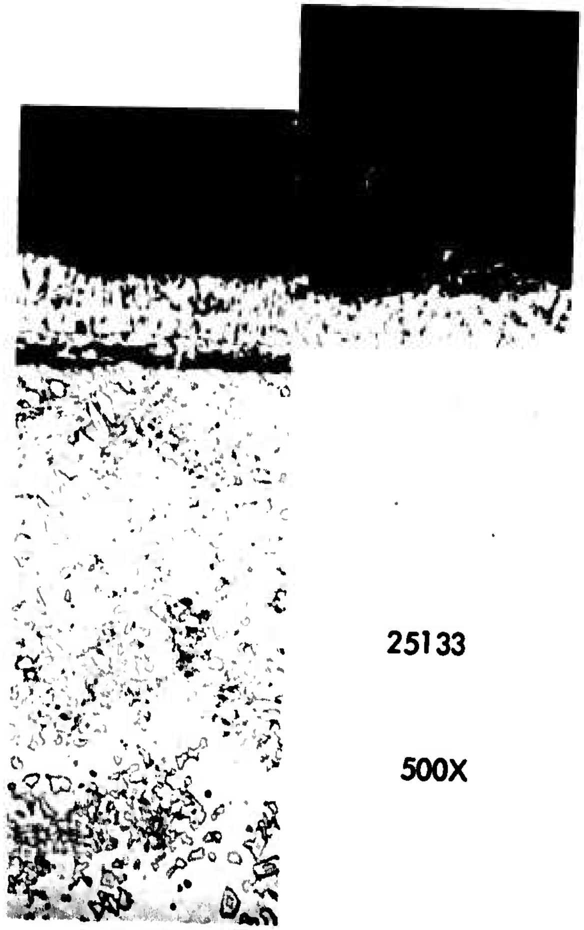

(ETCHED)

ALLOY 17-C

24 HOURS
1200°C
AIR

Figure 6. Effects of 7 Hour and 24 Hour Oxidation in Air at 1200°C on the Microstructure and Oxide-Metal Interface of Alloy 17 (Nb-15Al-15Co) at 500X.

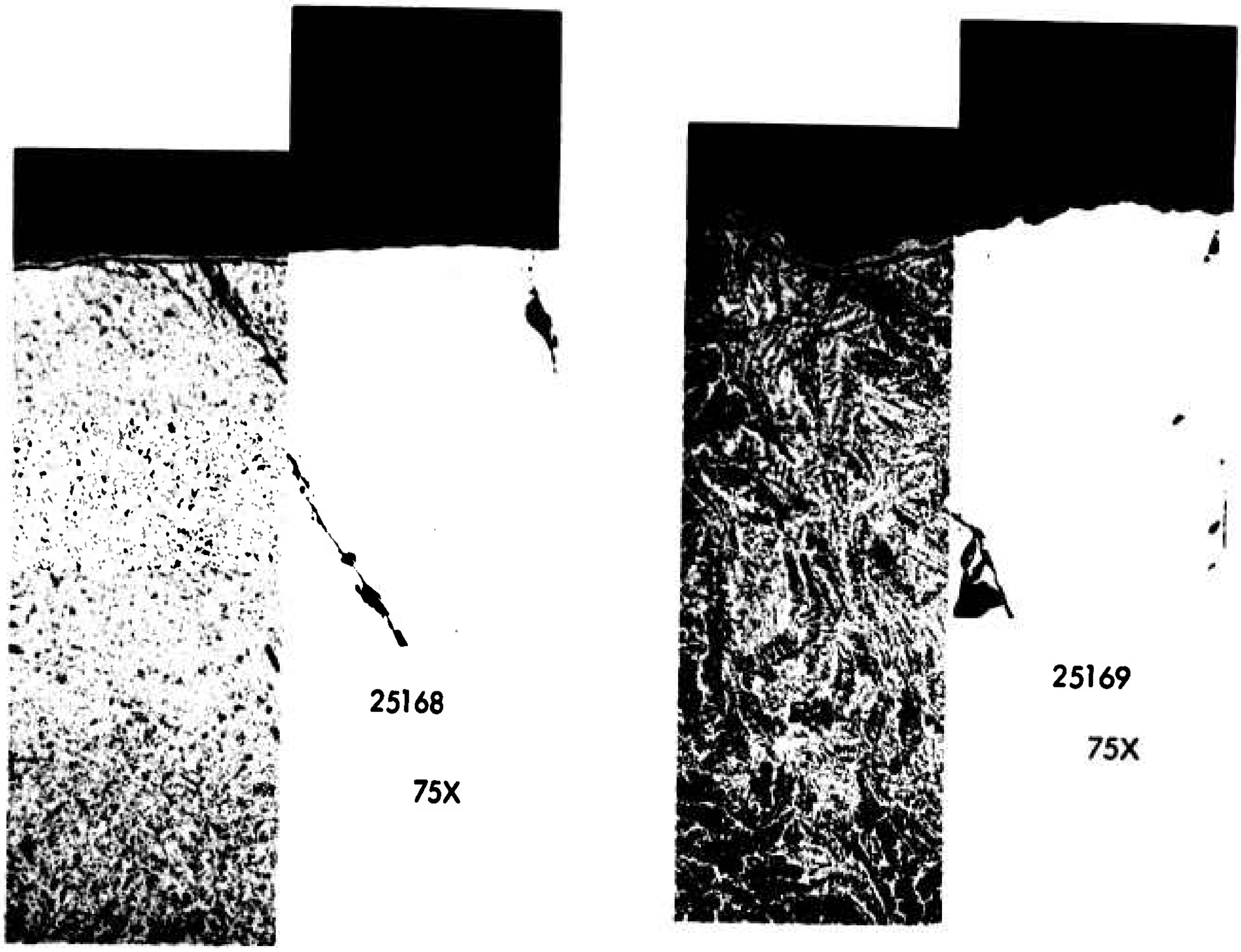

(ETCHED)

ALLOY 17 + Y

(ALLOY 32)

7 HOURS
1200°C
AIR

(ETCHED)

ALLOY 17 + Y_2O_3

(ALLOY 33)

7 HOURS
1200°C
AIR

Figure 7. Effects of Y and Y_2O_3 on the Microstructure and the Oxide Metal Interface of Alloy 17 at 75X.

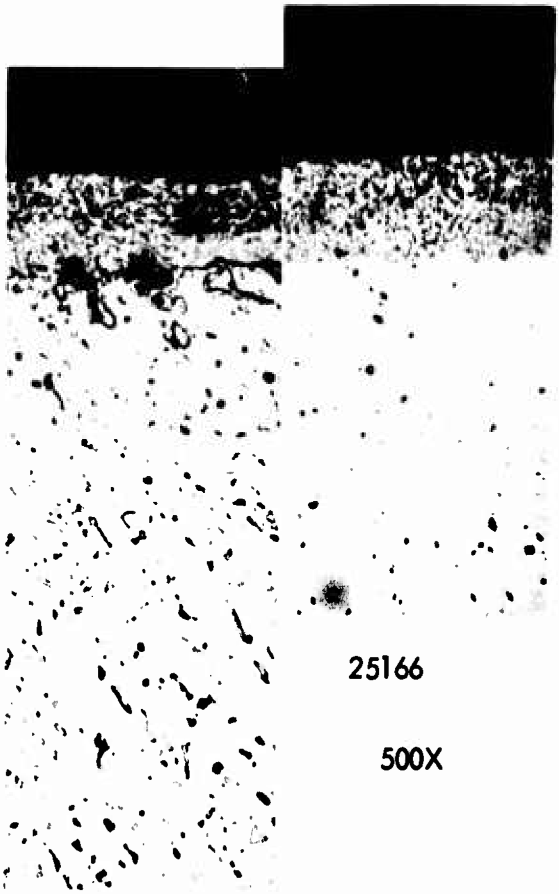

25166

500X

(ETCHED)

ALLOY 17 + Y
(ALLOY 32)

7 HOURS
1200°C
AIR

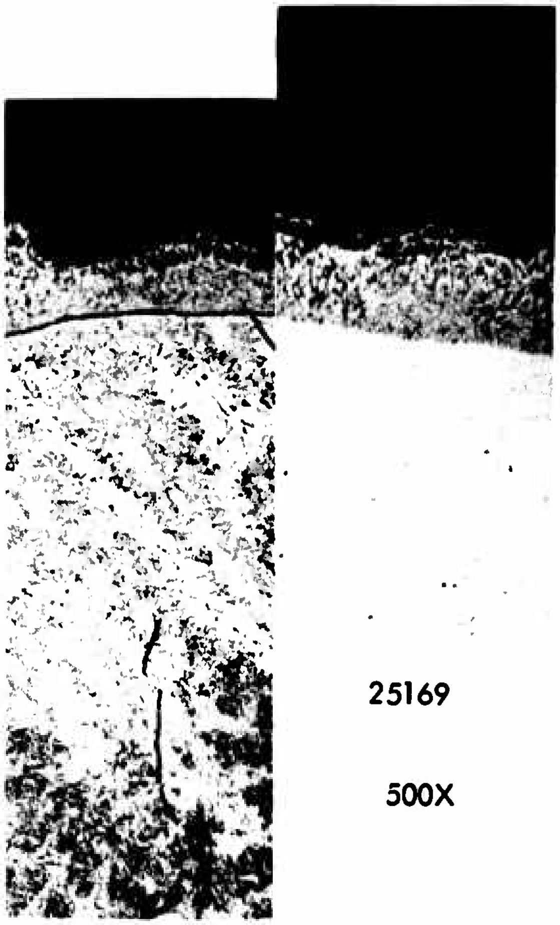

25169

500X

(ETCHED)

ALLOY 17 + Y_2O_3
(ALLOY 33)

7 HOURS
1200°C
AIR

Figure 8. Effects of Y and Y_2O_3 on the Microstructure and the Oxide Metal Interface of Alloy 17 at 500X.

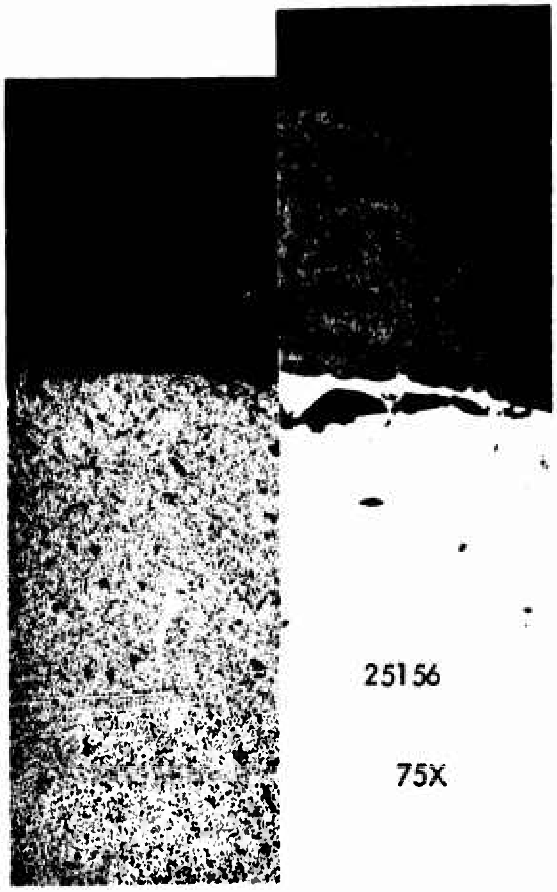

25156

75X

(ETCHED)

ALLOY 18-B

7 HOURS
1200°C
AIR

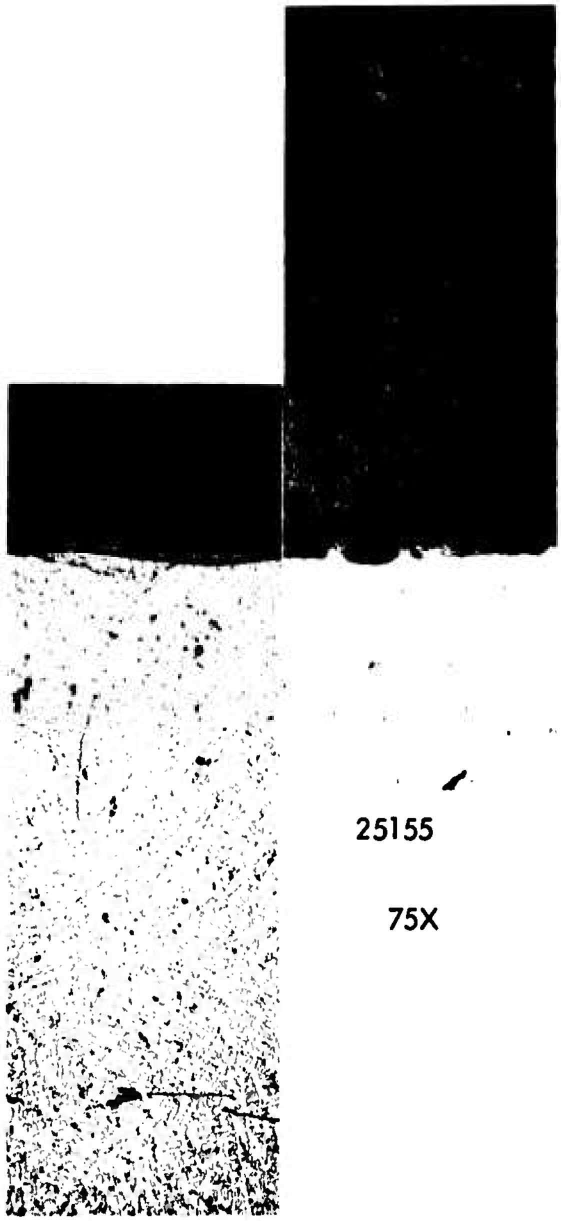

25155

75X

(ETCHED)

ALLOY 18-C

24 HOURS
1200°C
AIR

Figure 9. Effects of 7 Hour and 24 Hour Oxidation in Air at 1200°C on the Microstructure and Oxide-Metal Interface of Alloy 18 (Nb-20$NbAl_3$-20$NbCo_2$) at 75X.

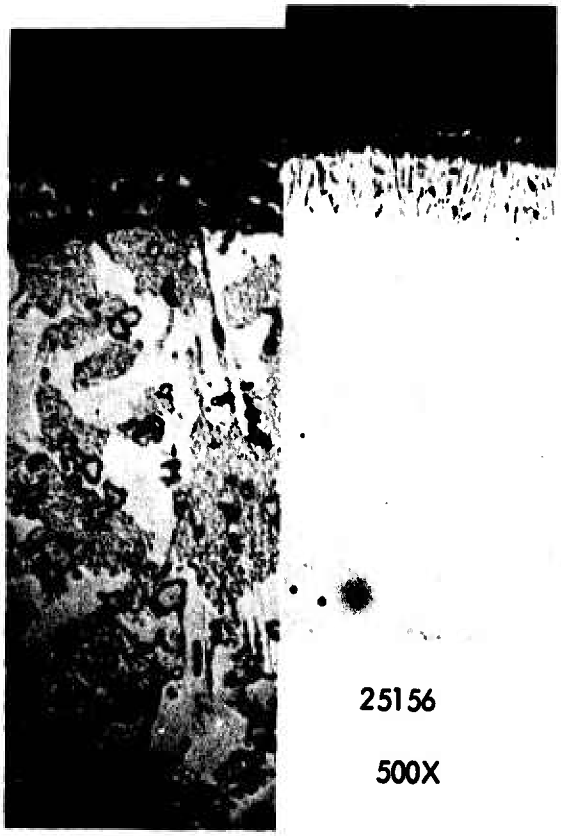

(ETCHED)

ALLOY 18-B

7 HOURS
1200°C
AIR

(ETCHED)

ALLOY 18-C

24 HOURS
1200°C
AIR

Figure 10. Effects of 7 Hour and 24 Hour Oxidation in Air at 1200°C on the Microstructure and Oxide-Metal Interface of Alloy 18 (Nb-20$NbAl_3$-20$NbCo_2$) at 500X.

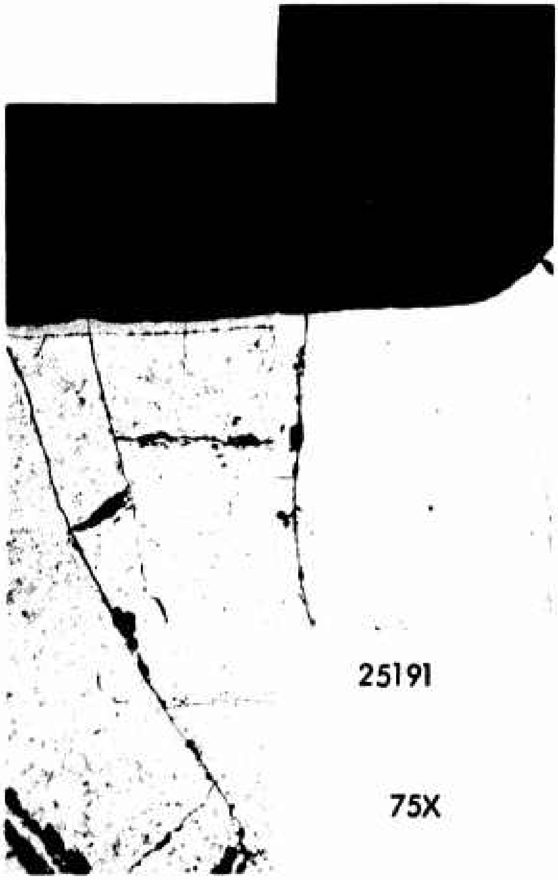

(ETCHED)

ALLOY 19-B

7 HOURS
1200°C
AIR

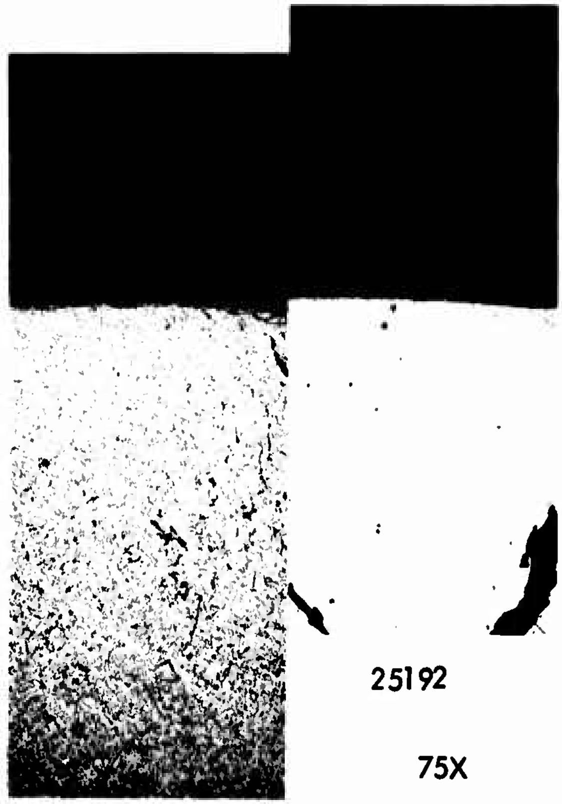

(ETCHED)

ALLOY 19-C

24 HOURS
1200°C
AIR

Figure 11. Effects of 7 Hour and 24 Hour Oxidation in Air at 1200°C on the Microstructure and Oxide-Metal Interface of Alloy 19 (Nb-10Al-20NbCo$_2$) at 75X.

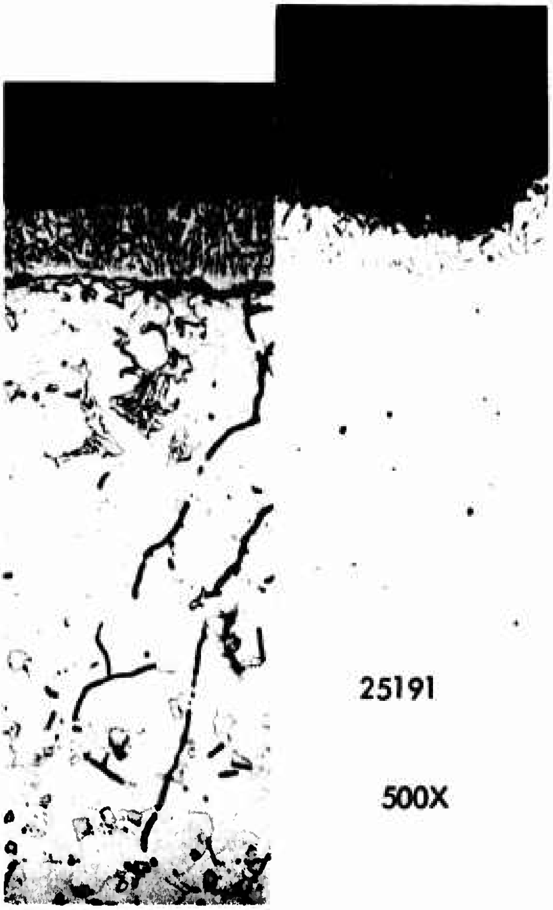

25191

500X

(ETCHED)

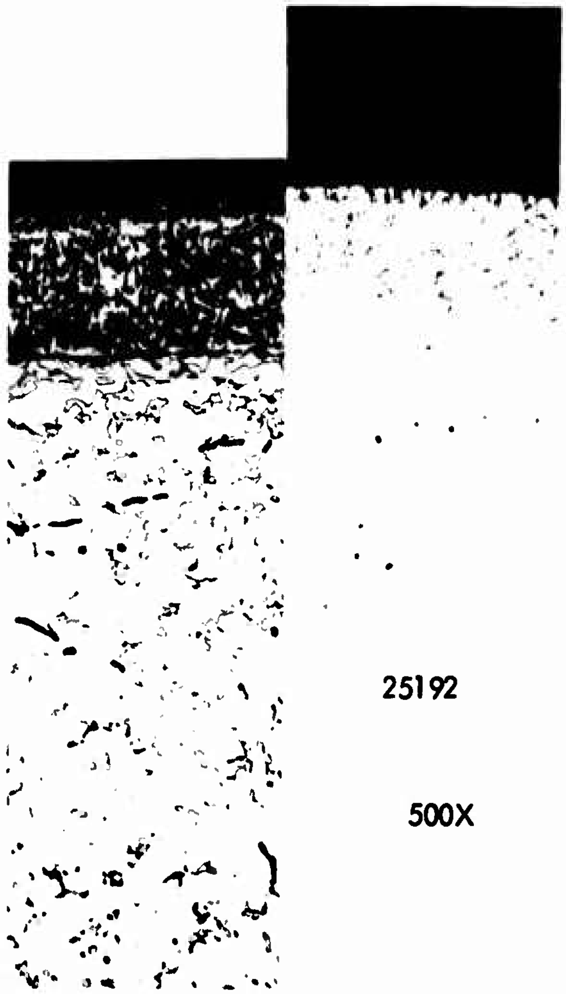

25192

500X

(ETCHED)

ALLOY 19-B

7 HOURS
1200°C
AIR

ALLOY 19-C

24 HOURS
1200°C
AIR

Figure 12. Effects of 7 Hour and 24 Hour Oxidation in Air at 1200°C on the Microstructure and Oxide-Metal Interface of Alloy 19 (Nb-10Al-20$NbCo_2$) at 500X.

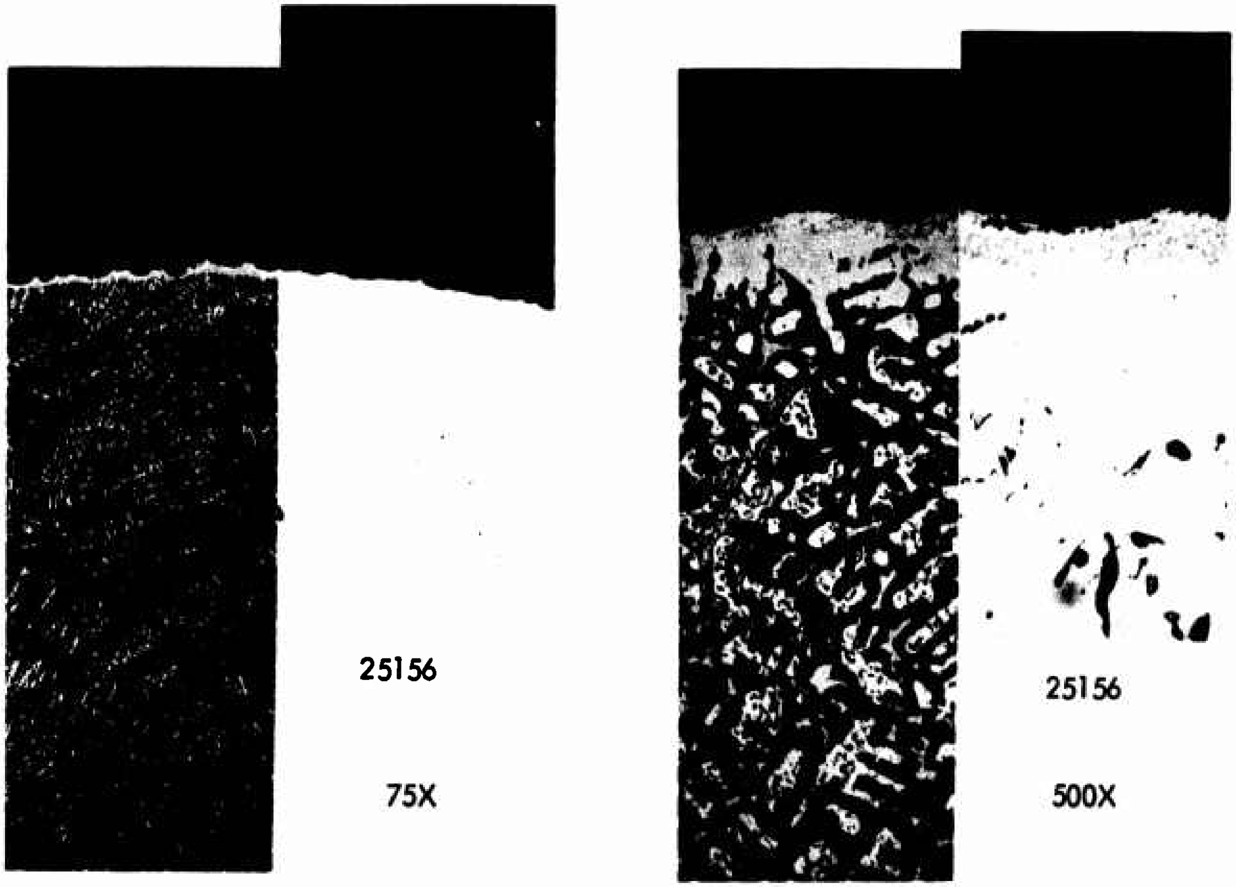

(ETCHED) (ETCHED)

ALLOY 20
7 HOURS
1200°C
AIR

Figure 13. The Effect of a 7 Hour Oxidation Exposure in Air on Alloy 20 (Nb-15$NbAl_3$-15$NbCo_2$) at 75 and 500X.

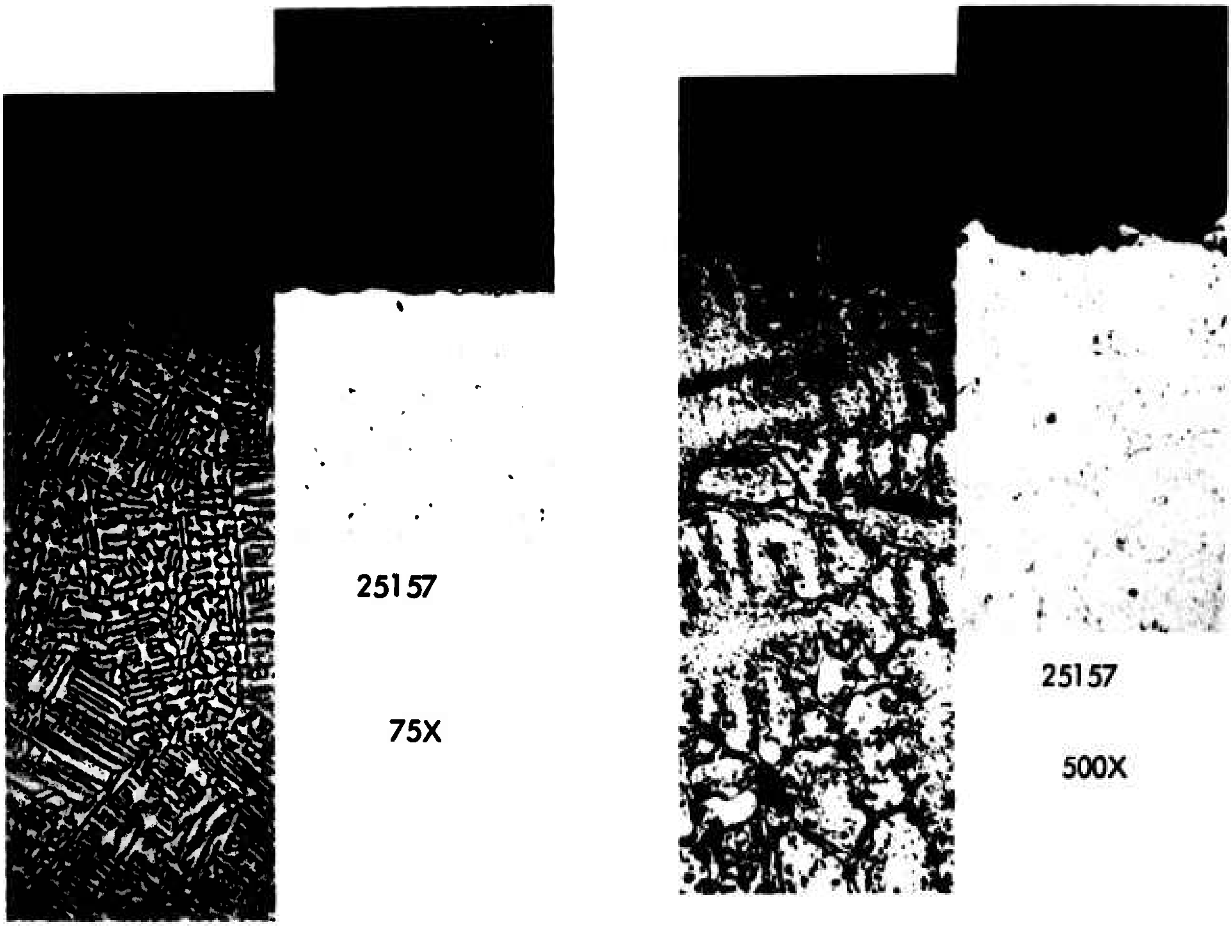

(ETCHED)

(ETCHED)

ALLOY 21

7 HOURS
1200°C
AIR

Figure 14. The Effect of a 7 Hour Oxidation Exposure in Air on Alloy 21 (Nb-15$NbAl_2$-15$NbCo_2$) at 75 and 500X.

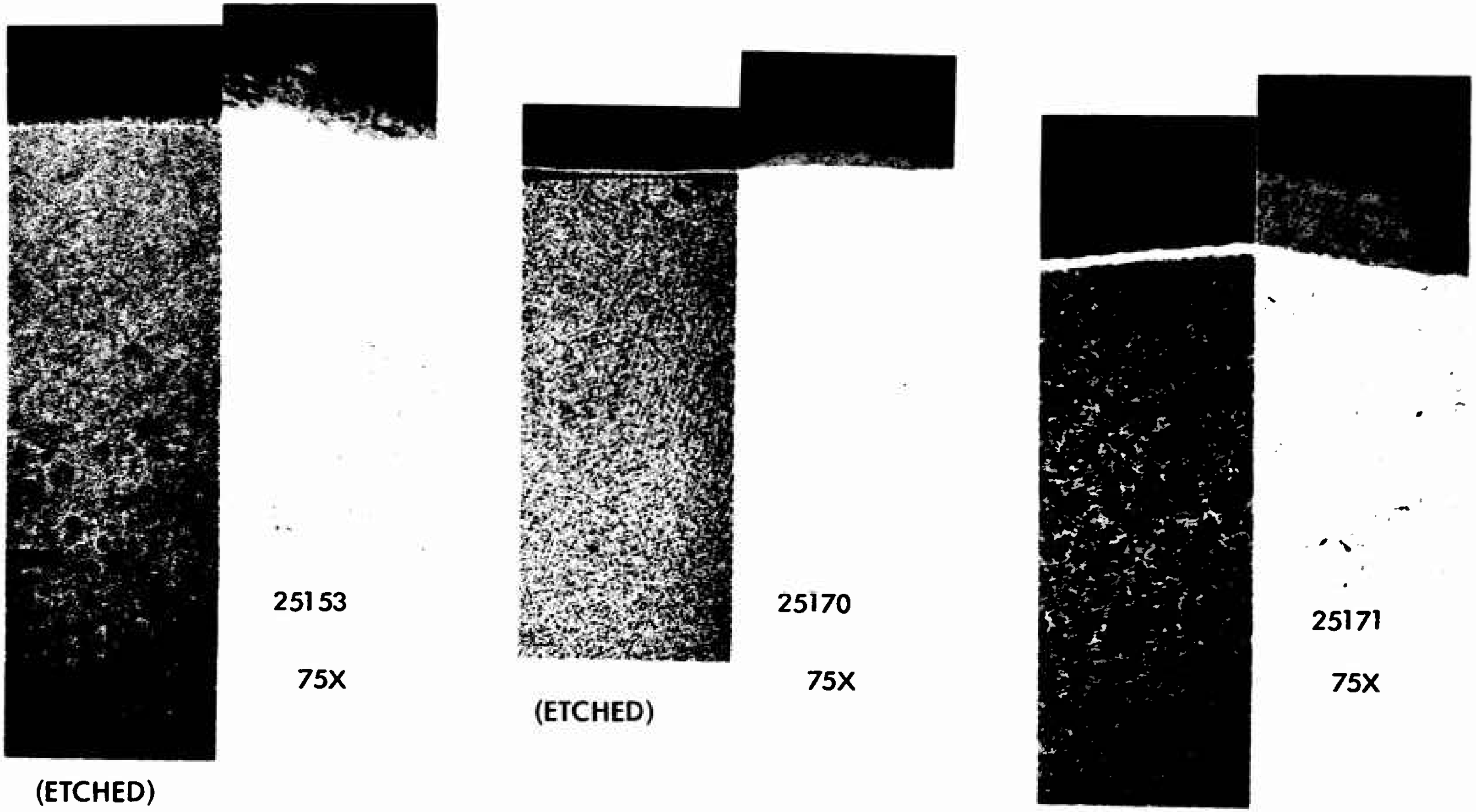

ALLOY 22

ALLOY 22 + Y
(ALLOY 34)

ALLOY 22 + Y_2O_3
(ALLOY 35)

7 HOURS - 1200°C - AIR

Figure 15. Effects of Y and Y_2O_3 on the Microstructure and Oxide Metal Interface of Alloy 22 (Nb-10NbCr$_2$-15NbAl$_3$-15NbCo$_2$) at 75X.

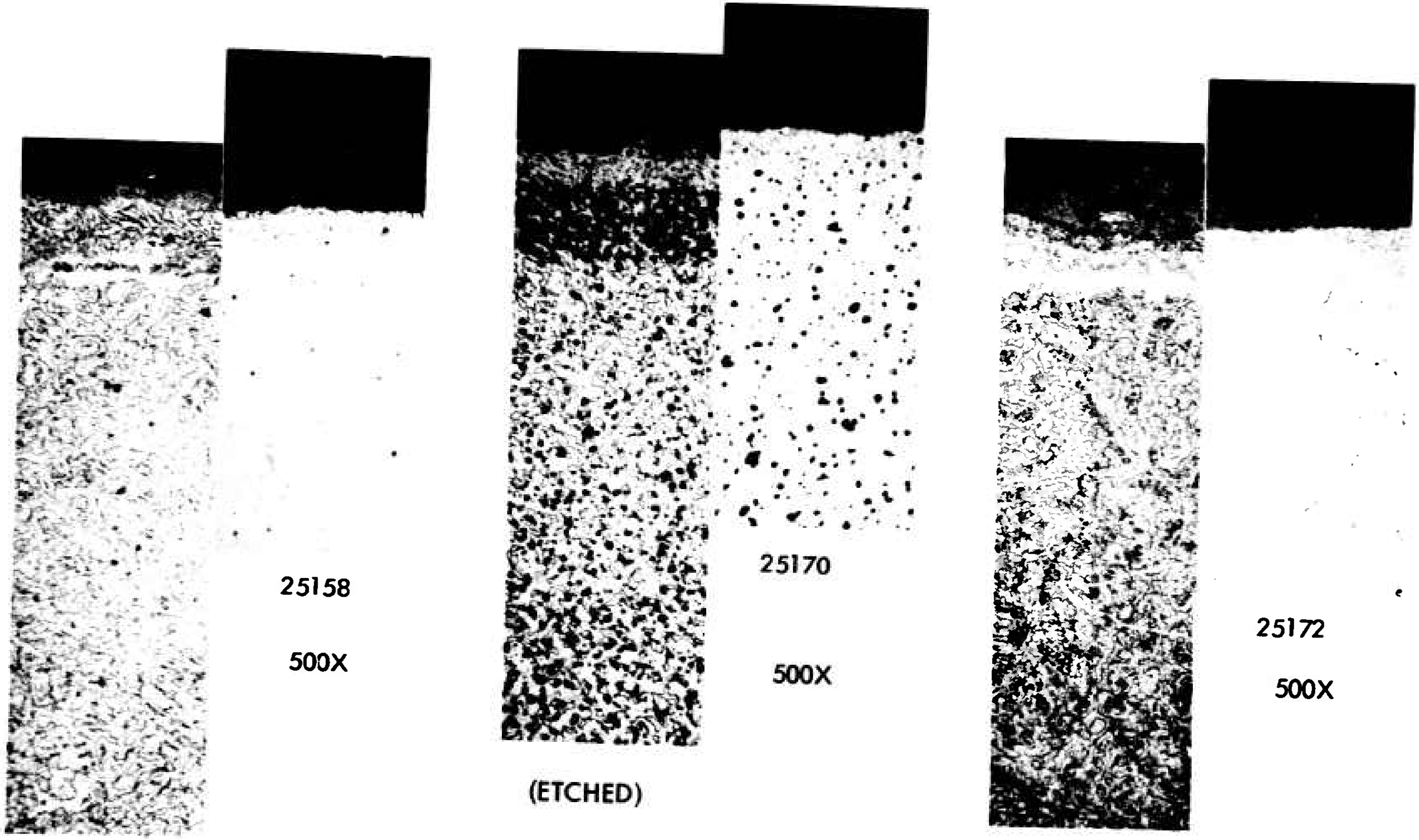

(ETCHED) (ETCHED) (ETCHED)

ALLOY 22

ALLOY 22 + Y
(ALLOY 34)

ALLOY 22 + Y_2O_3
(ALLOY 35)

7 HOURS - 1200°C - AIR

Figure 16. Effects of Y and Y_2O_3 on the Microstructure and Oxide Metal Interface of Alloy 22 (Nb-$10NbCr_2$-$15NbAl_3$-$15NbCo_2$) at 500X.

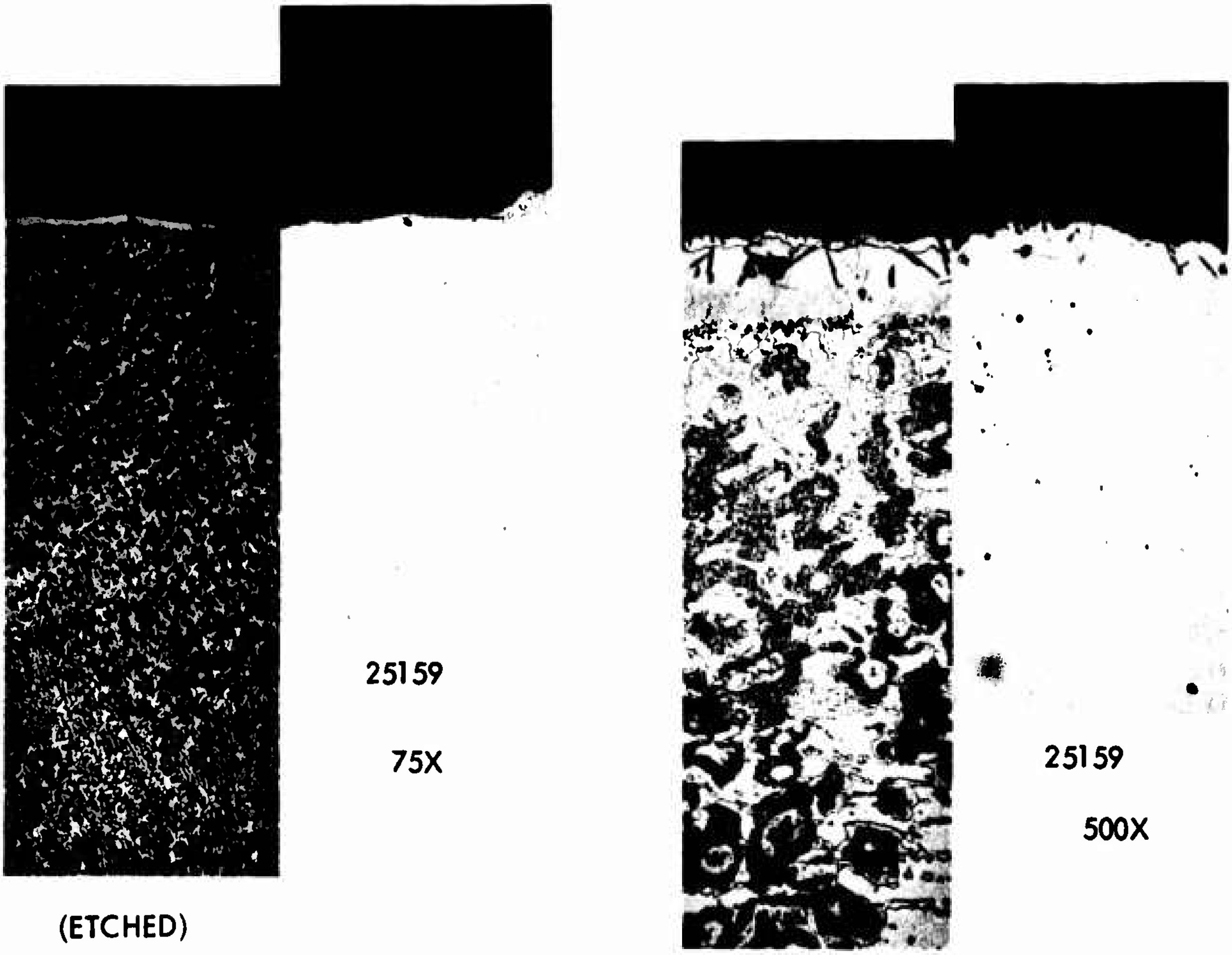

(ETCHED) (ETCHED)

ALLOY 23

7 HOURS
1200°C
AIR

Figure 17. The Effect of a 7 Hour Oxidation Exposure in Air on Alloy 23 (Nb-15$NbAl_3$-15$NbCo_2$-10NbNi) at 75X and 500X.

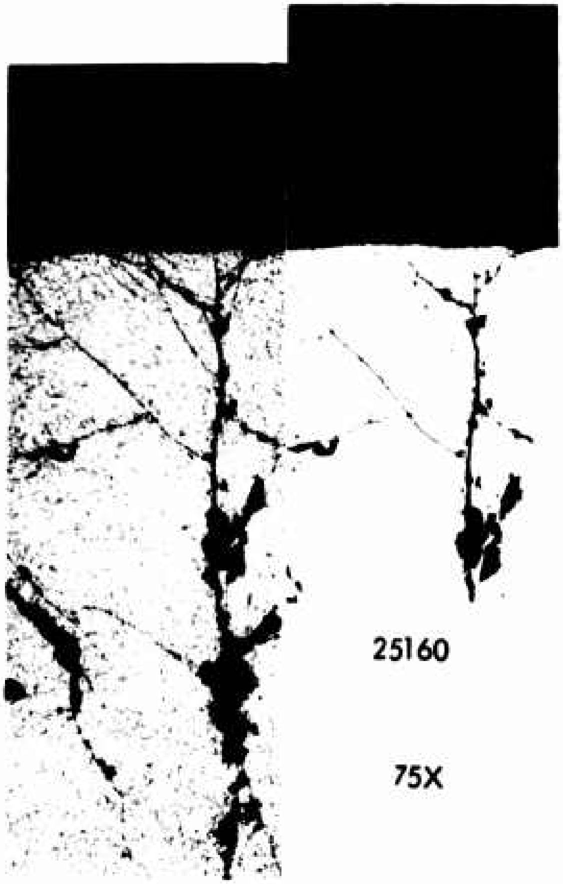

25160

75X

(ETCHED)

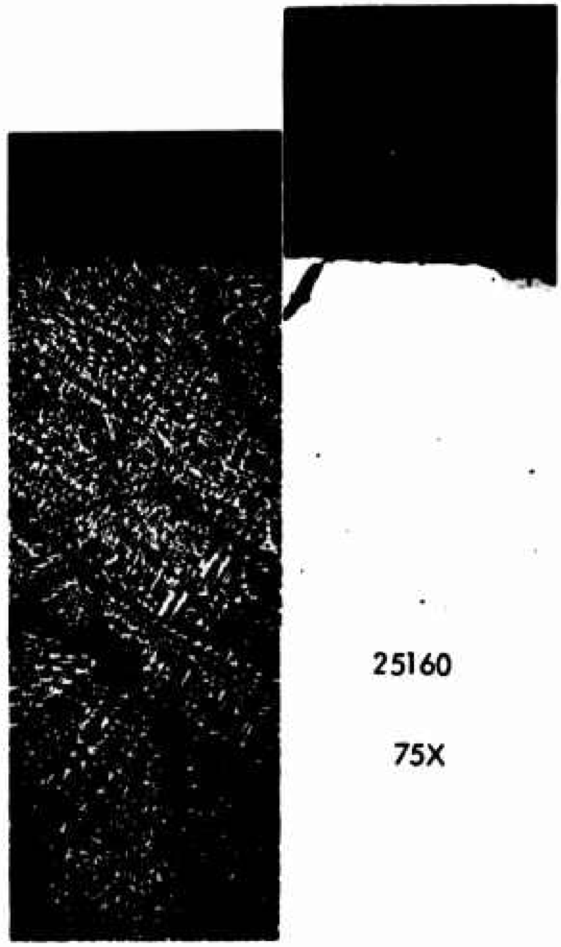

25160

75X

(ETCHED)

7 HOURS
1200°C
AIR

24 HOURS
1200°C
AIR

ALLOY 24

Figure 18. Effects of 7 Hour and 24 Hour Oxidation in Air at 1200°C on the Microstructure and Oxide-Metal Interface of Alloy 24 (Nb-30$NbAl_3$-10$NbCo_2$) at 75X.

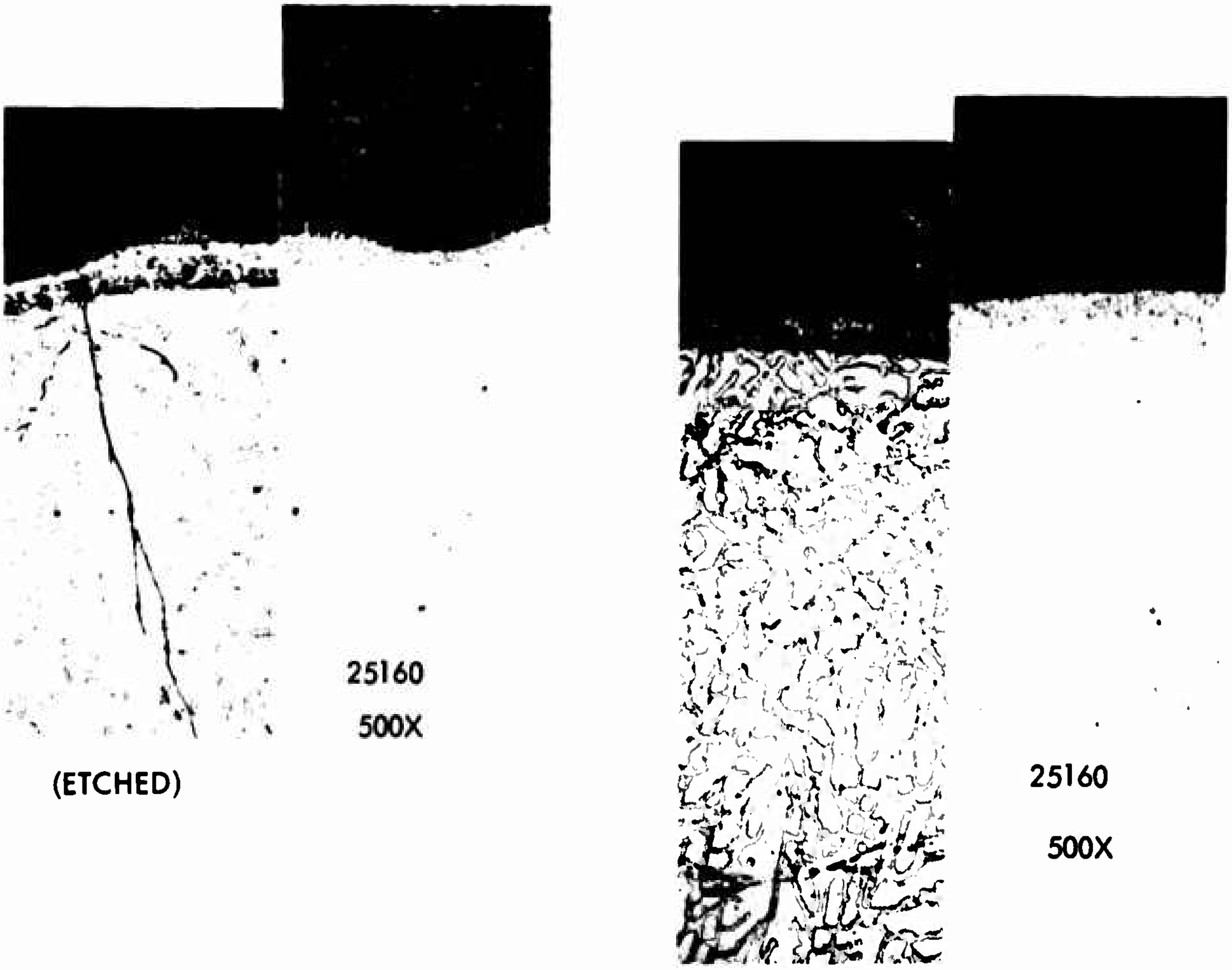

(ETCHED)

7 HOURS
1200°C
AIR

24 HOURS
1200°C
AIR

ALLOY 24

Figure 19. Effects of 7 Hour and 24 Hour Oxidation in Air at 1200°C on the Microstructure and Oxide-Metal Interface of Alloy 24 (Nb-30$NbAl_3$-10$NbCo_2$) at 500X.

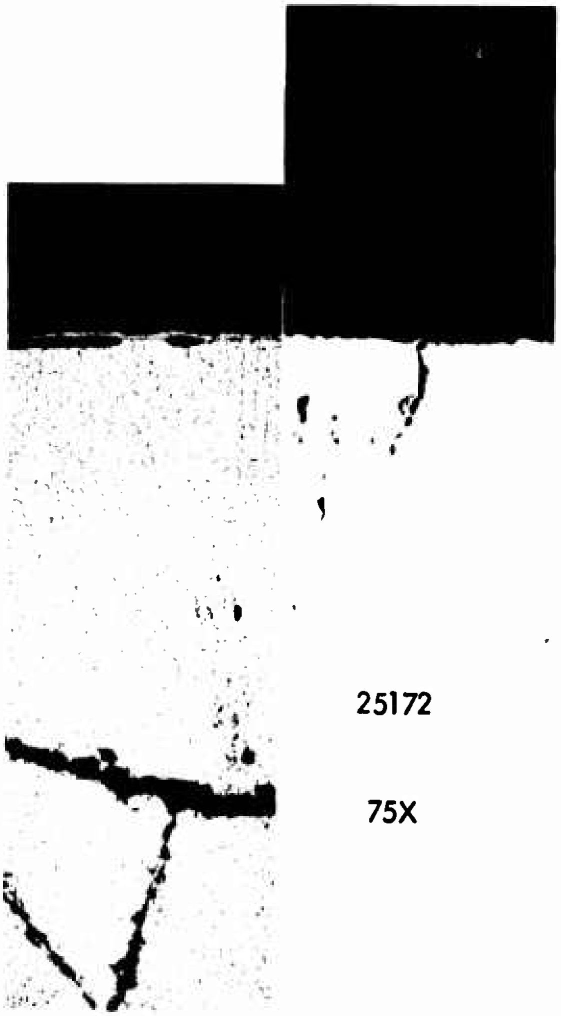

(ETCHED)

ALLOY 24 + Y

(ALLOY 36)

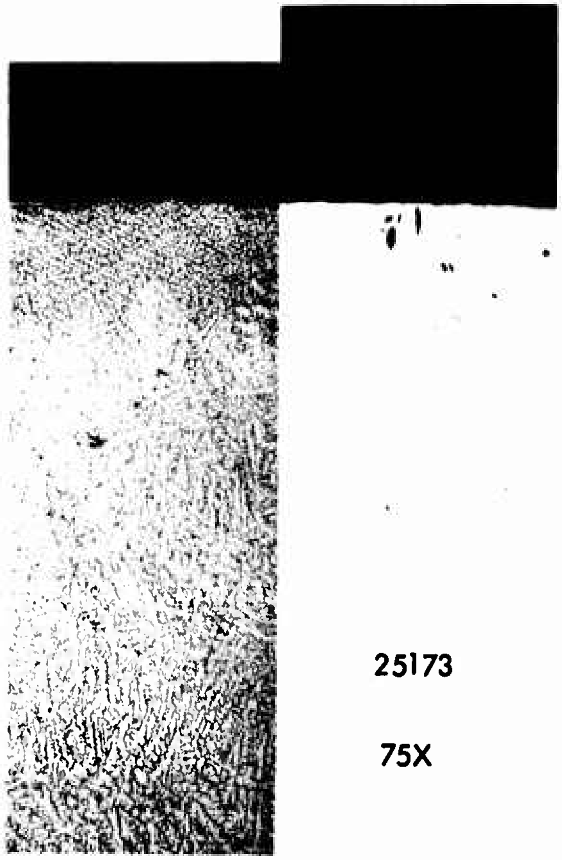

(ETCHED)

ALLOY 24 + Y_2O_3

(ALLOY 37)

7 HOURS
1200°C
AIR

Figure 20. Effects of Y and Y_2O_3 on the Microstructure and Oxide Metal Interface of Alloy 24 ($Nb-30NbAl_3-10NbCo_2$) at 75X.

(ETCHED) 25172

500X

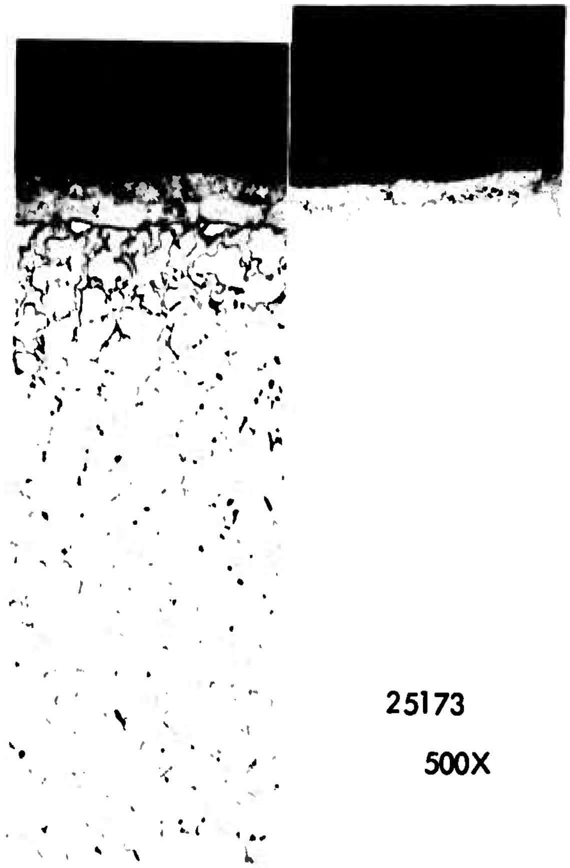

25173

500X

(ETCHED)

ALLOY 24 + Y

(ALLOY 26)

ALLOY 24 + Y_2O_3

(ALLOY 37)

7 HOURS
1200°C
AIR

Figure 21. Effects of Y and Y_2O_3 on the Microstructure and Oxide Metal Interface of Alloy 24 ($Nb-30NbAl_3-10NbCo_2$) at 500X.

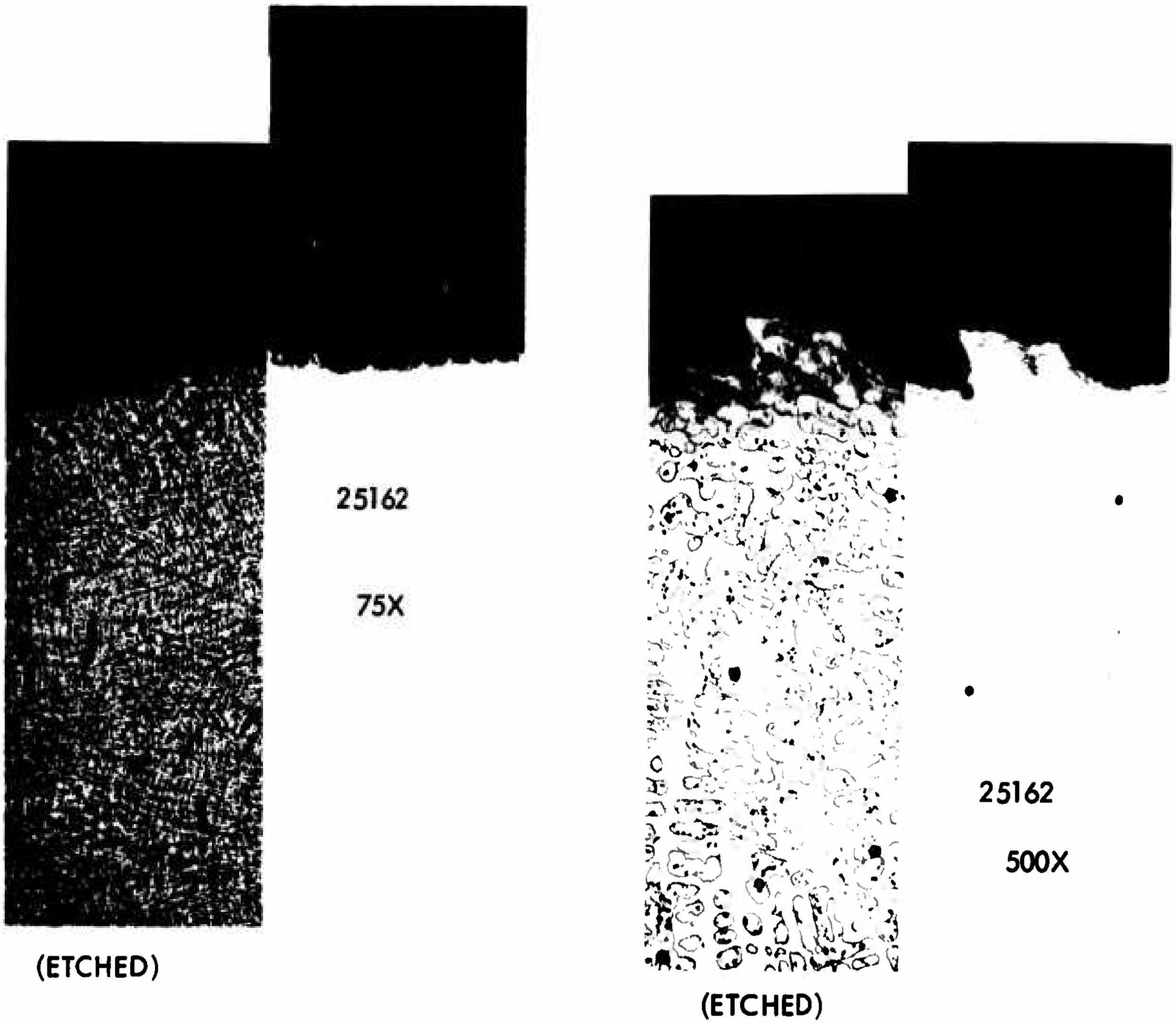

ALLOY 25

7 HOURS
1200°C
AIR

Figure 22. The Effect of a 7 Hour Oxidation Exposure in Air on Alloy 25 (Nb-10$NbAl_3$-30$NbCo_2$) at 75X and 500X.

Figure 3 shows the effects on the microstructure of adding Y and Y_2O_3 to alloy 13 (Nb-25NbAl$_3$-10Co (Nb-11.6Al-10Co)). Without the electron beam microprobe analysis it is difficult to see a real difference on the oxide-metal interface, with the exception that the metal oxide thickness is small for alloy 13 as would be expected from the measured oxidation rates. Figure 4 shows the metal affected zone at 500X. The affected metal zone is about 30μ, while the oxide scale for alloy 13 is 140 to 150μ thick. Alloy 17 oxidized for ~7 and ~24 hours is shown in Figures 5 and 6 . While the oxide is thicker as a result of the longer oxidation, a 3 fold increase in oxidation time, the affected metal zone increases only about 5 to 10μ.

Figures 7 and 8 are the photomicrographs of alloy 17 with Y and Y_2O_3 added. Both of these additions increased the metal affected zone by ~10-15μ. Figures 9 and 10 show the effects of oxidation on alloy 18. The metal affected zone of the alloy oxidized for ~24 hours (18-C) is actually thinner than that of the alloy oxidized for ~7 hours. Note the coarsening of the microstructure as the time at 1200°C is increased. The metal oxide interface of alloy 19 is shown in Figures 11 and 12 for oxidation times of ~7 and ~24 hours. For this alloy, the metal affected zone increased from ~20-23μ for the 7 hour oxidation to ~40-45μ for the 24 hour 1200°C exposure. The microstructures of alloy 20 and 21 are shown in Figures 13 and 14 . Both structures appear to be definite coarse 2 phase structures and did not show good oxidation properties.

Figures 15 and 16 show the results of Y and Y_2O_3 additions to alloy 22. The yttrium addition increased the depth of the metal affected zone from ~25μ to 40μ. Figure 17 characterizes the oxide metal interface of alloy 23.

Figures 18 through 21 characterize the oxide metal interface of alloy 24, oxidized for both ~7 and ~24 hours and for alloys 36 and 37 which is alloy 24 with Y and Y_2O_3,

respectively. The microstructure of alloy 25 is shown in Figure 22. For most of the alloys the depth of the metal affected zone is between 20 and 40 microns (5 to 10 mils).

3.2.3 Oxidation Behavior of Nb-Fe-Al Alloys

Alloys 14, 15, and 16 exhibited the best oxidation behavior for the Nb-Fe-Al alloys investigated. The parabolic rate constants are shown in Table 4. Both alloys 15 and 16 exhibited a decreasing parabolic rate constant as oxidation times increased. For these alloys, the parabolic oxidation constants were found to range from 0.042 to 0.33 $(mg/cm^2)^2/min.$, corresponding to a metal consumption rate of from ~1.8 mils/100 hours to about 4.5 mils/100 hours, excluding the metal affected zone in the substrate. As reported for the Nb-Co-Al alloys, the addition of Y or Y_2O_3 to Nb-Fe-Al alloys caused an increase in the oxidation rate in air.

3.2.4 Metallography of the Oxide-Metal Interfaces (Nb-Fe-Al Alloys)

Figures 23 through 30 characterize the oxide metal interface and the metal affected zone for the Nb-Fe-Al alloys. For alloys 14 (Figures 29 and 30) and 16 (Figures 24, 25, and 26) the metal affected zone is less than 20μ. However, for alloys 11 (Figure 23) and 15 (Figures 27 and 28) the metal affected zone is ~70μ (~17 mils). As the oxidation time is increased from ~7 hours to ~24 hours at 1200°C, the metal affected zone for alloy 16 does not increase with time, while for alloy 15, the depth of the metal affected zone does increase with increased oxidation time.

3.2.5 Nb-Cr; Nb-Cr-Al Alloys

The Nb-Cr alloy 12 exhibited the lowest oxidation rate for this group of alloys. Alloy 3 exhibited linear oxidation behavior and alloy 7 oxidized at a rate equivalent to ~20-23 mils/100 hours. Alloy 31 was the Nb-Cr-Al-Co alloy designated DU-1 and reported in the

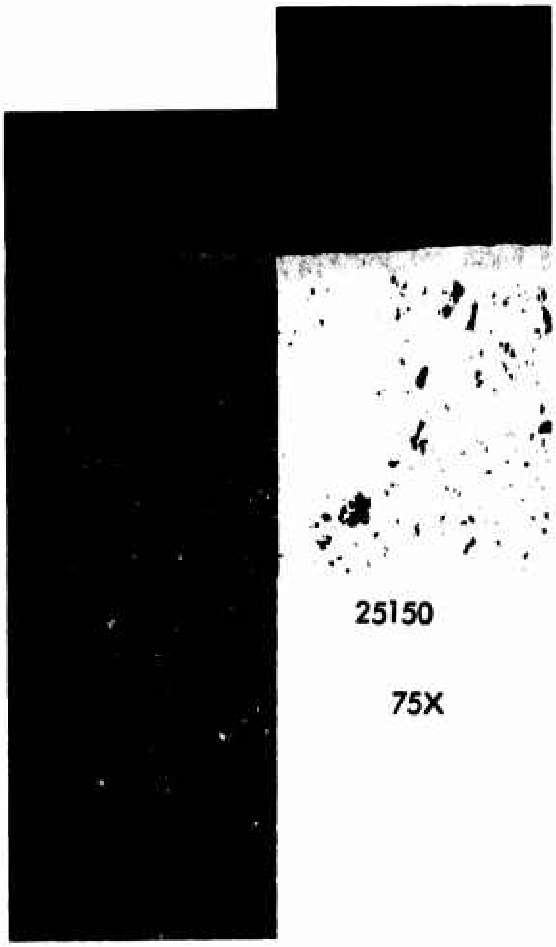

25150

75X

(ETCHED)

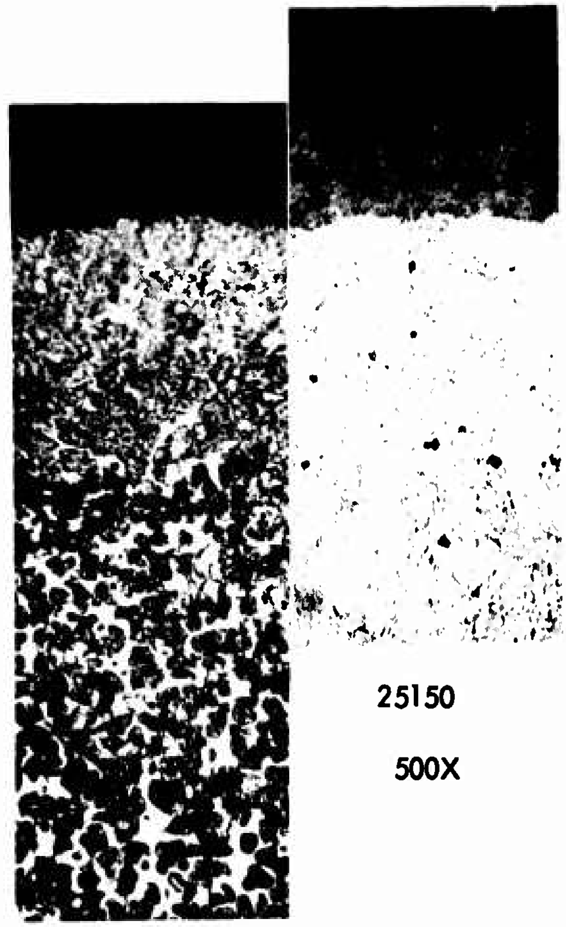

25150

500X

(ETCHED)

ALLOY 11

7 HOURS
1200°C
AIR

Figure 23. The Effect of a 7 Hour Oxidation Exposure in Air on Alloy 11 (Nb-25NbAl$_3$-25NbFe$_2$ at 75X and 500X.

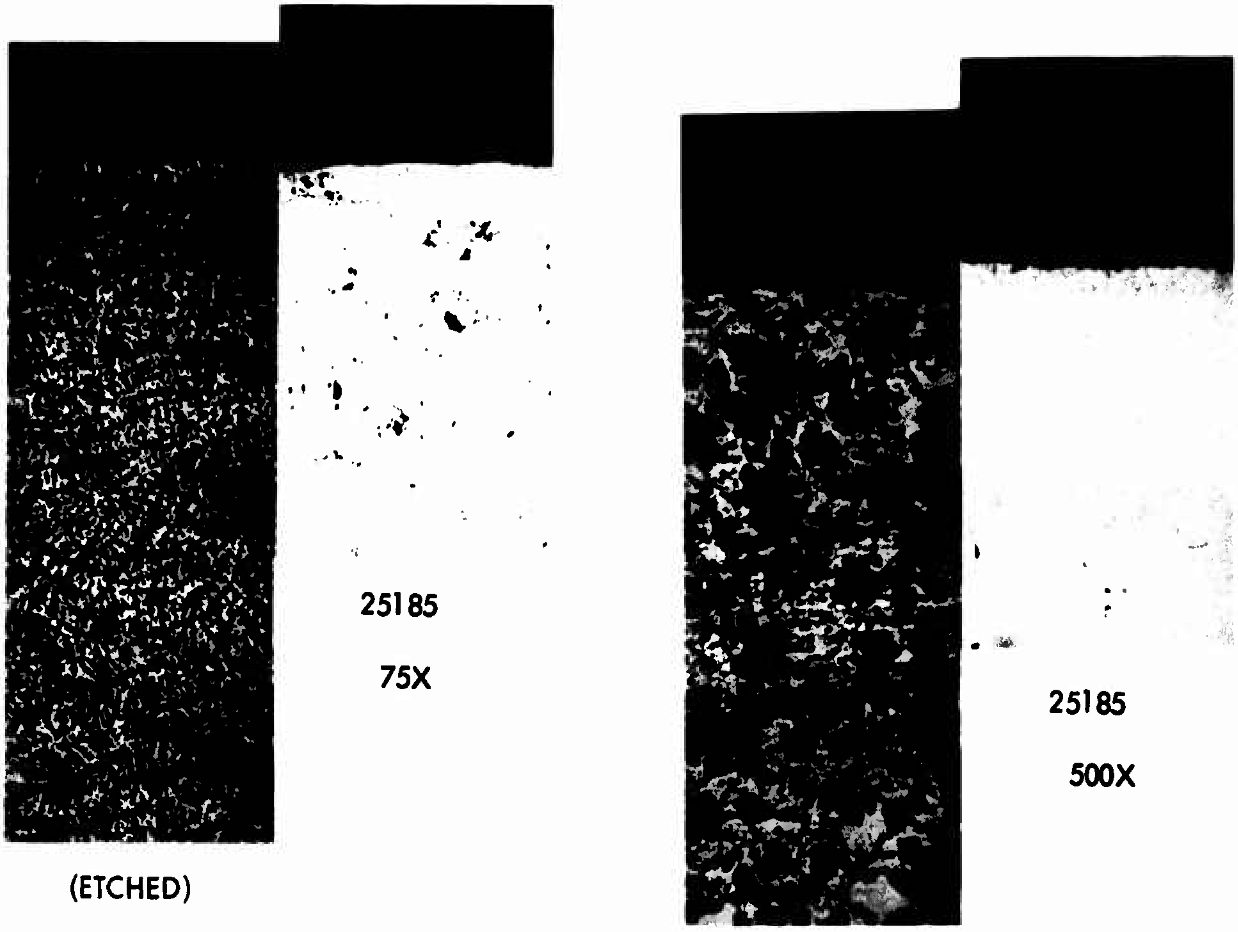

ALLOY 14

7 HOURS
1200°C
AIR

Figure 24. The Effect of a 7 Hour Oxidation Exposure in Air on Alloy 14 (Nb-10Al-30$NbFe_2$) at 75X and 500X.

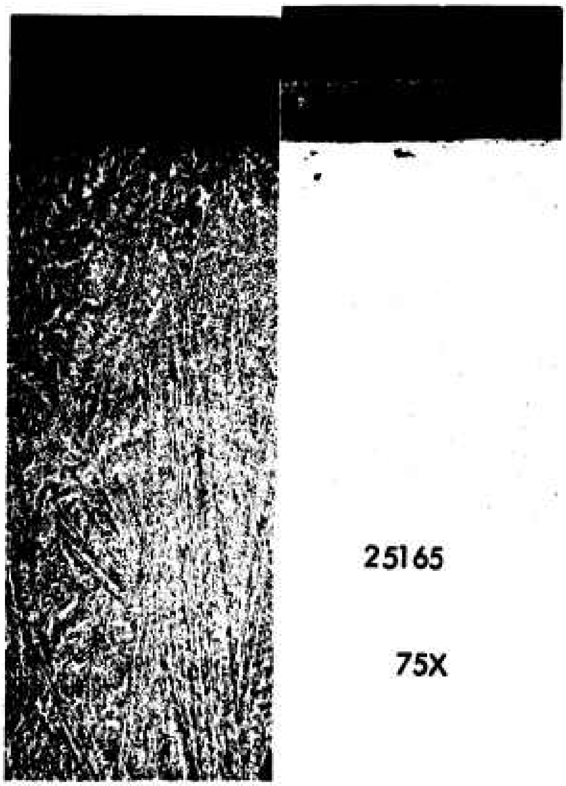

(ETCHED)

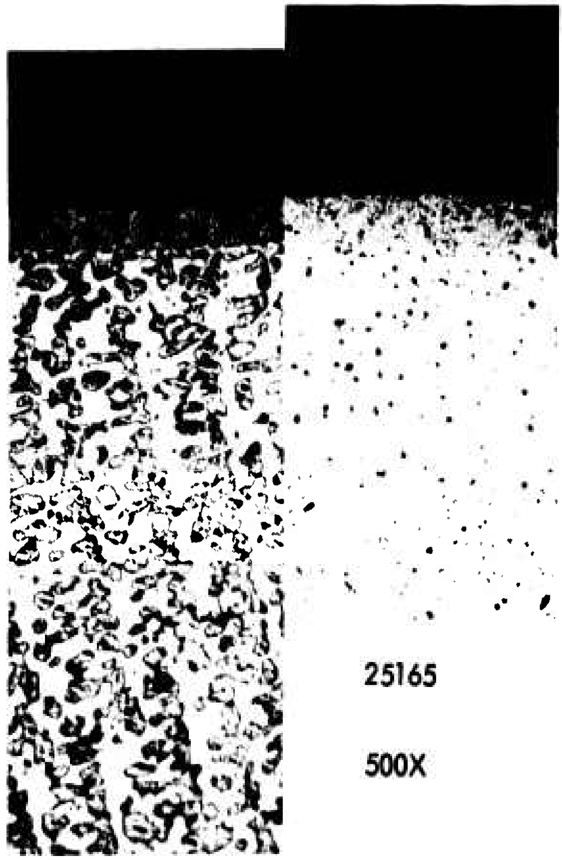

(ETCHED)

ALLOY 14 + Y
(ALLOY 28)

7 HOURS
1200°C
AIR

Figure 25. Effects of Y in the Microstructure and Oxide Metal Interface of Alloy 14 (Nb-10Al-30NbFe_2) at 75X and 500X.

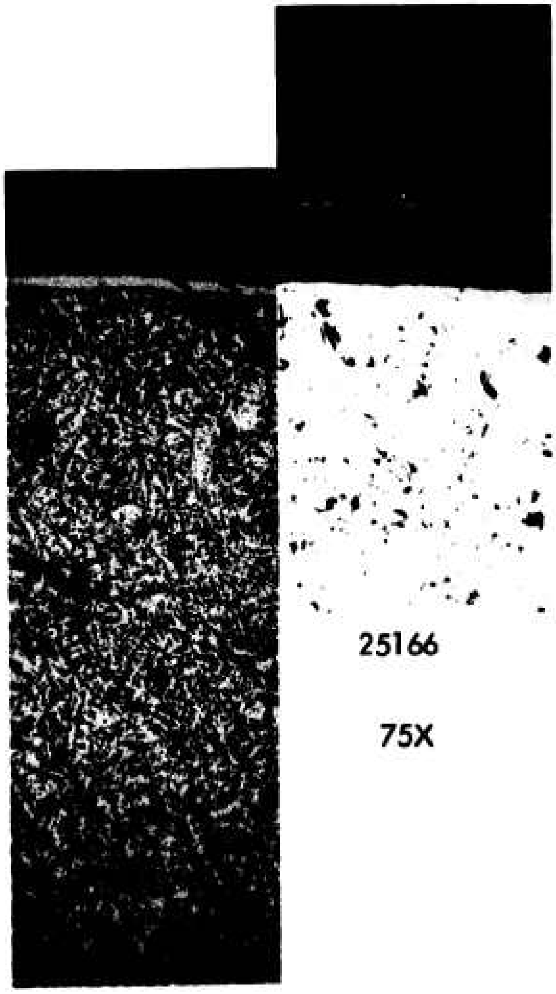

25166

75X

(ETCHED)

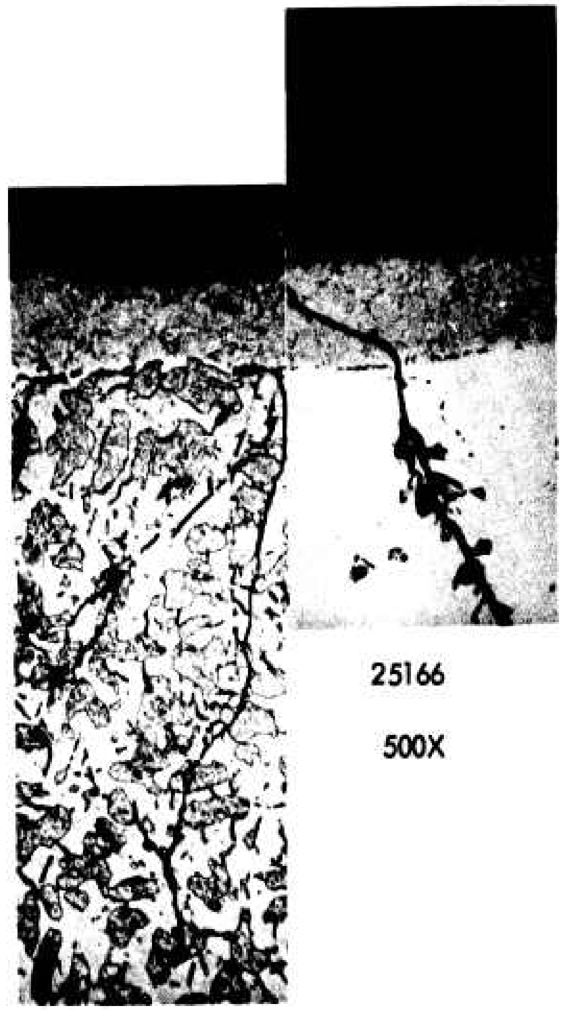

25166

500X

(ETCHED)

ALLOY 14 + Y_2O_3
(ALLOY 29)

7 HOURS
1200°C
AIR

Figure 26. Effect of Y_2O_3 in the Microstructure and Oxide Metal Interface of Alloy 14 (Nb-10Al-30$NbFe_2$) at 75 and 500X.

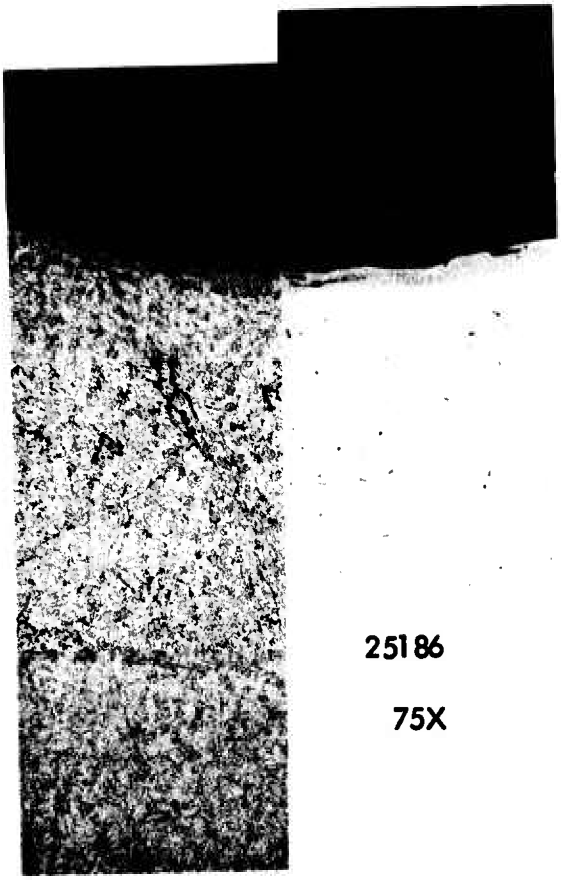

25186

75X

(ETCHED)

7 HOURS
1200°C
AIR

25187

75X

(ETCHED)

24 HOURS
1200°C
AIR

ALLOY 15

Figure 27. Effects of 7 Hour and 24 Hour Oxidation in Air at 1200°C on the Microstructure and Oxide-Metal Interface of Alloy 15 (Nb-10Al-30Fe) at 75X.

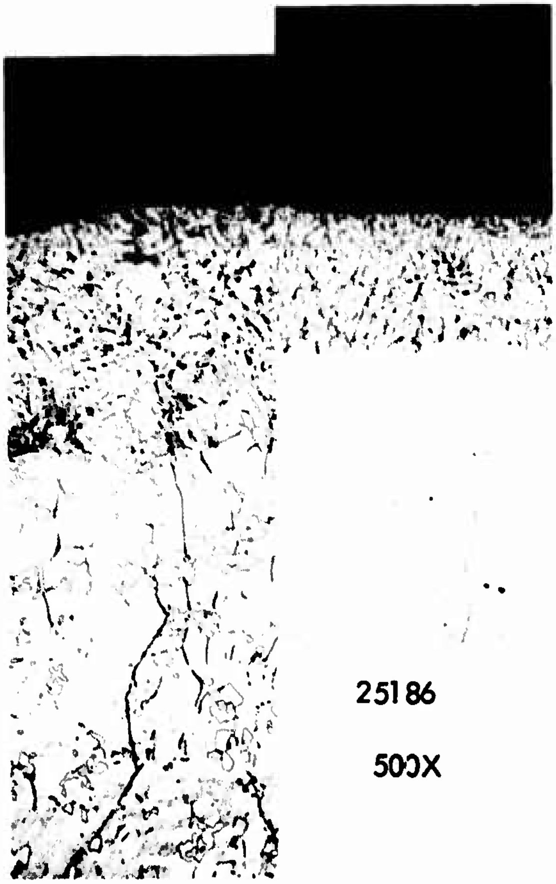

25186

500X

(ETCHED)

7 HOURS
1200°C
AIR

25187

500X

(ETCHED)

24 HOURS
1200°C
AIR

ALLOY 15

Figure 28. Effects of 7 Hour and 24 Hour Oxidation in Air at 1200°C on the Microstructure and Oxide-Metal Interface of Alloy 15 (Nb-10Al-30Fe) at 500X.

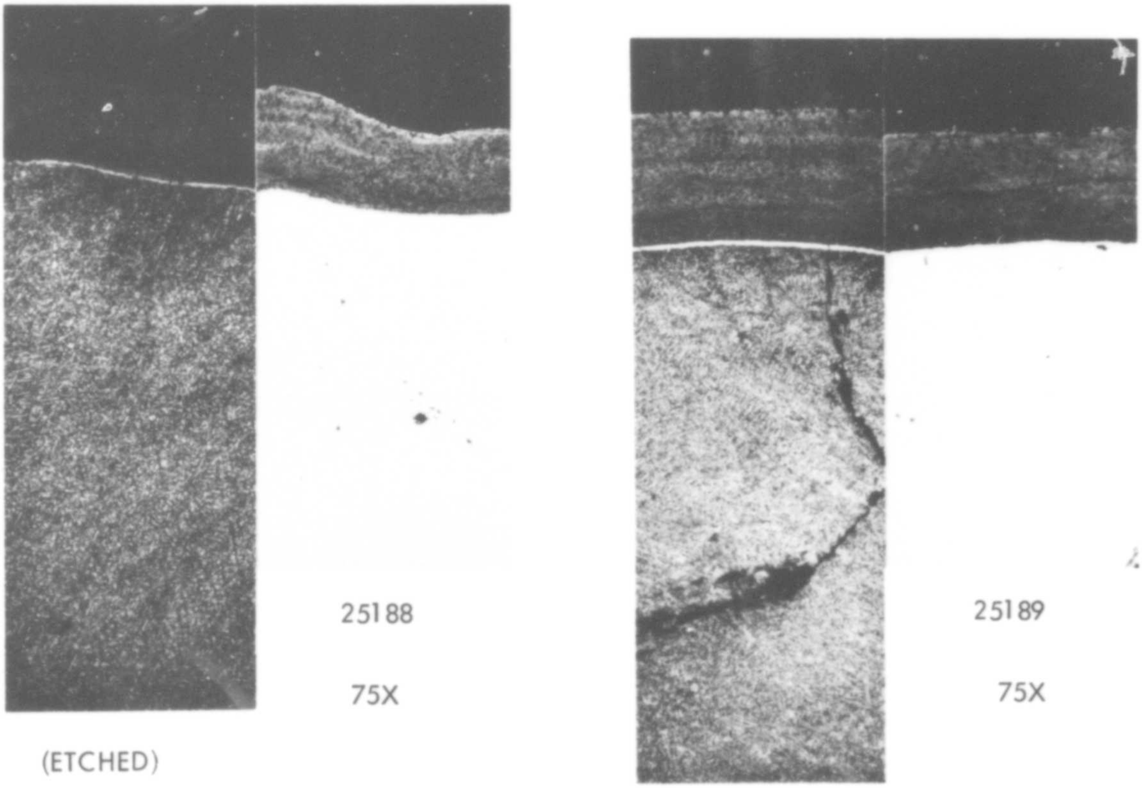

25188

75X

(ETCHED)

7 HOURS
1200°C
AIR

25189

75X

(ETCHED)

24 HOURS
1200°C
AIR

ALLOY 16

Figure 29. Effects of 7 Hour and 24 Hour Oxidation in Air at 1200°C on the Microstructure and Oxide-Metal Interface of Alloy 16 (Nb-25NbAl$_3$-15Fe) at 75X.

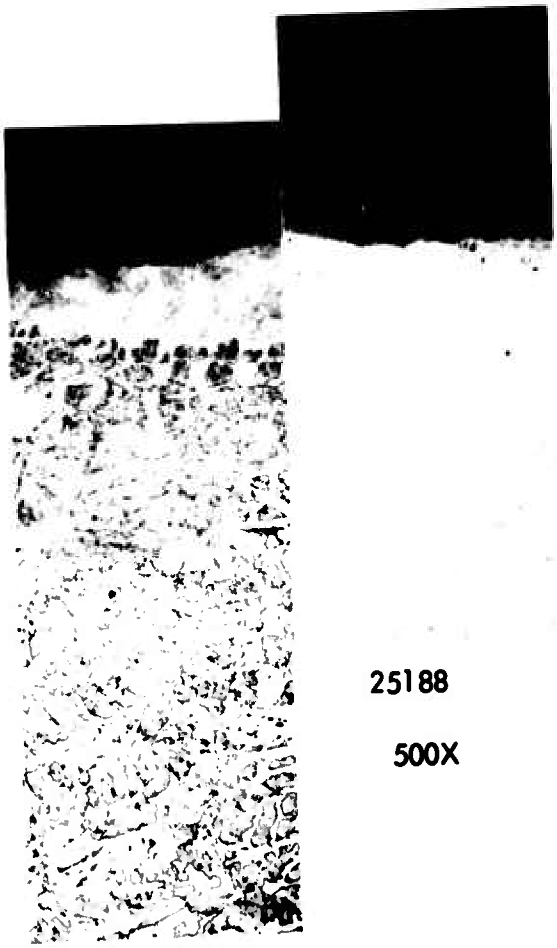

(ETCHED)

7 HOURS
1200°C
AIR

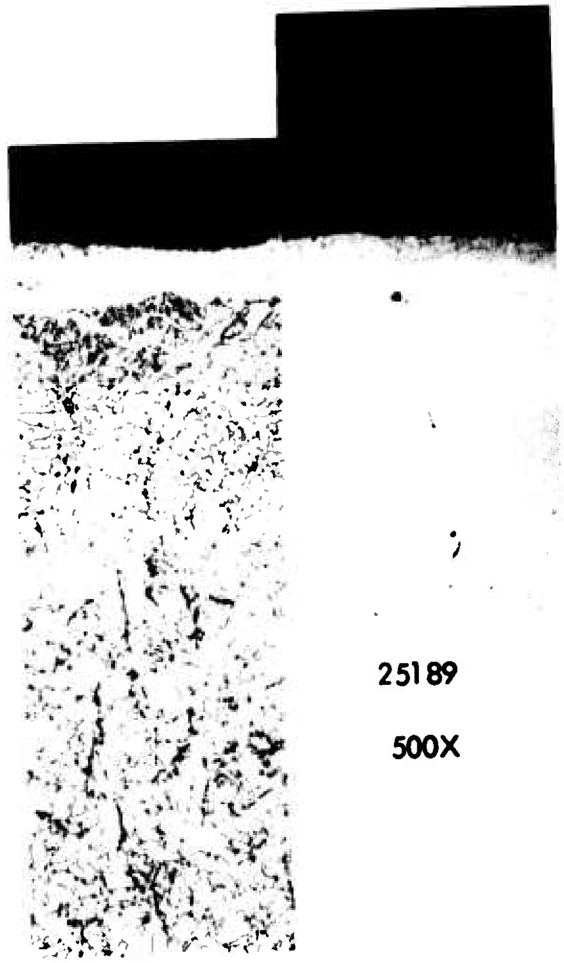

(ETCHED)

24 HOURS
1200°C
AIR

ALLOY 16

Figure 30. Effects of 7 Hour and 24 Hour Oxidation in Air at 1200°C on the Microstructure and Oxide-Metal Interface of Alloy 16 (Nb-25NbAl$_3$-15Fe) at 500X.

Phase III final report. Alloy 31 resulted when Y_2O_3 was added to the DU-1 alloy composition. An attempt was made to add Y, but the alloy cracked on cooling when it was arc-melted. The parabolic oxidation constant of 0.092 $(mg/cm^2)^2/min$ with Y_2O_3 compares with a parabolic oxidation constant of ~0.040 reported for the alloy without Y_2O_3.

3.2.6 Metallography of the Nb-Cr, Nb-Cr-Al, and Nb-Cr-Co-Al Alloys

Figure 31 to 34 present the microstructures of the oxide metal interface for the Nb-Cr base alloys. Both alloy 3 and 7 exhibited segregated structures similar to those exhibited by alloy 20 for the Nb-Co-Al system. Inherent with this structure seems to be relatively poor oxidation behavior. Figure 33 shows the microstructure of alloy 12. Although this alloy exhibited a low oxidation rate, the metal affected zone is over 160µ (40 mils) deep. This kind of metal affected zone has been shown to be characteristic of Nb-Cr alloy systems. Figure 34 shows the microstructure of the DU-1 + Y_2O_3 alloy which also exhibits a large metal affected zone. Both $NbCr_2$ and DU-1 reported during Phase III of this program exhibited similar behavior.

Microhardness determinations were made on the alloys evaluated and are given in Table 6.

3.3 X-RAY DIFFRACTION ANALYSIS OF THE OXIDE FILMS

The results of the x-ray analysis are presented in detail in Appendix C where the d-spacings in angstroms, an estimate of the relative intensity in the case where the results were taken from a Debye-Scherrer film and calculated relative intensities measured from the x-ray diffractometer strip chart trace, are listed. Also indicated for each film studied are the lines which correspond to particular compounds as reported by the ASTM index. Where no indication is given, the constituent or phase responsible for that particular line or lines could not be readily determined.

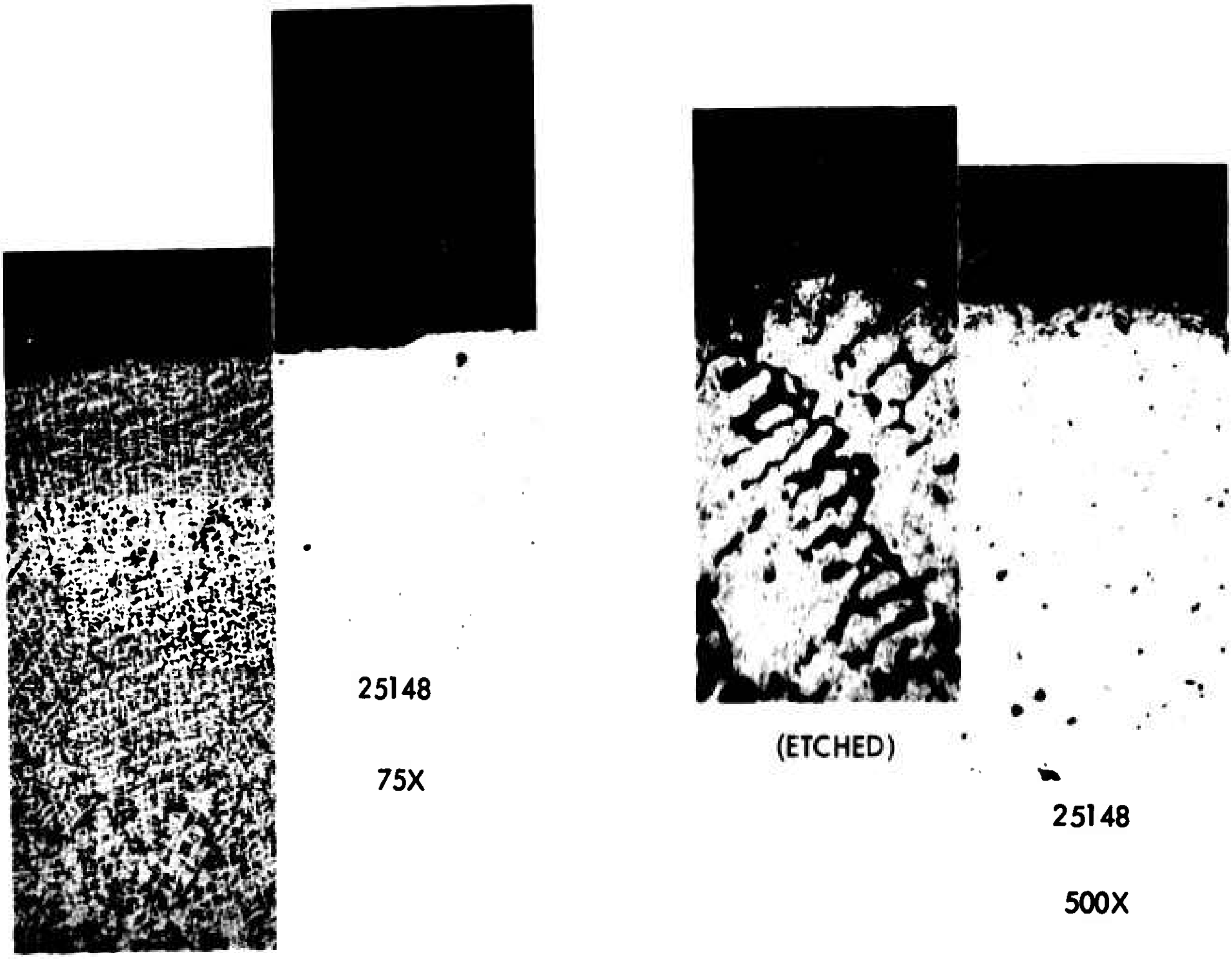

(ETCHED)

ALLOY 3

7 HOURS
1200°C
AIR

Figure 31. The Effect of a 7 Hour Oxidation Exposure in Air on Alloy 3 ($Nb-35NbCr_2-30Nb_2Al$) at 75X and 500X.

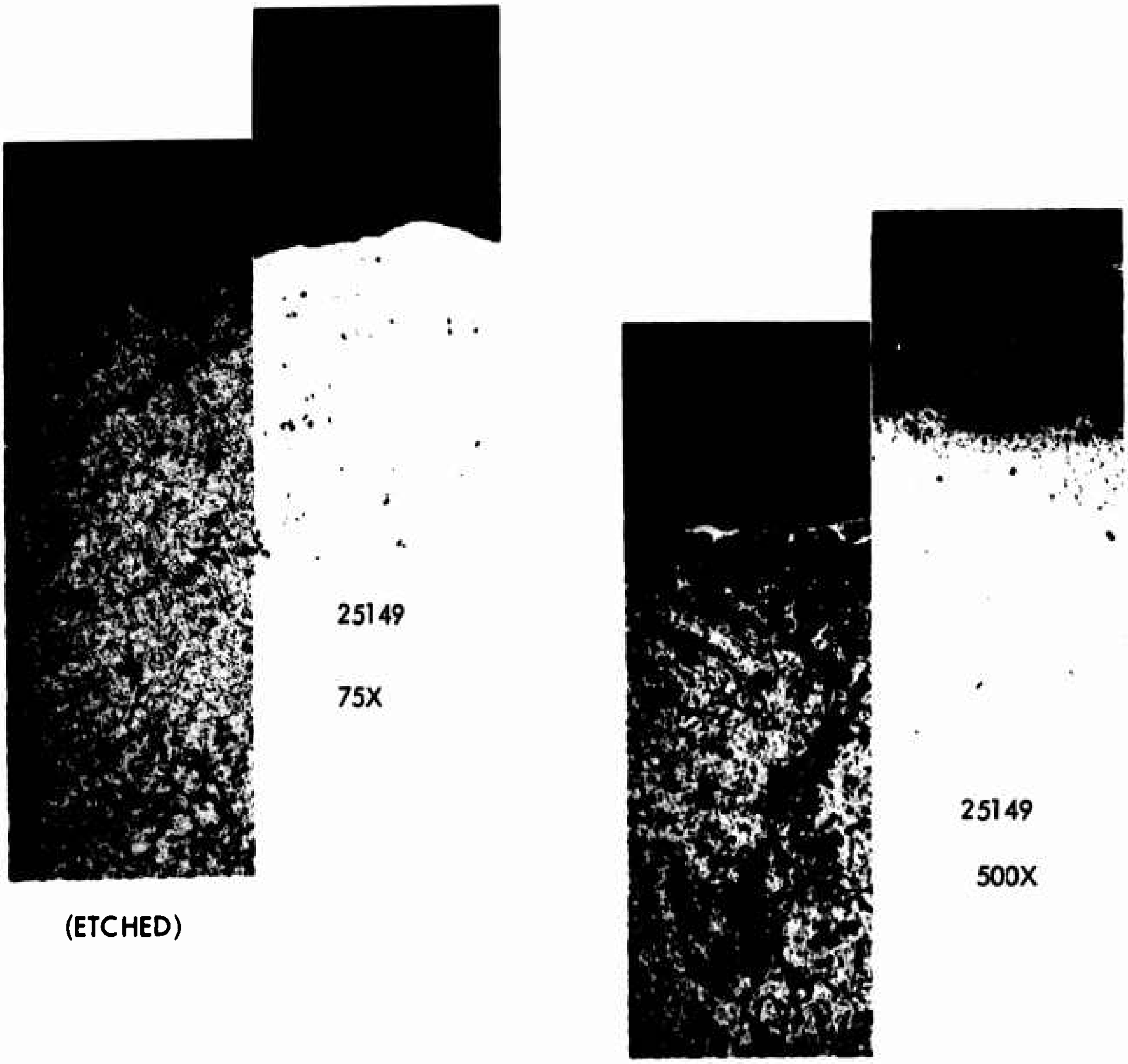

25149

75X

(ETCHED)

25149

500X

(ETCHED)

ALLOY 7

7 HOURS
1200°C
AIR

Figure 32. The Effect of a 7 Hour Oxidation Exposure in Air on Alloy 7 (Nb-15$NbCr_2$-10$NbAl_3$-4Al-9Cr) at 75X and 500X.

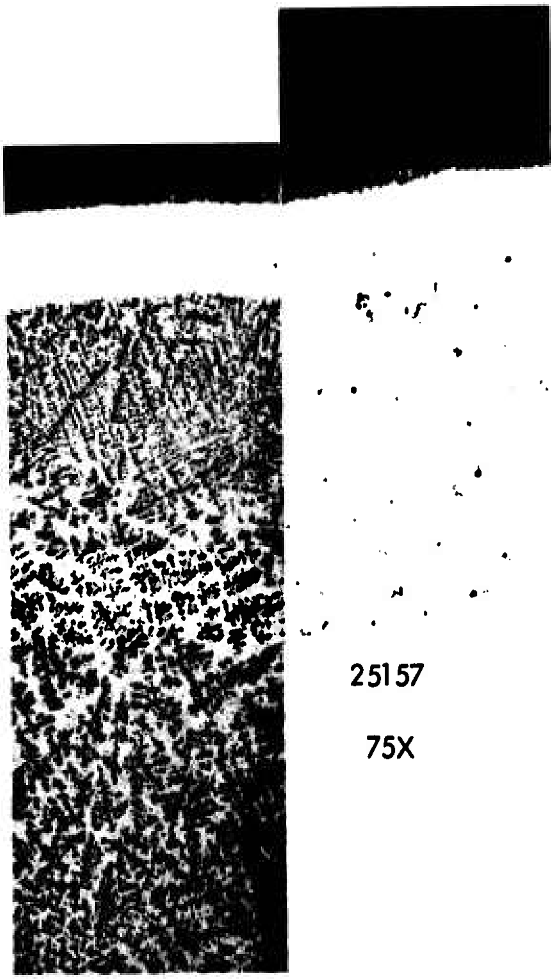

25157

75X

(ETCHED)

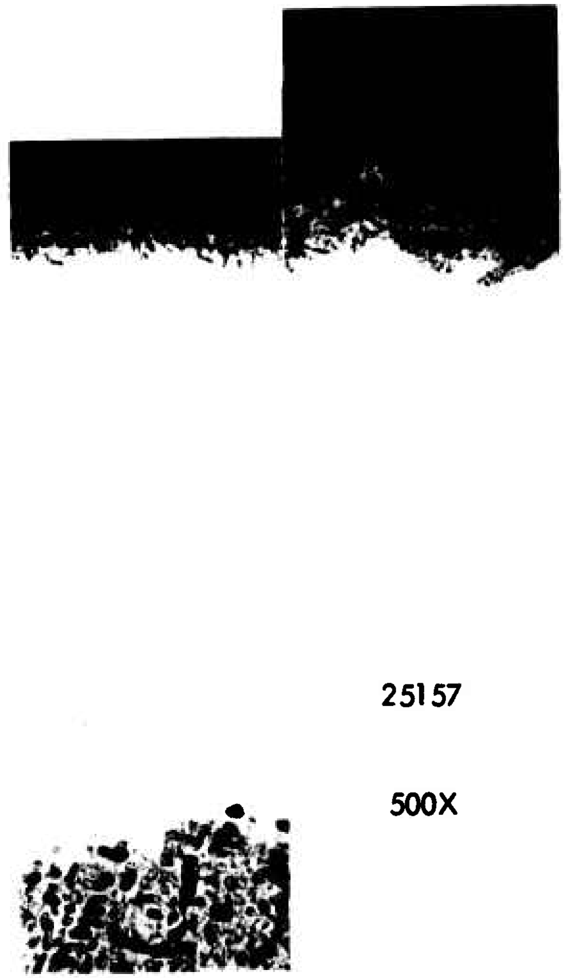

25157

500X

(ETCHED)

ALLOY 12

7 HOURS
1200°C
AIR

Figure 33. The Effect of a 7 Hour Oxidation Exposure in Air on Alloy 12 (Nb-40NbCr$_2$-10Cr) at 75X and 500X.

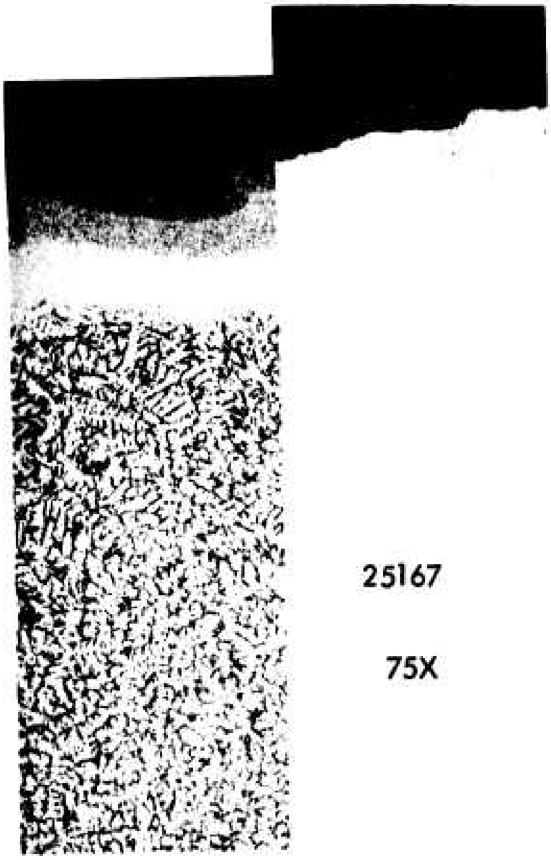

25167

75X

(ETCHED)

25167

500X

(ETCHED)

ALLOY 31

7 HOURS
1200°C
AIR

Figure 34. The Effect of a 7 Hour Oxidation Exposure in Air on Alloy 31 (Nb-9.8Al-18.8Cr-14.7Co-1.96Y_2O_3) at 75X and 500X.

Table 6. Average Vickers Hardness Numbers for the Nb Alloys After Oxidation

Alloy No.	VHN	Alloy No.	VHN
Nb-Fe-Al Alloys		Nb-Cr-Al Alloys	
11-B	814	3-B	514
14-B	850	7-B	798
15-B	847		
15-C	881	Nb-Cr Alloy	
16-B	860	12-B	763
16-C	844		
28-B	831	Nb-Cr-Al-Co Alloy	
29-B	829	31-B	865
Nb-Co-Al Alloys			
13-B	842		
17-B	747		
17-C	846		
18-B	821		
18-C	860		
19-B	717		
19-C	792		
20-A	667		
21-A	336		
22-B	806		
23-A	662		
24-C	779		
24-C	789		
25-A	579		
26-B	809		
27-B	852		
32-B	892		
33-B	860		
34-B	756		
35-B	768		
36-B	747		
37-B	782		

The ASTM index contained no $CoNbO_4$ or $CoNb_2O_4$ cards. These compounds were arc melted from Nb_2O_5 and Co_3O_4 or Co_2O_3, and the diffraction pattern was determined and is presented in Appendix C. The oxide structures determined from the x-ray analysis are categorized below according to the alloy designation. Table 7 gives a brief summary of the compounds formed on the oxides for the alloys. Table 8 gives some observations concerning the visual appearances of these oxides during sampling.

3.3.1 Nb-Cr Alloy

The Nb-Cr alloys 1-5-10-12 had similar oxide structures. Basically, these were a good match to card 20-311, $CrNbO_4$, a tetragonal oxide with $a_o = 4.635$ Å and $c_o = 3.005$ Å. Alloy 5 also showed some α-Al_2O_3, the source of which is not clear unless some Al_2O_3 from the sintering or oxidation supports contaminated the scale. These are Nb-Cr alloys with no Al addition.

The oxide formed on alloy 12 exhibited only the $CrNbO_4$ structure. However, alloy 1-A and 1-B and 12-A showed additional lines which closely matched a monoclinic NbO_2 (19-859). Alloy 5 showed an especially complex oxide with possible lines for $CrNbO_4$ (20211), NbO_2 (19-859), Cr_2O_3 (6-0504 , and $NbCr_2$ (5-0701). The elemental chromium content of alloys 1, 5, and 12 go from 18.5 to 22.2, to 31.1 weight percent Cr. At 31.1 wt. % Cr, the alloy tends to form the pure $NbCrO_4$ rutile structure. The difference between the alloy with the suffix A and suffix B are that the A alloys have been pressed and sintered while the B alloys have been arc melted. For alloy 12-A, the NbO_2 (19-859) phase is present along with the rutile $NbCrO_4$ while for the arc melted 12-B alloy only the rutile phase is present. For 12-A both Nb and $NbCr_2$ were present in the matrix. For 12-B after arc melting, a homogeneous Nb-Cr alloy was developed, and this difference was reflected in the respective oxide structures. Figure 35 is a photograph of the results of the dispersion x-ray analysis of the oxide removed from sample 12 showing Nb-Cr and a small amount of Fe in the oxide. The source of the iron is unknown.

Table 7. A Summary of the Oxides Formed on the Specific Alloys

	Powder or Diffraction	Compounds in Oxide	Strongest Unindexed Lines
Nb-Fe-Al			
11-A +	P	$NbAlO_4$(14-494); Al_2O_3-$9Nb_2O_5$ (16-545)	1.625
11-B	P	$NbAlO_4$(14-494)	2.92; 2.87
14-B	P	$NbAlO_4$(14-494); a-Fe_2O_3	-
14-B	D	$FeNbO_4$(16-374); a - Fe_2O_3	-
14-C *	D	Al_2O_3-Nb_2O_5(16-545)	2.56; 1.87; 1.74
15-B	P	$NbAlO_4$(14-494); $FeNbO_4$(16-358)	3.32; 2.95; 2.54; 2.49; 1.425
15-C	P	" " " "	2.87; 2.65; 1.665
15-B	D	" " " "	-
16-A	P	-	2.53; 2.33-4; 2.23; 2.19
16-B	P	$NbAlO_4$(14-494)	2.96; 2.86
16-C	P	" "	2.88; 1.67
28-B	D	a-Fe_2O_3	-
29-B	D	a-Fe_2O_3	-
Nb-Co-Al			
13-A	P	$AlNbO_4$(14-494); Al_2O_3-$9Nb_2O_5$(16-545)	2.88; 1.44
13-B	P	" " " " "	3.30; 2.93
17-A	P	Al_2O_3-$9Nb_2O_5$(16-545)	3.65; 2.95; 2.48; 1.725; 1.53; 1.45
17-B	P	$NbAlO_4$(14-494)	3.52; 2.91
17-C	P	" "	3.59; 3.51
18-A	P	-	2.39; 2.32; 2.28; 2.23; 2.17; 1.357
19-A	P	$NbAlO_4$ (14-494)	3.40; 2.93; 2.04; 1.675
19-B	P	-	3.70; 3.51; 2.92
19-C	P	-	3.70; 3.51; 3.39; 2.67; 1.568
20-A	P	Al_2O_3-$9Nb_2O_5$(16-545)	2.95; 2.68; 2.40
21-A	P	" " "	2.95; 2.65-2.70; 2.40
22-A	P	Al_2O_3-$9Nb_2O_5$(16-545); NbO_2(19-859)	2.95; 2.68; 2.40
22-B	P	-	3.67; 3.55; 3.29; 2.79; 2.69; 2.53
23-A	P	Al_2O_3-$9Nb_2O_5$(16-545)	2.95
24-A	P	Al_2O_3-$9Nb_2O_5$(16-545)	2.34; 2.22-3; 2.185
24-B	P	$NbAlO_4$(14-494)	3.65; 3.53; 3.41
24-C	P	" "	-

* After grinding

\+ A denotes pressed and sintered alloy

B denotes arc melted alloy oxidized for 7 hours

C denotes arc melted alloy oxidized for 24 hours

Table 7 (Continued)

	Powder or Diffraction	Compounds in Oxide	Strongest Unindexed Lines
25-A	P	Al_2O_3-$9Nb_2O_5$ (16-545)	2.95; 1.725; 1.705; 1.45
26-B	P	$AlNbO_4$(14-494)	
26-B	D		2.95; 2.87; 2.79; 2.59; 2.56; 2.45; 1.87; 1.45
27-B	P		3.70; 3.51; 3.39; 3.07; 2.91; 1.57
31-B	D		3.28; 2.53; 1.71
32-B	D		2.95; 1.87; 3.57
33-B	D		2.95; 1.87; 3.64; 1.71; 1.53; 1.45
36-B		$NbAlO_4$(14-494); Al_2O_3-$9Nb_2O_5$(16-545)	2.97; 1.73
37-B		" " " " "	2.95; 2.49; 1.45
Nb-Cr-Nb-Cr-Al			
1-A and 1-B	P	$CrNbO_4$(20-311); NbO_2(19-859)	-
5-A		$CrNbO_4$(20-311); NbO_2(19-859); $NbCr_2$(5-0701)	-
5-B		Cr_2O_3(6-0504); $NbCr_2$(5-0701); NbO_2(19-859) and $CrNbO_4$	2.78; 2.085
12-A		$NbCrO_4$(20-311); NbO_2(19-859)	3.67
12-B		$NbCrO_4$(20-311)	-

Table 8. Comments on Oxide Characteristics While Sampling for X-ray Powder Analysis

Sample No.	
13-B	The coating chipped off easily in large pieces.
14-B	Silvery thick coating; large piece broke off easily; Debye Scherrer film with Co/Fe radiation; strip chart traces on flat surface with Co/Fe radiation before and after grinding surface.
15-B	Gray thick coating; large pieces broke off easily; Debye Scherrer film and strip chart trace of flat surface with Co/Fe radiation.
15-C	Silver-gray thick coating; Debyb Scherrer film with Co/Fe radiation.
16-B	Gray thick coating; Debyb Scherrer film with Co/Fe radiation.
16-C	Gray thick coating; chipped off easily; Debye Scherrer film with Co/Fe radiation.
17-B	Purplish-gray coating; difficult to remove; Debyb Scherrer film with Co/Fe radiation.
17-C	A large piece of the bluish colored surface came off easily.
19-B	Dull gray with trace of purple coating; difficult to remove; Debyb
19-C	Dark gray with purple trace; large crack made removal fairly easy; Debyb Scherrer film with Co/Fe radiation.
22-B	The dark gray surface coating was very difficult to chip off.
24-B	The dark purplish-gray surface contained a crack which made removal easy. Without the pre-existing crack, removal would have been difficult.
24-C	The dark gray surface coating was difficult to chip off.

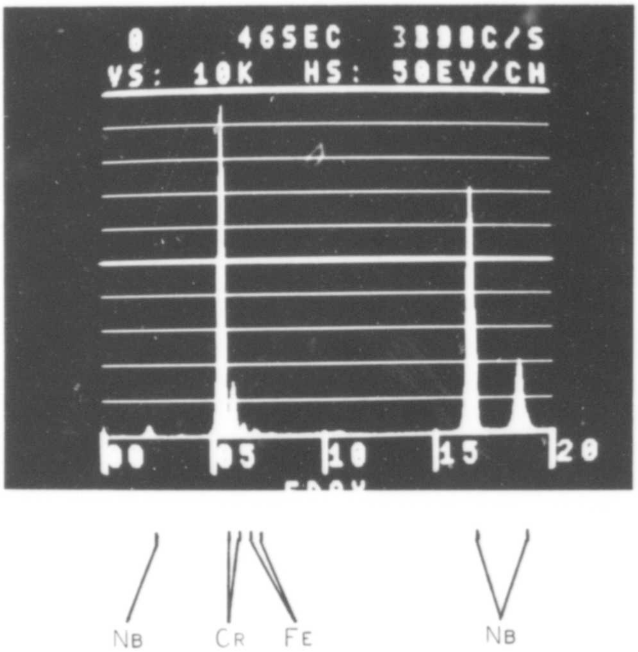

Figure 35. Energy Dispersion X-ray Analysis (EDAX) of the Oxide Formed on Alloy 12-B(Nb-40NbCr$_2$-10Cr).

3.3.2 Nb-Fe-Al Alloy

Alloys 11, 14, 15, 16, 28, and 29 are Nb-Fe-Al alloys. Alloy 11 shows a good correlation to card 14-494 an $AlNbO_4$ rutile structure and the compounds Al_2O_3-$9Nb_2O_5$ and possibly Al_2O_3-$25Nb_2O_5$, card file numbers 16-545 and 16-546, respectively. It is quite similar to the oxide grown on DU-4, the Nb-Fe-Al alloy examined during Phase III. Alloy 16, however, is very difficult to match to any card in the index. This is quite interesting in light of the fact that the iron in alloy 16 is elemental at 15 wt.% and was made by powder techniques, while the iron in alloy 11, at 13.7 wt.%, was alloyed as the $NbFe_2$ intermetallic, and the DU-4 alloy was arc-melted. This indicates that the iron addition as an intermetallic does influence the structure of the oxide formed.

The oxide from alloy 14 is described by the d-spacings listed in column 1 of Table C-6. This column represents powder pattern data taken from the entire oxide cross section. This oxide is predominantly $NbAlO_4$ (14-494) with some α-Fe_2O_3 present. The second column in Table C-6 shows the results of the x-ray diffractometer trace made on the outside surface of the oxide while still intact on the metal surface. This oxide appears to be a mixture of $FeNbO_4$ and α-Fe_3O_4. From the previous program Phase III, the oxide formed on DU-4 alloy was shown by microprobe analysis to have an iron-rich layer of oxide on the surface and then an iron depleted layer further into the oxide with an iron buildup in the metal matrix just below the oxide metal interface. The surface after grinding ($\approx$20 mils) gives the structure, shown in the third column which is difficult to analyze, fitting none of the ASTM cards for the Nb-Fe-O-Al systems. However, some comments should be made about the strip chart traces. The lack of a sufficiently large flat surface area introduces two difficulties. First, if the surface area does not contain the entire beam, then the signal-to-noise ratio will be decreased. Second, it is difficult to accurately align a small flat surface in the diffractometer. This causes a decrease in the signal-to-noise ratio and a shift in the positions of the Bragg

* See Appendix C.

reflection peaks. If the flat surface on your samples were larger (e.g., not cut in half) we should be able to obtain accurately positioned Bragg reflection peaks with higher signal-to-noise ratios.

The peaks being compared for alloy 14 should, however, be relatively oriented to each other since they were taken from the same surface. These results do show a gross difference between the outer oxide structure and the oxide below the surface.

The oxide from alloy 15 was shown to be composed of $NbAlO_4$ (14-494) and $FeNbO_4$ (16-358) (orthorhombic). The oxide grown on alloy 16 is difficult to identify. Some $NbAlO_4$ (14-494) can be identified in the scales. Alloy 15-C and 16-C have been oxidized for 24 hours. The oxides are quite similar to the 15-B and 16-B which were grown on the same alloy for only 7 hours. Both of these alloys exhibited increased oxidation resistance as the oxidation time increased, and it appears that the oxide associated with the 15-C and 16-C alloys is more protective.

Alloys 28 and 29 are alloy 14 with Y, and Y_2O_3, respectively, added to the system. The defractometer scan of the surface indicates the formation of α-Fe_2O_3 (13-534) at the oxide surface as the predominant oxide constituent.

Figures 36 through 39 give the results of the EDAX analysis on the Nb-Fe-Al alloys. A slight amount of Cr and Co appear in the oxide of alloy 11 (Figure 36) and a small amount of Ti (Figure 37) appears in the oxide of alloy 15. The alloy with Y added (alloy 28) exhibits Y in the oxide. However, no Y was observed for alloy 29 in which Y_2O_3 was added. This indicates that possibly the Y_2O_3 is remaining in the metal matrix.

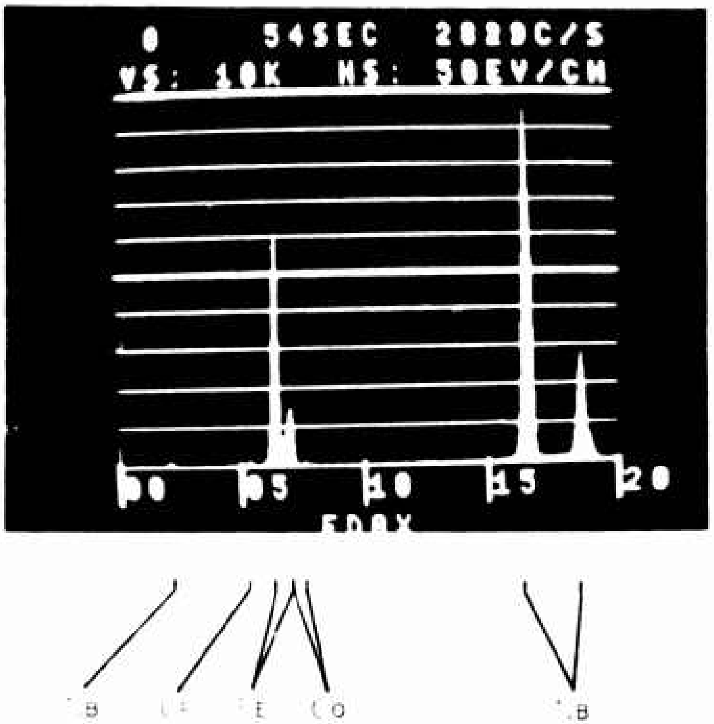

(a) ALLOY 11-B

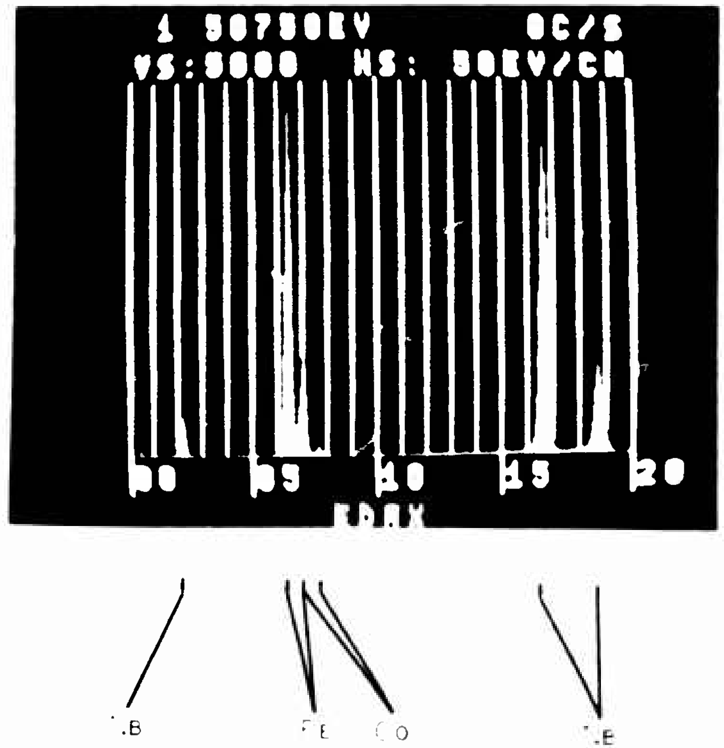

(b) ALLOY 14-B

Figure 36. Energy Dispersion X-ray Analysis (EDAX) of the Oxide Formed on (a) Alloy 11 (Nb-25$NbAl_3$-25$NbFe_2$) and on (b) Alloy 14 (Nb-10Al-30$NbFe_2$).

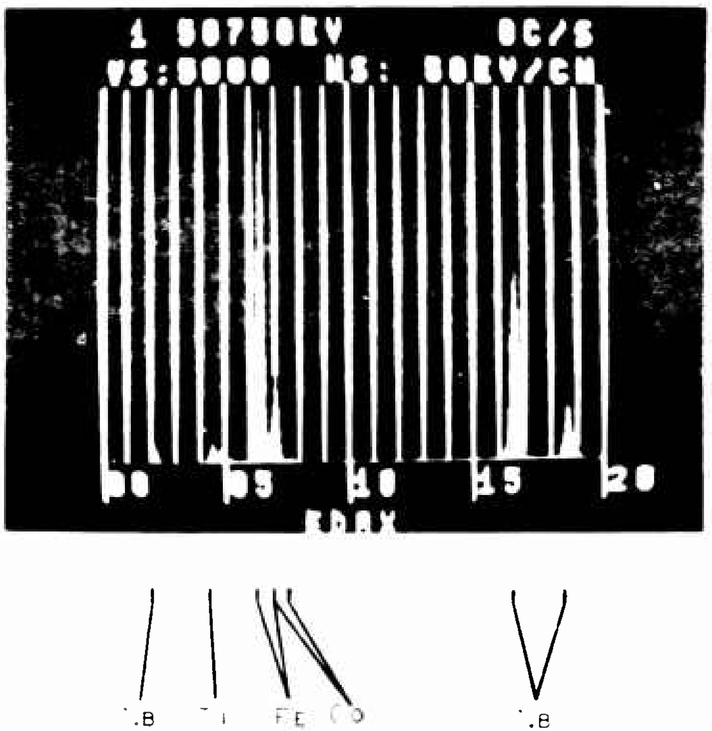

(a) ALLOY 15 - 7 hours at 1200°C in air.

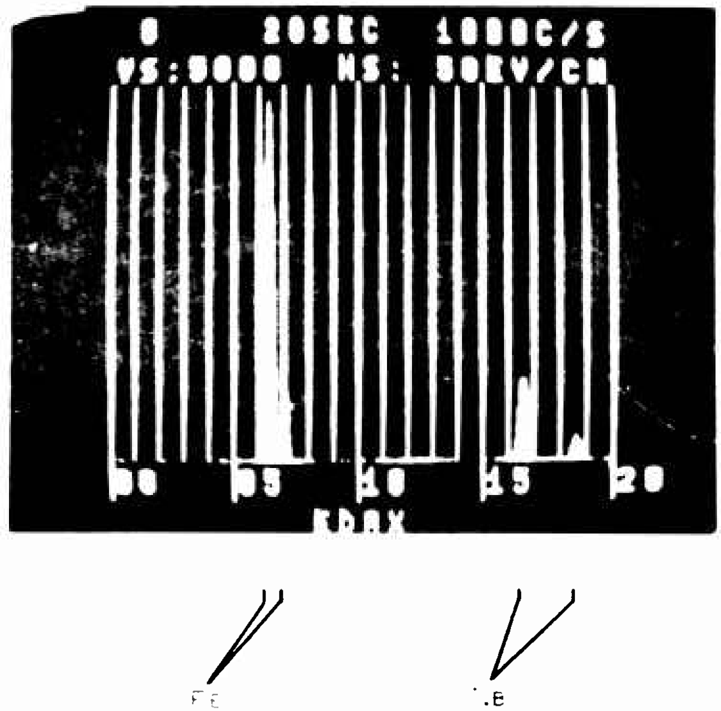

(b) ALLOY 15 - 24 hours at 1200°C in air.

Figure 37. Energy Dispersion X-ray Analysis (EDAX) of the Oxide Formed on Alloy 15 (Nb-10Al-30Fe) after 7 and 24 Hours Exposure to Air at 1200°C.

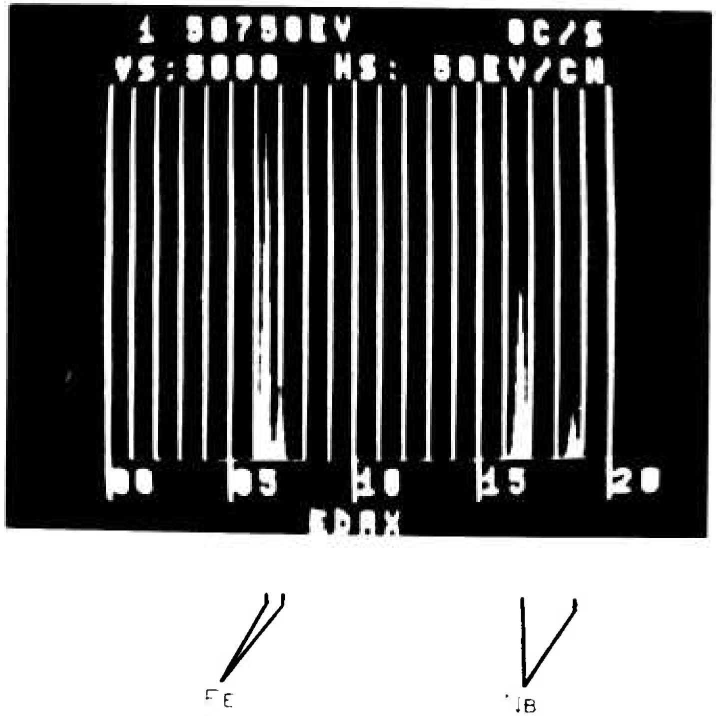

(a) Alloy 16 - 7 hours at 1200°C in air.

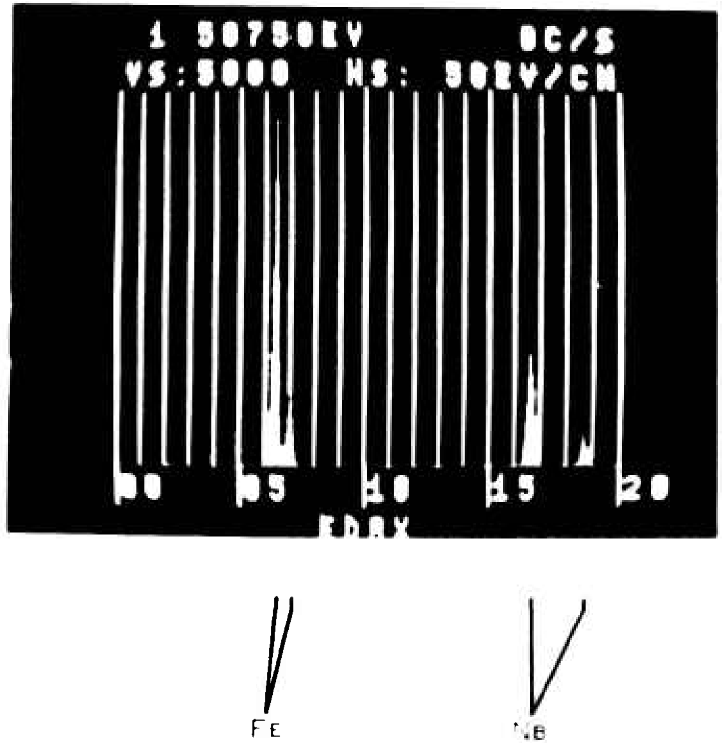

(b) ALLOY 16 - 24 hours at 1200°C in air.

Figure 38. Energy Dispersion X-ray Analysis (EDAX) of the Oxide formed on Alloy 16 (Nb-25NbAl$_3$-15Fe) after 7 and 24 Hours Exposure to Air at 1200°C.

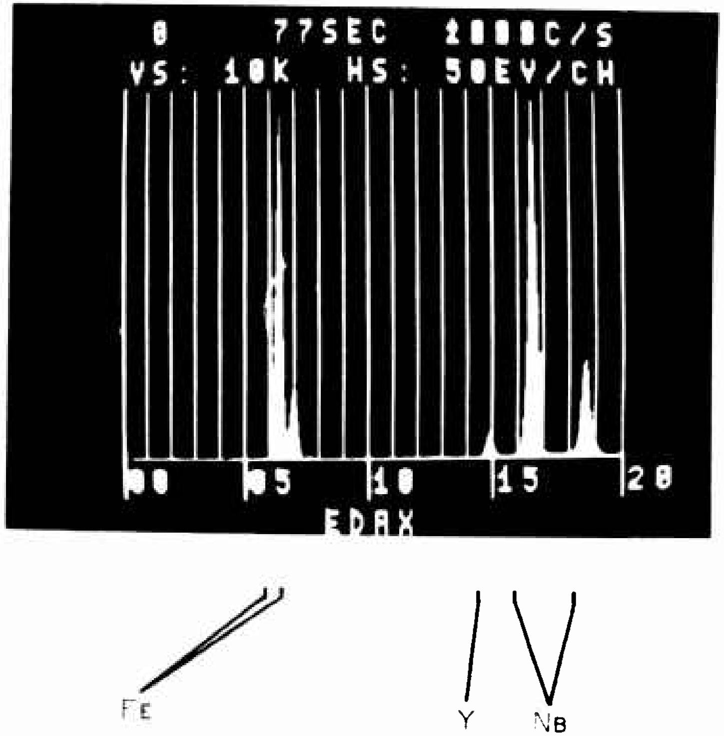

(a) ALLOY 28 (Y)

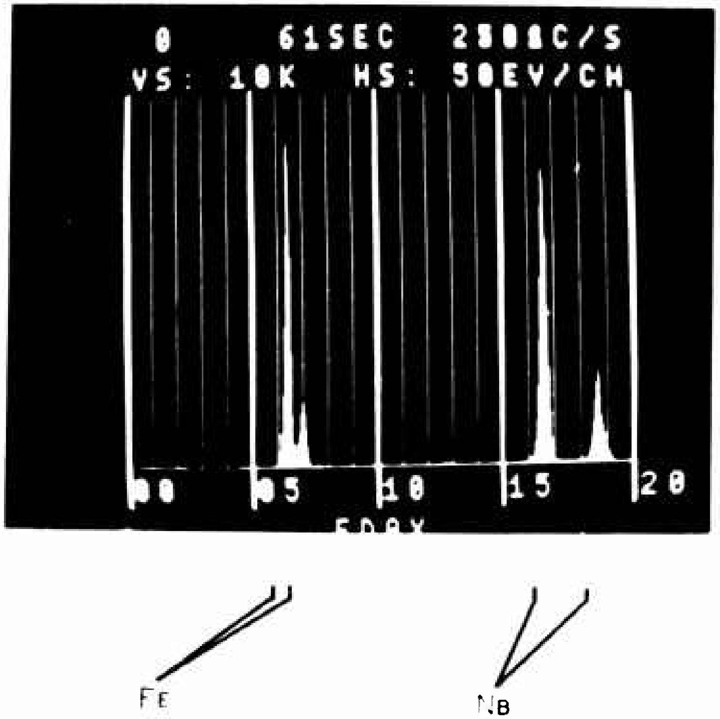

(b) ALLOY 29 (Y_2O_3)

Figure 39. Energy Dispersion X-ray Analysis (EDAX) of the Oxide Formed on Alloy 14 (Nb-30NbFe$_2$-10Al) with (a) Y (Alloy 28) and (b) Y_2O_3 (Alloy 29).

Although $NbAlO_4$ is identified by diffraction analysis, the EDAX photographs show no Al in the oxide. Presumably, this is because Al is an extremely light element and cannot be expected to be shown.

3.3.3 Nb-Co-Al Alloy

Alloys 13 and 17 through 27 and 32 through 37 are Nb-Co-Al alloys. The scales formed on these alloys are difficult to characterize. All appear to have a rutile type oxide structure. Some of the x-ray films do match $AlNbO_4$ (14-494). None of the patterns match the $Nb_2Co_4O_9$ (hemitite) (13-494). There is no card for the columbite Nb_2CoO_6 or the rutile $NbCoO_4$ both possible structures in this system[5]. These samples have been prepared, and the x-ray analysis of these results is shown in Appendix C.

All of these Nb-Co-Al alloys show the Al_2O_3-$9Nb_2O_5$ and Al_2O_3-$25Nb_2O_5$ structures except 18 and 25. A 2.95 d Å line becomes increasingly strong as one goes from alloys 19 → (24, 13) → (20, 22, 23) → 21 → 17 → 25. This sequence also shows a higher cobalt or cobalt/aluminum ratio as one progresses from 19 to 25. Alloy 17 has 15 wt.% elemental cobalt, alloy 21 has 8.4 wt.% cobalt to 1.9 wt.% Al, and alloy 25 has a 16.8 wt.% Co to 4.4 wt.% Al. From this trend, the assumption that the 2.95 d Å line is from a $NbCoO_4$ rutile or Nb_2CoO_6 columbite is quite reasonable. In fact, a fairly close match of some of the lines in the Nb-Co-Al alloys can be made against a columbite structure of Nb-Ni-O, (15-159). The x-ray analysis of the $NbCoO_4$ oxide and the Nb_2CoO_6 oxide do show strong lines at several d spacings between 2.90 to 2.95.

The composition of the oxide scales as determined by EDAX is shown in Figure 40 through 46 for the Nb-Co-Al alloys. These analysis indicate that all of the elements in alloys are present in the scale although the Al peak is quite low.

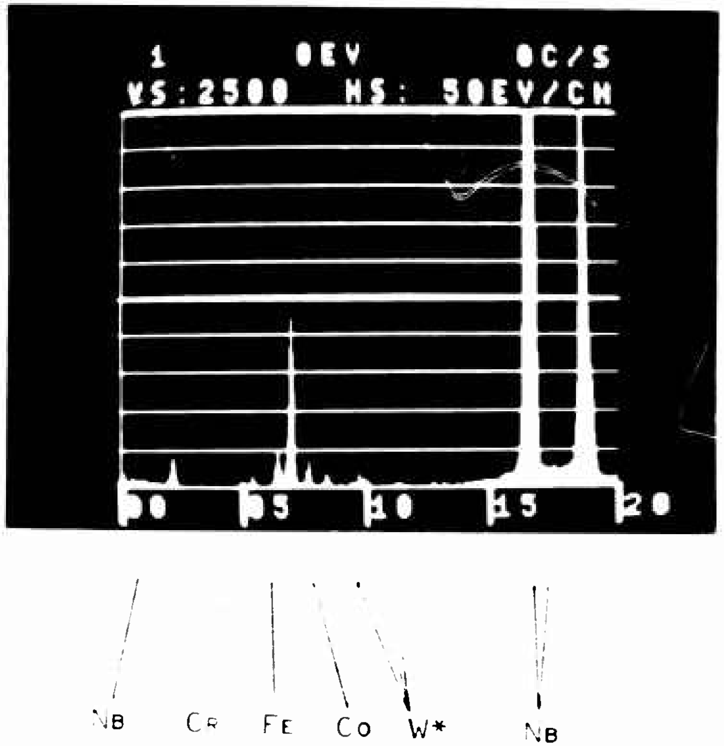

(a) ALLOY 13

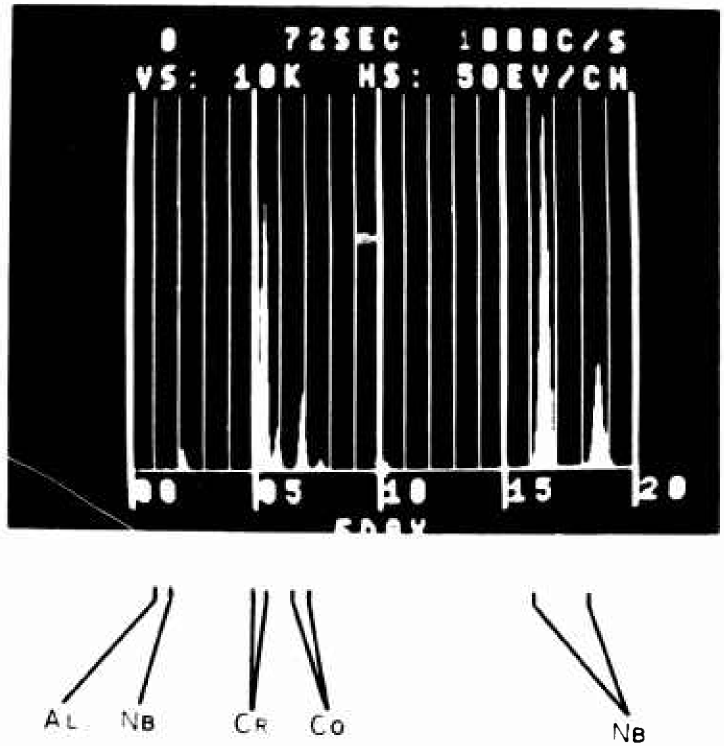

(b) ALLOY 31

Figure 40. Energy Dispersion X-ray Analysis (EDAX) of the Oxide Formed on Alloy 31 (Nb-9.8Al-18.6Cr-14.7Co-1.961 $2O_3$) and Alloy 13 (Nb-25$NbAl_3$-10Co).

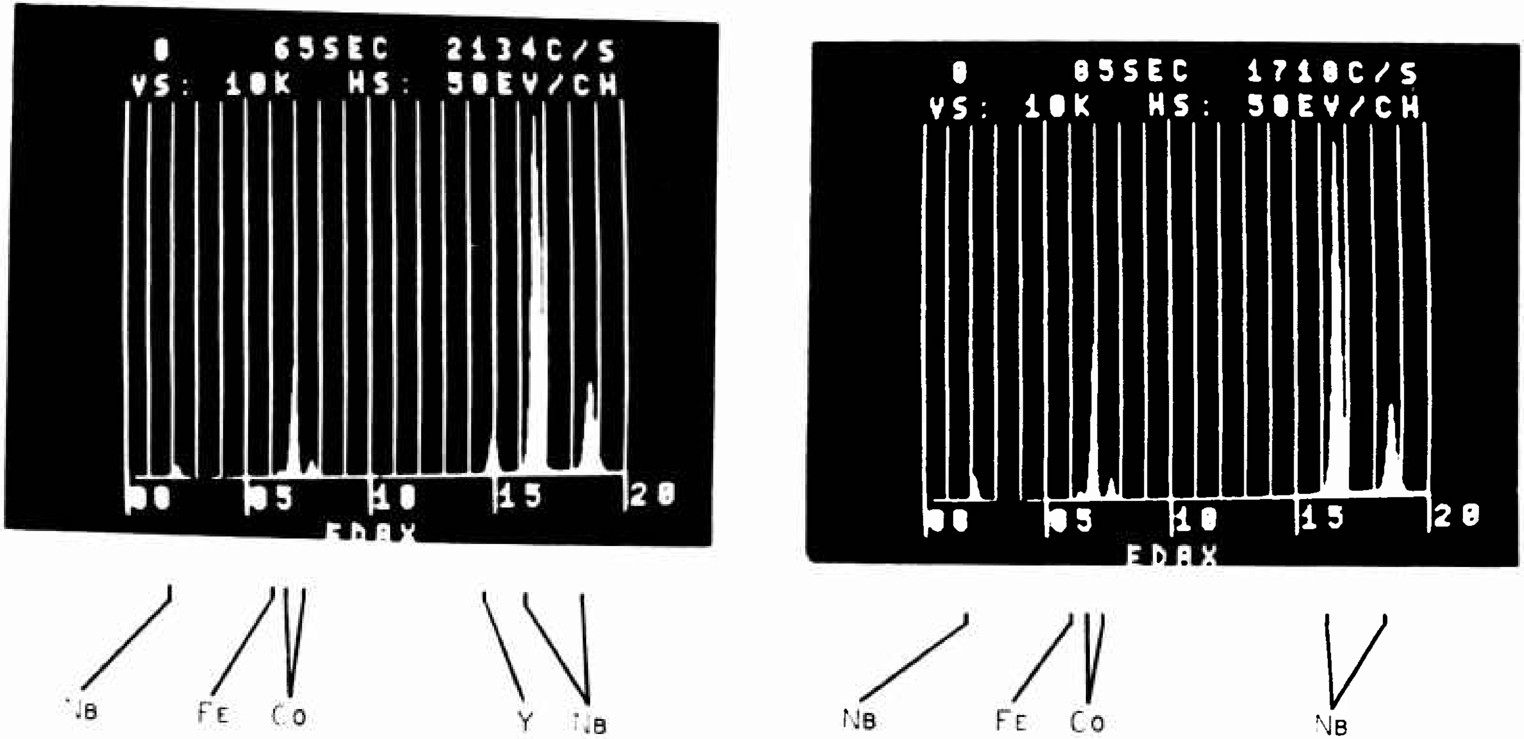

(a) ALLOY 26 (Y)

(b) ALLOY 27 (Y_2O_3)

Figure 41. Energy Dispersion X-ray Analysis (EDAX) of the Oxide Formed on Alloy 13 (Nb-25NbAl$_3$-10Co) with (a) Y (Alloy 26) and (b) Y_2O_3 (Alloy 27).

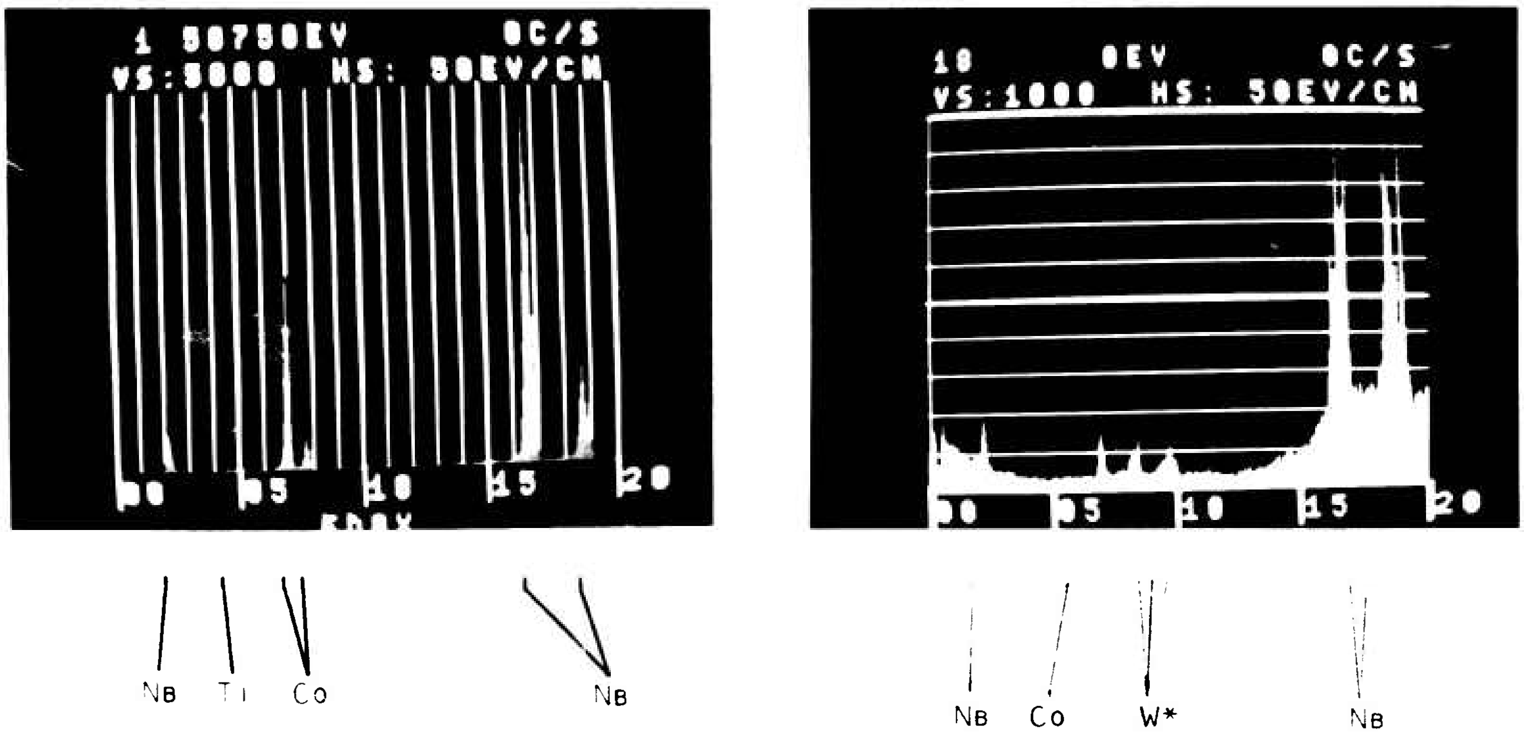

*W - EXCITATION ENERGY

(a) ALLOY 17 - 7 hours at 1200°C in air.

(b) ALLOY 17 - 24 hours at 1200°C in air.

Figure 42. Energy Dispersion X-ray Analysis (EDAX) of the Oxide Formed on Alloy 17 (Nb-15Al-15Co) after 7 and 24 Hours Exposure to Air at 1200°C.

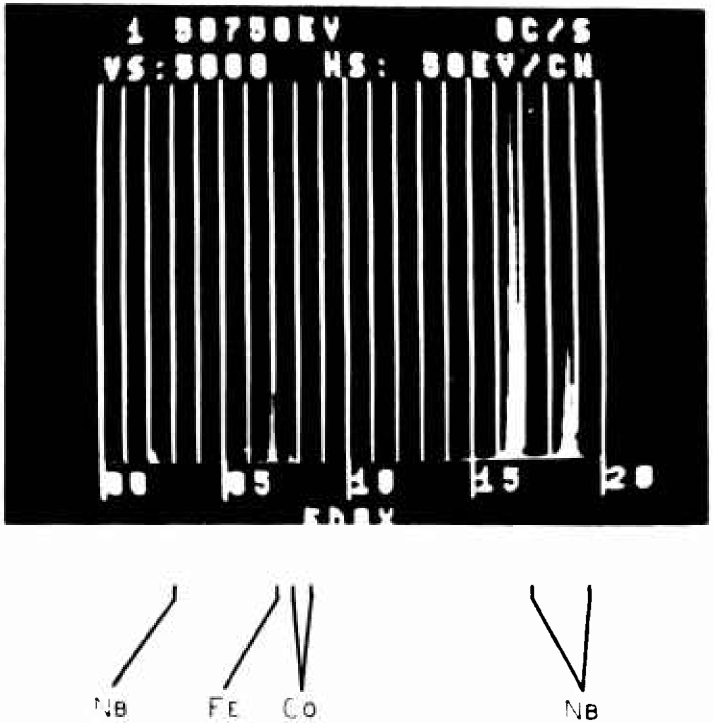

(a) ALLOY 19 - 7 hours at 1200°C in air.

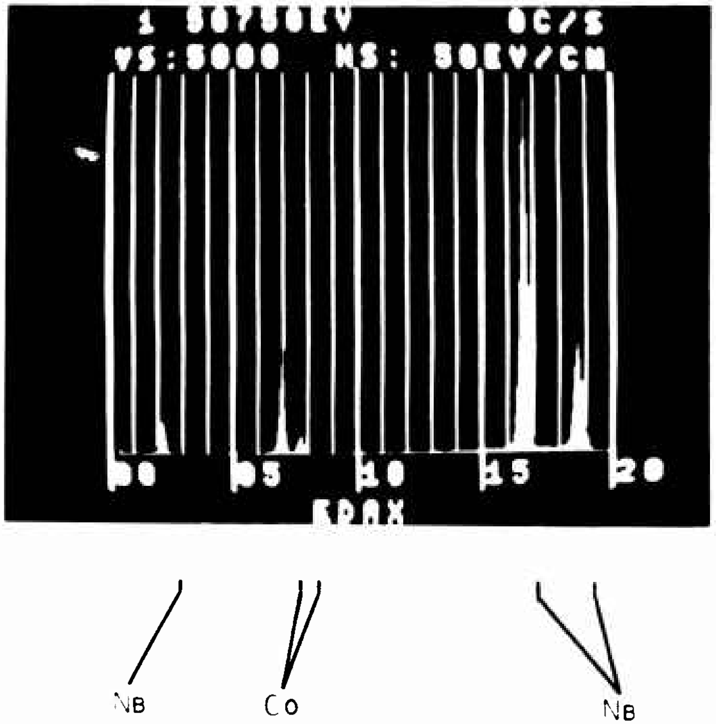

(b) ALLOY 19 - 24 hours at 1200°C in air.

Figure 43. Energy Dispersion X-ray Analysis (EDAX) of the Oxide Formed on Alloy 19 (Nb-10Al-20 NbCo_2) after 7 and 24 Hours Exposure to Air at 1200°C.

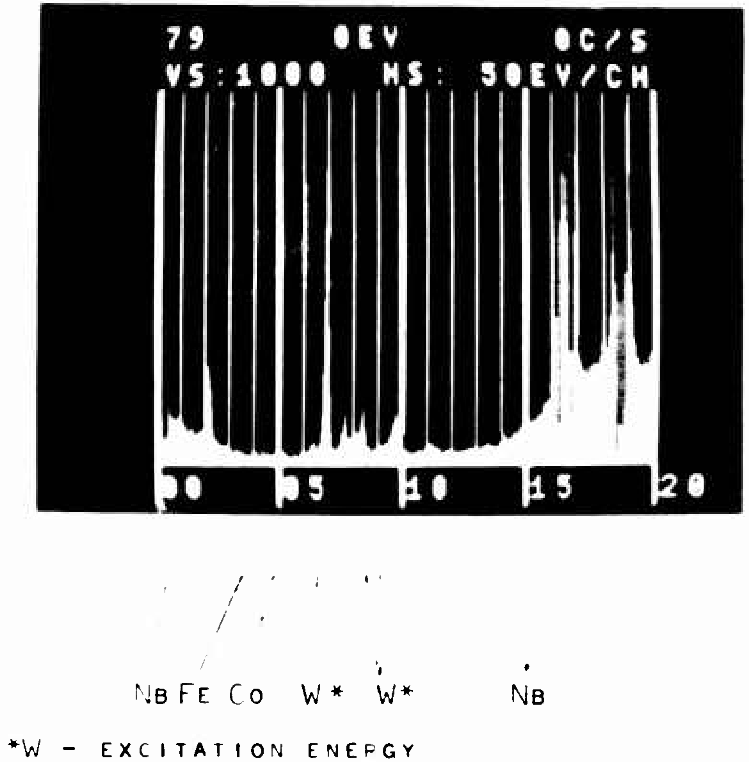

(a) ALLOY 24 - 7 hours at 1200°C in air.

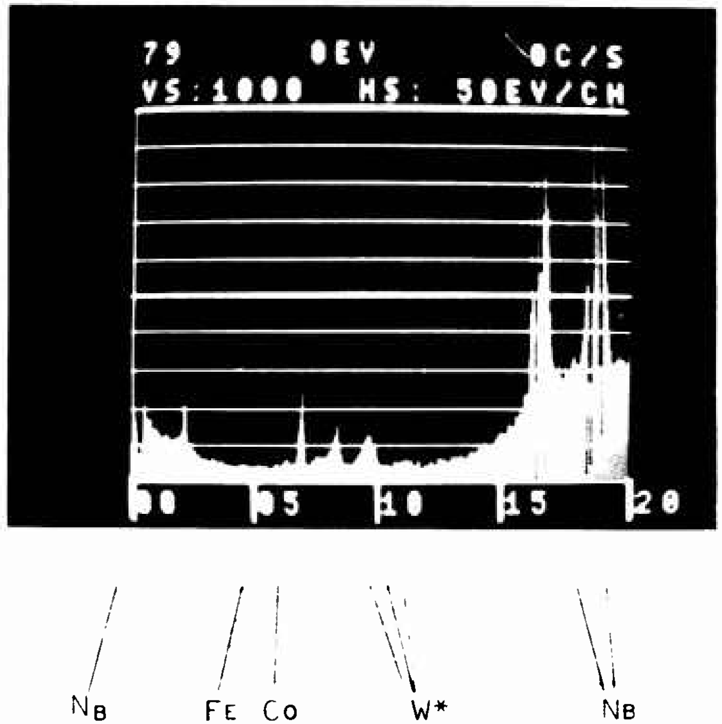

(b) ALLOY 24 - 24 hours at 1200°C in air.

Figure 44. Energy Dispersion X-ray Analysis (EDAX) of the Oxide Formed on Alloy 24 ($Nb-30NbAl_3-10NbCo_2$) after 7 and 24 Hours Exposure to Air at 1200°C.

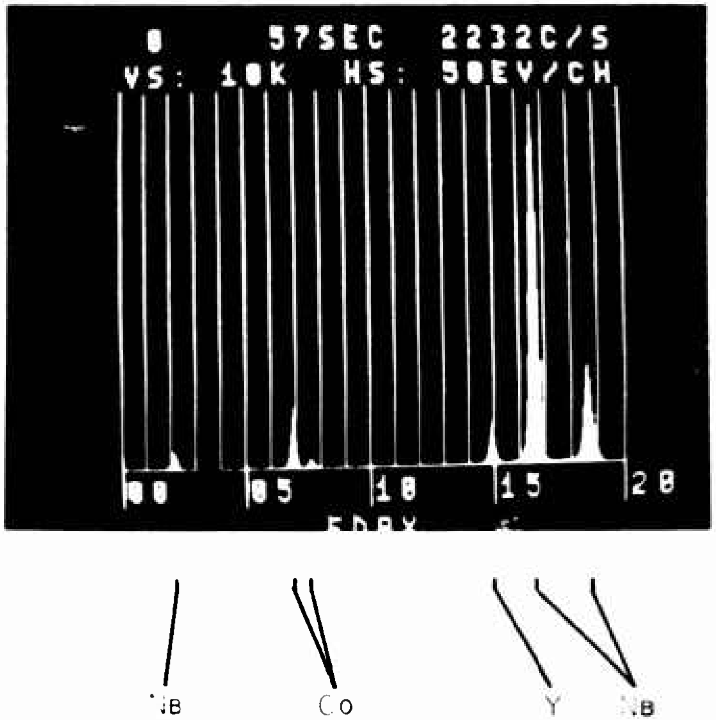

(a) ALLOY 32 (Y)

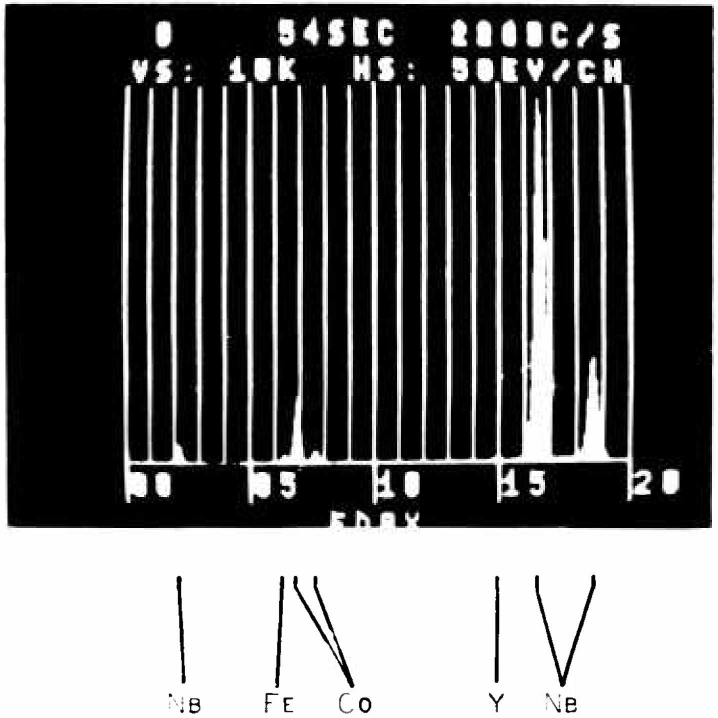

(b) ALLOY 37 (Y_2O_3)

Figure 45. Energy Dispersion X-ray Analysis (EDAX) of the Oxide Formed on (a) Alloy 17 (Nb-15Al-15Co) with Y (Alloy 32) and (b) Alloy 24 (Nb-30NbAl$_3$-10NbCo) with Y_2O_3 (Alloy 30)

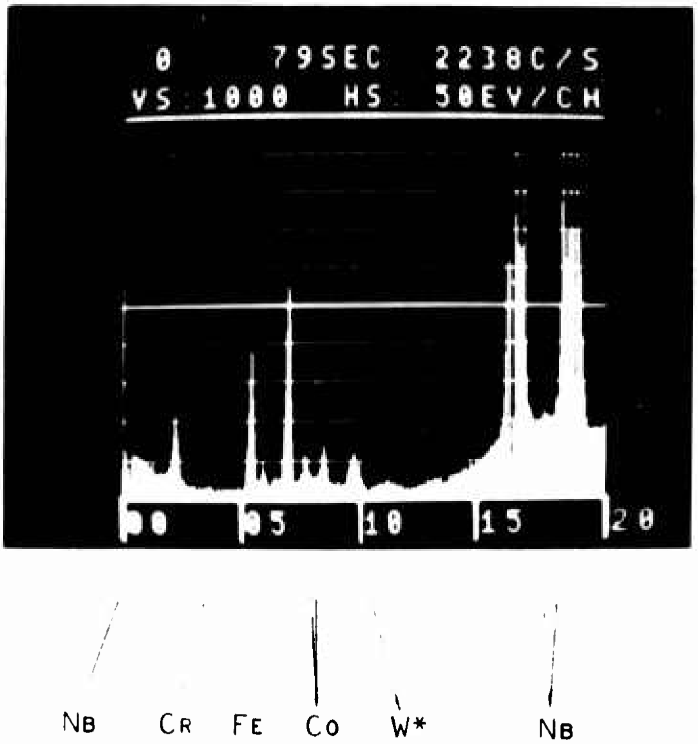

* Tungsten Excitation

Figure 46. Energy Dispersion X-ray Analysis (EDAX) of the Oxide Formed on Alloy 22 ($Nb-10NbCr_2-15NbAl_3-15NbCo_2$)

Table C-14 presents the diffraction results for the oxides formed on alloy 24 in the pressed and sintered state as well as for the arc-melted alloy oxidized for 420 and 1410 minutes. Definite differences are apparent for each oxide. Noted by an asterisk on the table are the lines that match the rutile $NbAlO_4$ oxide structure. The oxide seems to reach a more stable structure and becomes the predominant oxide as the oxidation time increases. The oxide of 24-B does not give the definite strong $NbAlO_4$ pattern. Although it is close to this pattern, a strong 3.53 line on 24-B apparently shifts to a strong 3.56 line on 24-C. The medium intensity 3.65 line on 24-B disappears on 24-C. A 2.68 medium line on 24-C does not appear on 24-B. Sample 24-A meanwhile has a strong 2.34 line and definite lines at 2.49 - 2.54, 2.41, and 2.22 - 2.23. These lines seem to indicate Al-Nb compounds such as 12-85 ($AlNb_3$), 14-458 (AlNb), 15-598 ($AlNb_2$), and 13-146 ($AlNb_3$). The compounds are feasible due to the mixing of $NbAl_3$ and Nb during the sintering process for 24-A. The conclusion drawn from these results is that a definite time period is required to form a protective oxide structure on some of the alloys.

Alloy 17 (Table C-9) is another alloy for which x-ray results of the oxide formed during a 7 hour and 24 hour oxidation exposure have been determined. The same conclusion can be reached as indicated above for alloy 24. The $NbAlO_4$ structure appears to stabilize as time at temperature increases. Again, there is a distinctly different oxide formed in the pressed and sintered sample when compared with the arc-melted sample. The compound Al_2O_3-$9Nb_2O_5$ appears as one of the components in the oxide on the pressed and sintered sample.

The d-spacings are presented in Tables C-13 and C-5 for alloys 22 and 13, respectively. Both of these samples cannot be positively indexed, although Al_2O_3-$9Nb_2O_5$ is present in the oxide formed on the pressed and sintered sample for alloy 22.

Alloy 18 gives an oxide whose structure is distinctly different from the other oxides. Alloys 20, 21, and 22 gives a similar oxide structure in the as-pressed and sintered configuration. Mostly, the compound Al_2O_3-$9Nb_2O_5$ is formed. The oxides on the Nb-Co-Al alloys with Y and Y_2O_3 added have been examined using the diffraction technique while the oxide is still on the sample. With the exception of alloys 36 and 37 and 26, it is not possible to determine the constituents of the oxides. The oxides for 26, 36, and 37 do contain $AlNbO_4$ (14-494) as the predominant oxide species.

Again some of the lines obtained for $CoNbO_4$ and $CoNb_2O_6$ appear to match some of the lines which cannot be positively identified as being associated with a given species listed in the ASTM card index.

4.0 DISCUSSION OF RESULTS

Figures 47 and 48 are ternary phase "maps" of the composition investigated. The oxidation behavior is also a definite function of alloy composition and good and bad behavior is denoted by an "iso-oxidation" line on each figure. If one examines the oxide phases listed in Table 7 in light of the compositions plotted in Figures 47 and 48 in most cases the rutile oxides $NbAlO_4$ and $FeNbO_4$ are associated with the alloys with the slowest oxidation rates. On the other hand, the alloys which exhibit the poorest oxidation performance contain Al_2O_3-$9Nb_2O_5$ type oxides. In the case of the best Nb-Cr alloy, the rutile phase $CrNbO_4$ was associated with alloys with good oxidation performance. These results confirm the findings of the Phase III program. However, it is very difficult to locate and analyze the oxide scales to determine if any spinel-type compounds are present.

Within the context of several summaries of the state-of-the-art of our understanding of the oxidation behavior of niobium alloys in a paper by Prof. Stringer at the AGARD Specialists meeting[4] and in an article by Kofstad[5], a more detailed understanding of the mechanisms of oxidation of Nb alloys is required. Throughout this present program; i.e., Phase I to Phase IV, we have attempted to provide an understanding of the oxidation behavior by attempting to characterize the scales formed on alloys previously reported to possess good oxidation behavior with little regard to the other alloy properties such as strength and ductility. In taking this approach, we have established the role the rutile structures play in the formation of a protective oxide on these alloys. The question still remains, "is there some other oxide layer or intermetallic layer which is rate controlling, or have we sufficiently lowered the melting point or increased the plasticity of the scales formed on these oxides and only increased the oxide structural integrity"? The Nb-Al-V system and the Nb-Ti-W both studied by Wlodek [6, 7] gave good oxidation performance based on the formation or stabilization of the NbO structure. However, these best alloys had parabolic oxidation

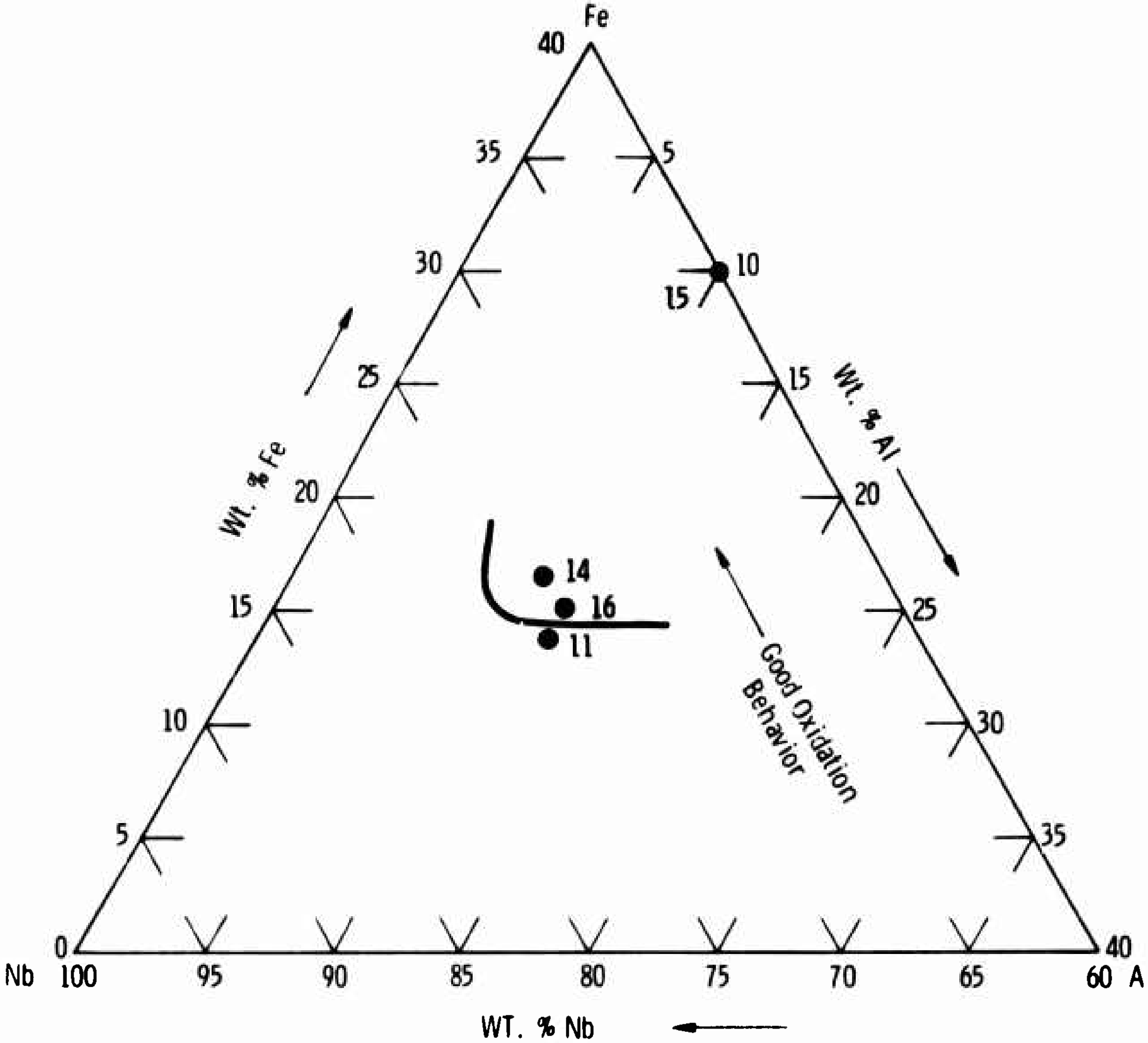

TERNARY MAP Nb-Fe-Al SYSTEM

Figure 47. Ternary Plot of Elemental Compositions Showing the Region Where Parabolic Oxidation Constant (k_p) Being Less than or Greater than 1.0 $(mg/cm^2)^2/min$.

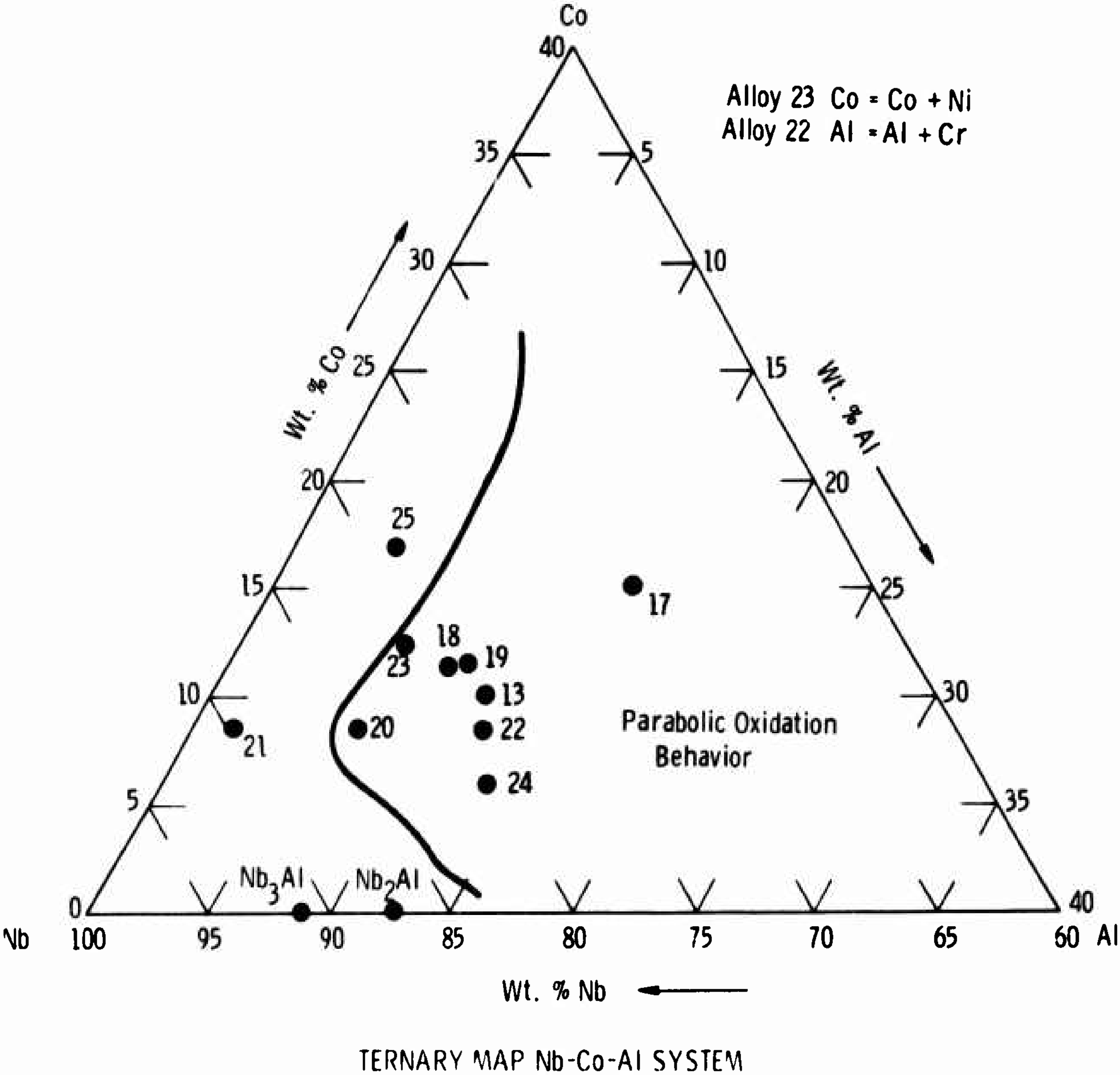

Figure 48. Ternary Plot of Elemental Compositions Showing Regions of Parabolic and Linear Oxidation in the Nb-Co-Al System

constants of the order of 17.6 $(mg/cm^2)^2$/min at 1200°C or a metal consumption rate of ~35 mils/100 hours compared with the metal consumption rates measured in this program of 3.0 to 6 mils/100 hours.

Rapp and Goldberg[8] have suggested that rhenium, a noble metal, when added to a Nb-Zr alloy, tended to accumulate in the metal below the oxide metal interface. Microprobe results determined during Phase III of this progran do, in fact, show that Co, Ni, and Fe do accumulate in the metal substrate just below oxide metal interface. The accumulation of the more noble metals could decrease the chemical potential of the niobium. In alloys containing Al, Al_2O_3 formed by internal oxidation could react with the accumulated noble metal to form BAl_2O_4 spinels at the oxide metal interface. A lack of adequate phase information for the alloys and oxides make the detailed development of mechanisms extremely difficult.

The oxygen transport studies initiated during the program have indicated that some oxides, such as the rutile $CrNbO_4$, has a slower rate of oxygen transport through the oxides than $AlNbO_4$. Yet it has been shown in this study that $AlNbO_4$ is associated with the improved oxidation performance of the Nb-Fe-Al and Nb-Co-Al alloys, and these alloys show the same low oxidation as the NbCr alloys without the associated internal oxidation.

The best alloys examined during this program based on the oxidation behavior and metal contamination are summarized in Table 9. Alloy 15 gives a 4.3 mils/24 hours to metal loss and metal affected zone; alloy 16 gives 2.33 mils/24 hours; alloy 17 gives 2.45 mils/24 hours; alloy 24 gives 2.53 mils/24 hours; and alloy 19 gives 4.2 mils/24 hours all calculated at 1200°C oxidation temperature. Therefore, alloys 15, 16, and 24 are the best alloys based on minimizing the overall detrimental effects of oxygen on the alloy.

Table 9. Comparison of Depth of Metal Affected Zone and Oxidation Kinetics of the Most Promising Alloys

Alloy	Metal Affected Zone Depth (μ)	Metal Affected Zone Depth (mils)	Time (hrs)	Parabolic Constant $mg^2/cm^4/min$	Metal Consumption mils/ 24 hrs.*
15	60 90	2.36 3.54	7 24	0.042	0.76
16	19 20	0.75 0.79	7 24	0.17	1.54
17	18 25	0.71 1.0	7 24	0.15	1.45
24	6 16	0.2 0.63	7 24	0.26	1.9
19	22 40	0.87 1.6	7 24	0.47	2.6
22	30	1.2	7	0.30	2.1
14	30	1.2	7	0.24	1.8

*Based on metal consumption during oxidation.

5.0 CONCLUSIONS

1. Nb-Co-Al and Nb-Fe-Al alloys give improved oxidation behavior

73.4Nb-15Fe-11.6Al	$k_p = 0.17$	3.3 mils/100 hrs.	1200°C
60Nb-30Fe-10Al	$k_p = 0.043$	1.6 mils/100 hrs.	1200°C
80.5 Nb-5.6Co-13.9Al	$k_p = 0.26$	4.1 mils/100 hrs.	1200°C

2. Long time oxidation tests (approximately 24 hours) are required to form the most protective scale on these alloys.

3. Oxygen diffusion rate measurements on Co_3O_4-Nb_2O_5 indicate a complex temperature-oxygen partial pressure-oxide phase equilibrium relationship.

4. The buildup of Co and/or Fe in the metal at the oxide-metal interface contribute to the decreased oxygen penetration into the base metal.

5. $NbAlO_4$, $NbCrO_4$, and $NbFeO_4$ rutile-type oxides are responsible for the improved oxidation behavior of these alloys.

6.0 REFERENCES

1. Svedberg, R. C., "Modification and Control of Oxide Structures on Metals and Alloys", WANL-PR(XXX)-001, April 1971.

2. Svedberg, R. C., "Modification and Control of Oxide Structures on Metals and Alloys (II)", WANL-FR-M-72-003, May 1972.

3. Svedberg, R. C., "Modification and Control of Oxide Structures on Metals and Alloys (III)", WANL-FR-M-73-003, February 1973.

4. Strunger, J., R. I. Jaffee, and T. F. Kearns", AGARD Conf. Proceedings No. 120, "High Temperature Corrosion of Aerospace Alloys", March 1973.

5. Promisel, N. E., (Ed.), The Science and Technology of Tungsten, Tantalum, Molybdenum, Niobium, and Their Alloys, Pergamon, N.Y., 1964, p 247.

6. Wlodek, S. T., AIME Met. Soc. Conference on Columbium Metallurgy, Vol. 10, 1961, p 175.

7. Wlodek, S. T., AIME Met. Soc. Conference on Columbium Metallurgy, Vol. 10, 1961, p 553.

8. Rapp, R. A. and G. N. Goldberg, Trans. AIME, Vol. 236, 1966, p 1619.

APPENDIX A

AIR OXIDATION WEIGHT GAIN DATA

3-B

TIME-MIN	WT-LOSS	WT-LOSS/AREA	(WT-LOSS/AREA)-SQR	
1.	.3	.2	.03	1
2.	2.8	1.6	2.50	2
3.	5.8	3.3	10.74	3
4.	6.1	3.4	11.88	4
5.	5.8	3.3	10.74	5
10.	7.3	4.1	17.01	6
15.	9.8	5.5	30.66	7
20.	13.0	7.3	53.94	8
25.	14.8	8.4	69.92	9
30.	17.1	9.7	93.34	10
40.	21.1	11.9	142.11	11
50.	25.3	14.3	204.31	12
60.	29.3	16.6	274.02	13
90.	43.5	24.6	603.99	14
120.	59.4	33.6	1126.23	15
150.	76.8	43.4	1882.68	16
180.	96.1	54.3	2947.82	17
210.	114.5	64.7	4184.70	18
240.	134.3	75.9	5757.12	19
270.	154.3	87.2	7599.51	20
300.	175.3	99.0	9808.83	21
330.	197.3	111.5	12425.32	22
360.	218.3	123.3	15211.11	23

7-B

TIME-MIN	WT-LOSS	WT-LOSS/AREA	(WT-LOSS/AREA)-SQR	
1.	.0	.0	.00	1
2.	3.5	1.9	3.70	2
3.	7.0	3.8	14.79	3
4.	7.5	4.1	16.98	4
5.	8.0	4.4	19.32	5
10.	10.0	5.5	30.19	6
15.	12.5	6.9	47.17	7
20.	15.2	8.4	69.75	8
25.	17.0	9.3	87.25	9
30.	18.5	10.2	103.32	10
40.	23.0	12.6	159.70	11
50.	26.5	14.6	212.01	12
60.	30.0	16.5	271.71	13
90.	40.0	22.0	483.03	14
120.	48.0	26.4	695.57	15
150.	55.8	30.7	940.00	16
180.	62.0	34.1	1160.49	17
210.	68.0	37.4	1395.97	18
240.	73.0	40.1	1608.60	19
270.	77.5	42.6	1813.26	20
300.	82.0	45.1	2029.95	21
330.	86.0	47.3	2232.82	22
360.	90.0	49.5	2445.36	23
390.	93.5	51.4	2639.25	24

10-A

TIME-MIN	WT-LOSS	WT-LOSS/AREA	(WT-LOSS/AREA)-SQR
1.	1.5	.5	.28
2.	3.0	1.1	1.13
3.	6.0	2.1	4.53
4.	7.0	2.5	6.16
5.	8.5	3.0	9.09
10.	13.5	4.8	22.92
15.	17.5	6.2	38.51
20.	21.7	7.7	59.21
25.	25.0	8.9	78.59
30.	27.5	9.8	95.10
40.	33.0	11.7	136.94
50.	37.0	13.1	172.15
60.	41.5	14.7	216.57
90.	53.0	18.8	353.23
120.	64.0	22.7	515.06
150.	73.0	25.9	670.11
180.	80.0	28.4	804.79

11-A

TIME-MIN	WT-LOSS	WT-LOSS/AREA	(WT-LOSS/AREA)-SQR
1.	1.0	.3	.07
2.	3.0	.8	.62
3.	7.0	1.8	3.36
4.	8.0	2.1	4.39
5.	10.5	2.7	7.56
10.	18.0	4.7	22.20
15.	23.5	6.2	37.85
20.	28.2	7.4	54.50
25.	31.0	8.1	65.86
30.	34.0	8.9	79.22
40.	38.0	9.9	98.96
50.	42.5	11.1	123.78
60.	46.5	12.2	148.18
90.	56.0	14.7	214.91
120.	64.5	16.9	285.10
150.	72.0	18.8	355.25
180.	78.0	20.4	416.93
210.	84.5	22.1	489.31
240.	90.0	23.6	555.08
270.	95.5	25.0	625.00
300.	101.0	26.4	699.06
330.	106.5	27.9	777.27
360.	111.5	29.2	851.97
390.	114.0	29.8	890.60

11-B

TIME-MIN	WT-LOSS	WT-LOSS/AREA	(WT-LOSS/AREA)-SQR	
1.	.0	.0	.00	1
2.	2.5	1.4	2.06	2
3.	6.0	3.4	11.89	3
4.	6.5	3.7	13.95	4
5.	7.5	4.3	18.58	5
10.	11.0	6.3	39.97	6
15.	13.5	7.8	60.20	7
20.	17.1	9.8	96.58	8
25.	18.2	10.5	109.41	9
30.	20.2	11.6	134.77	10
40.	23.0	13.2	174.73	11
50.	25.8	14.8	219.86	12
60.	28.0	16.1	258.95	13
90.	34.8	20.0	400.00	14
120.	39.0	22.4	502.38	15
150.	44.0	25.3	639.45	16
180.	48.2	27.7	767.35	17
210.	52.8	30.3	920.81	18
240.	57.6	33.1	1095.84	19
270.	62.0	35.6	1269.65	20
300.	66.0	37.9	1438.76	21
330.	70.0	40.2	1618.44	22
360.	73.5	42.2	1784.33	23

12-A

TIME-MIN	WT-LOSS	WT-LOSS/AREA	(WT-LOSS/AREA)-SQR
1.	63.0	16.4	267.77
2.	89.5	23.2	540.41
3.	98.5	25.6	654.56
4.	101.0	26.2	688.21
5.	104.5	27.1	736.73
10.	110.5	28.7	823.76
15.	114.0	29.6	876.78
20.	117.7	30.6	934.61
25.	120.0	31.2	971.50
30.	122.0	31.7	1004.15
40.	126.5	32.9	1079.59
50.	131.0	34.0	1157.77
60.	134.5	34.9	1220.46
90.	146.0	37.9	1438.08
120.	158.0	41.0	1684.20
150.	169.5	44.0	1938.29
180.	180.0	46.8	2185.67
210.	188.5	49.0	2397.18
240.	196.5	51.0	2604.98
270.	203.0	52.7	2780.17
300.	209.0	54.3	2946.94
330.	213.0	55.3	3060.82

12-B

TIME-MIN	WT-LOSS	WT-LOSS/AREA	(WT-LOSS/AREA)-SQR	
1.	-1.0	-.6	.31	1
2.	-1.0	-.6	.31	2
3.	1.0	.6	.31	3
4.	1.0	.6	.31	4
5.	.7	.4	.15	5
10.	2.0	1.1	1.25	6
15.	2.7	1.5	2.28	7
20.	4.2	2.3	5.51	8
25.	5.2	2.9	8.44	9
30.	6.0	3.4	11.24	10
40.	6.5	3.6	13.19	11
50.	7.0	3.9	15.29	12
60.	7.5	4.2	17.56	13
90.	9.0	5.0	25.28	14
120.	10.0	5.6	31.21	15
150.	11.5	6.4	41.28	16
180.	12.0	6.7	44.94	17
210.	13.2	7.4	54.38	18
240.	14.0	7.8	61.17	19
270.	15.0	8.4	70.22	20
300.	16.0	8.9	79.90	21
330.	16.3	9.1	82.92	22
360.	16.8	9.4	88.09	23
390.	17.5	9.8	95.58	24
420.	18.0	10.1	101.12	25

13-A

TIME-MIN	WT-LOSS	WT-LOSS/AREA	(WT-LOSS/AREA)-SQR
1.	2.0	.6	.31
2.	5.5	1.5	2.31
3.	8.5	2.3	5.51
4.	10.0	2.8	7.63
5.	11.0	3.0	9.23
10.	14.5	4.0	16.04
15.	17.5	4.8	23.37
20.	20.7	5.7	32.70
25.	23.0	6.4	40.37
30.	24.5	6.8	45.81
40.	27.0	7.5	55.63
50.	30.0	8.3	68.68
60.	32.0	8.8	78.14
90.	38.0	10.5	110.19
120.	43.0	11.9	141.10
150.	48.0	13.3	175.82
180.	52.5	14.5	210.33
210.	57.0	15.7	247.93
240.	61.5	17.0	288.62
270.	66.0	18.2	332.41
300.	69.5	19.2	368.60
330.	73.5	20.3	412.25
360.	78.0	21.5	464.27
390.	81.5	22.5	506.87
420.	84.5	23.3	544.87

14-B

TIME-MIN	WT-LOSS	WT-LOSS/AREA	(WT-LOSS/AREA)-SQR
1.	2.5	.8	.58
2.	3.7	1.1	1.26
3.	6.4	1.9	3.78
4.	6.3	1.9	3.67
5.	6.5	2.0	3.90
10.	8.8	2.7	7.15
15.	10.5	3.2	10.19
20.	13.0	4.0	15.61
25.	14.0	4.3	18.11
30.	14.8	4.5	20.24
40.	16.0	4.9	23.65
50.	17.0	5.2	26.70
60.	18.2	5.5	30.60
90.	20.8	6.3	39.97
120.	22.8	6.9	48.03
150.	25.0	7.6	57.74
180.	27.0	8.2	67.35
210.	28.7	8.7	76.10
240.	30.0	9.1	83.15
270.	31.7	9.6	92.84
300.	33.2	10.1	101.83
330.	14.5	4.4	19.42
360.	35.8	10.9	118.41
390.	36.6	11.1	123.76
420.	38.0	11.6	133.41

15-B

TIME-MIN	WT-LOSS	WT-LOSS/AREA	(WT-LOSS/AREA)-SQR
1.	3.0	.8	.58
2.	4.5	1.1	1.31
3.	7.5	1.9	3.64
4.	7.0	1.8	3.17
5.	7.0	1.8	3.17
10.	8.5	2.2	4.68
15.	9.5	2.4	5.84
20.	11.7	3.0	8.86
25.	12.5	3.2	10.12
30.	13.5	3.4	11.80
40.	15.3	3.9	15.16
50.	16.5	4.2	17.63
60.	18.0	4.6	20.98
90.	20.5	5.2	27.21
120.	22.5	5.7	32.78
150.	24.5	6.2	38.86
180.	26.5	6.7	45.47
210.	28.3	7.2	51.85
240.	29.5	7.5	56.35
270.	31.2	7.9	63.03
300.	32.5	8.3	68.39
330.	33.7	8.6	73.53
360.	35.0	8.9	79.31
390.	36.0	9.2	83.91
420.	37.0	9.4	88.64
450.	37.5	9.5	91.05

15-C

TIME-MIN	WT-LOSS	WT-LOSS/AREA	(WT-LOSS/AREA)-SQR	
1.	1.5	.3	.08	1
2.	2.0	.4	.14	2
3.	3.8	.7	.52	3
4.	3.3	.6	.39	4
5.	3.0	.6	.32	5
10.	3.0	.6	.32	6
15.	3.5	.7	.44	7
20.	5.5	1.0	1.08	8
25.	6.3	1.2	1.42	9
30.	6.8	1.3	1.65	10
40.	7.5	1.4	2.01	11
50.	8.3	1.6	2.46	12
60.	9.3	1.8	3.09	13
90.	11.3	2.1	4.56	14
120.	13.3	2.5	6.32	15
150.	14.3	2.7	7.31	16
180.	15.3	2.9	8.37	17
210.	16.5	3.1	9.73	18
240.	18.0	3.4	11.58	19
270.	18.3	3.5	11.97	20
300.	19.5	3.7	13.59	21
330.	20.3	3.8	14.73	22
360.	21.5	4.1	16.52	23
390.	22.3	4.2	17.77	24
420.	23.3	4.4	19.40	25
450.	23.5	4.4	19.73	26
480.	24.5	4.6	21.45	27
510.	25.3	4.8	22.87	28
540.	25.8	4.9	23.79	29
570.	26.5	5.0	25.09	30
600.	27.1	5.1	26.24	31
630.	27.3	5.2	26.63	32
660.	28.3	5.3	28.62	33
690.	28.8	5.4	29.64	34
720.	29.3	5.5	30.68	35
750.	29.8	5.6	31.73	36
780.	30.3	5.7	32.81	37
810.	31.3	5.9	35.01	38
840.	31.5	6.0	35.46	39
870.	32.1	6.1	36.82	40
900.	33.1	6.3	39.15	41
930.	33.3	6.3	39.63	42
960.	33.8	6.4	40.62	43
990.	34.3	6.5	42.04	44
1020.	35.1	6.6	44.03	45
1050.	35.3	6.7	44.53	46
1080.	35.8	6.8	45.60	47
1110.	36.5	6.9	47.61	48
1140.	37.1	7.0	49.19	49
1170.	37.3	7.1	49.72	50
1200.	38.3	7.2	52.42	51
1230.	38.3	7.2	52.42	52
1260.	38.8	7.3	53.80	53
1290.	39.3	7.4	55.19	54
1320.	39.5	7.5	55.75	55
1350.	40.3	7.6	58.04	56
1380.	40.5	7.7	58.61	57
1410.	41.3	7.8	60.95	58

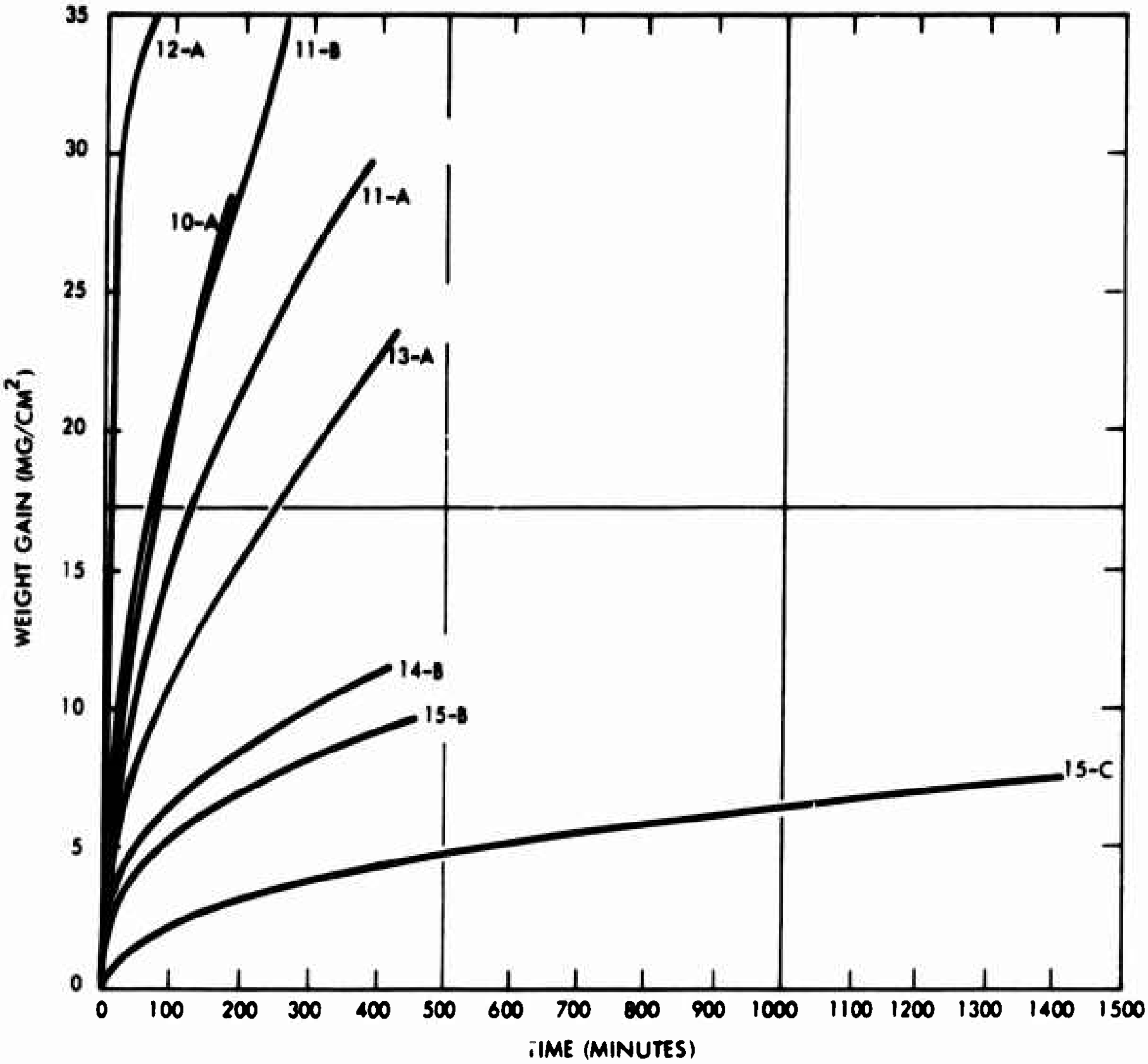

Figure A-1. Oxidation Behavior of Experimental Niobium Alloys at 1200°C

16-B

TIME-MIN	WT-LOSS	WT-LOSS/AREA	(WT-LOSS/AREA)-SQR
1.	3.0	.7	.47
2.	4.0	.9	.84
3.	7.0	1.6	2.58
4.	8.5	1.9	3.80
5.	9.0	2.1	4.26
10.	11.5	2.6	6.96
15.	13.5	3.1	9.59
20.	16.2	3.7	13.81
25.	17.5	4.0	16.11
30.	18.5	4.2	18.00
40.	20.5	4.7	22.11
50.	22.5	5.2	26.63
60.	23.5	5.4	29.05
90.	26.5	6.1	36.94
120.	29.5	6.8	45.78
150.	32.0	7.3	53.87
180.	34.5	7.9	62.61
210.	36.5	8.4	70.08
240.	38.5	8.8	77.97
270.	40.5	9.3	86.29
300.	42.5	9.7	95.02
330.	43.5	10.0	99.54
360.	45.0	10.3	106.53
390.	46.5	10.7	113.75
420.	48.0	11.0	121.20

16-C

TIME-MIN	WT-LOSS	WT-LOSS/AREA	(WT-LOSS/AREA)-SQR	
1.	-.3	-.1	.01	1
2.	1.2	.3	.08	2
3.	4.5	1.1	1.13	3
4.	4.7	1.1	1.23	4
5.	4.5	1.1	1.13	5
10.	7.1	1.7	2.80	6
15.	8.5	2.0	4.02	7
20.	9.7	2.3	5.23	8
25.	11.4	2.7	7.23	9
30.	12.3	2.9	8.42	10
40.	14.0	3.3	10.90	11
50.	15.0	3.5	12.52	12
60.	16.2	3.8	14.60	13
90.	18.7	4.4	19.45	14
120.	20.5	4.8	23.38	15
150.	22.5	5.3	28.16	16
180.	24.0	5.7	32.04	17
210.	25.2	5.9	35.32	18
240.	26.7	6.3	39.65	19
270.	28.5	6.7	45.18	20
300.	29.5	7.0	48.41	21
330.	30.7	7.2	52.43	22
360.	32.0	7.5	56.96	23
390.	33.2	7.8	61.31	24
420.	34.3	8.1	65.44	25
450.	24.0	5.7	32.04	26
480.	25.2	5.9	35.32	27
510.	26.7	6.3	39.65	28
540.	28.5	6.7	45.18	29
570.	29.5	7.0	48.41	30
600.	30.7	7.2	52.43	31
630.	32.0	7.5	56.96	32
660.	33.2	7.8	61.31	33
690.	34.3	8.1	65.44	34
720.	24.0	5.7	32.04	35
750.	25.2	5.9	35.32	36
780.	26.7	6.3	39.65	37
810.	28.5	6.7	45.18	38
840.	29.5	7.0	48.41	39
870.	30.7	7.2	52.43	40
900.	32.0	7.5	56.96	41
930.	33.2	7.8	61.31	42
960.	34.3	8.1	65.44	43
990.	24.0	5.7	32.04	44
1020.	25.2	5.9	35.32	45
1050.	26.7	6.3	39.65	46
1080.	28.5	6.7	45.18	47
1110.	29.5	7.0	48.41	48
1140.	53.5	12.6	159.21	49
1170.	54.3	12.8	164.01	50
1200.	54.7	12.9	166.43	51
1230.	56.0	13.2	174.44	52
1260.	56.5	13.3	177.57	53
1290.	57.5	13.6	183.91	54
1320.	58.5	13.8	190.36	55
1350.	58.7	13.8	191.67	56
1380.	59.7	14.1	198.25	57
1410.	60.7	14.3	204.95	58
1440.	61.5	14.5	210.39	59
1470.	62.3	14.7	215.90	60
1500.	62.7	14.8	218.68	61
1530.	63.7	15.0	225.71	62

17-B

TIME-MIN	WT-LOSS	WT-LOSS/AREA	(WT-LOSS/AREA)-SQR
1.	2.5	.5	.28
2.	4.5	.9	.90
3.	7.0	1.5	2.18
4.	7.5	1.6	2.50
5.	8.0	1.7	2.85
10.	6.0	1.3	1.60
15.	9.0	1.9	3.61
20.	12.2	2.6	6.62
25.	13.5	2.8	8.11
30.	15.5	3.3	10.69
40.	17.5	3.7	13.63
50.	18.5	3.9	15.23
60.	20.0	4.2	17.80
90.	23.5	5.0	24.58
120.	25.5	5.4	28.94
150.	28.0	5.9	34.89
180.	29.5	6.2	38.73
210.	31.0	6.5	42.77
240.	33.0	7.0	48.47
270.	34.5	7.3	52.98
300.	35.5	7.5	56.09
330.	36.5	7.7	59.30
360.	37.5	7.9	62.59
390.	38.5	8.1	65.97
420.	39.5	8.3	69.44
450.	40.5	8.5	73.01

17-C

TIME-MIN	WT-LOSS	WT-LOSS/AREA	(WT-LOSS/AREA)-SQR	
1.	2.5	.5	.30	1
2.	4.0	.9	.76	2
3.	6.5	1.4	2.01	3
4.	6.2	1.4	1.83	4
5.	6.5	1.4	2.01	5
10.	8.5	1.9	3.44	6
15.	10.0	2.2	4.77	7
20.	12.5	2.7	7.45	8
25.	13.1	2.9	8.18	9
30.	14.0	3.1	9.34	10
40.	15.7	3.4	11.75	11
50.	17.0	3.7	13.78	12
60.	18.0	3.9	15.45	13
90.	16.0	3.5	12.20	14
120.	22.7	5.0	24.57	15
150.	24.7	5.4	29.08	16
180.	26.5	5.8	33.48	17
210.	28.0	6.1	37.38	18
240.	29.5	6.4	41.49	19
270.	30.5	6.7	44.35	20
300.	31.5	6.9	47.30	21
330.	32.5	7.1	50.35	22
360.	33.5	7.3	53.50	23
390.	34.5	7.5	56.74	24
420.	35.5	7.8	60.08	25
450.	36.5	8.0	63.51	26
480.	37.5	8.2	67.04	27
510.	38.3	8.4	69.93	28
540.	38.7	8.4	71.40	29
570.	39.5	8.6	74.38	30
600.	40.5	8.8	78.20	31
630.	41.3	9.0	81.31	32
660.	42.2	9.2	84.90	33
690.	42.5	9.3	86.11	34
720.	43.5	9.5	90.21	35
750.	44.3	9.7	93.56	36
780.	45.2	9.9	97.40	37
810.	45.8	10.0	100.00	38
840.	46.5	10.2	103.08	39
870.	47.3	10.3	106.66	40
900.	47.9	10.5	109.38	41
930.	48.5	10.6	112.14	42
960.	49.5	10.8	116.81	43
990.	50.3	11.0	120.62	44
1020.	51.3	11.2	125.46	45
1050.	51.7	11.3	127.42	46
1080.	52.5	11.5	131.40	47
1110.	53.3	11.6	135.43	48
1140.	54.3	11.9	140.56	49
1170.	55.0	12.0	144.21	50
1200.	55.5	12.1	146.84	51
1230.	56.5	12.3	152.18	52
1260.	57.3	12.5	156.52	53
1290.	58.0	12.7	160.37	54
1320.	59.0	12.9	165.95	55
1350.	59.7	13.0	169.91	56
1380.	60.5	13.2	174.49	57
1410.	61.5	13.4	180.31	58

18-B

TIME-MIN	WT-LOSS	WT-LOSS/AREA	(WT-LOSS/AREA)-SQR
1.	4.5	1.0	.91
2.	7.0	1.5	2.20
3.	10.5	2.2	4.95
4.	11.0	2.3	5.43
5.	12.0	2.5	6.46
10.	14.0	3.0	8.80
15.	16.0	3.4	11.49
20.	19.7	4.2	17.42
25.	21.0	4.4	19.79
30.	22.5	4.8	22.72
40.	25.5	5.4	29.19
50.	27.5	5.8	33.95
60.	30.0	6.4	40.40
90.	35.5	7.5	56.57
120.	40.5	8.6	73.63
150.	44.5	9.4	88.89
180.	48.5	10.3	105.58
210.	52.5	11.1	123.72
240.	55.5	11.8	138.26
270.	60.0	12.7	161.59
300.	62.5	13.2	175.34
330.	65.5	13.9	192.57
360.	68.5	14.5	210.62
390.	71.0	15.0	226.27
420.	74.0	15.7	245.80

18-C

TIME-MIN	WT-LOSS	WT-LOSS/AREA	(WT-LOSS/AREA)-SQR	
1.	1.5	.4	.12	1
2.	4.0	.9	.87	2
3.	7.0	1.6	2.67	3
4.	8.0	1.9	3.49	4
5.	9.0	2.1	4.42	5
10.	12.0	2.8	7.86	6
15.	14.0	3.3	10.70	7
20.	17.7	4.1	17.10	8
25.	19.0	4.4	19.71	9
30.	20.5	4.8	22.94	10
40.	23.5	5.5	30.15	11
50.	26.0	6.1	36.90	12
60.	28.5	6.7	44.34	13
90.	35.0	8.2	66.87	14
120.	39.5	9.2	85.17	15
150.	44.0	10.3	105.69	16
180.	48.5	11.3	128.41	17
210.	52.0	12.1	147.61	18
240.	55.5	13.0	168.15	19
270.	59.0	13.8	190.03	20
300.	62.5	14.6	213.24	21
330.	65.7	15.4	235.64	22
360.	69.0	16.1	259.90	23
390.	71.5	16.7	279.08	24
420.	74.5	17.4	302.99	25
450.	77.5	18.1	327.88	26
480.	80.5	18.8	353.76	27
510.	83.5	19.5	380.61	28
540.	86.5	20.2	408.46	29
570.	92.2	21.5	464.06	30
600.	94.5	22.1	487.50	31
630.	97.5	22.8	518.95	32
660.	100.0	23.4	545.90	33
690.	102.5	23.9	573.54	34
720.	105.5	24.6	607.60	35
750.	108.5	25.4	642.65	36
780.	111.5	26.1	678.68	37
810.	114.0	26.6	709.45	38
840.	116.7	27.3	743.45	39
870.	119.7	28.0	782.17	40
900.	122.5	28.6	819.19	41
930.	123.7	28.9	835.32	42
960.	128.5	30.0	901.40	43
990.	131.7	30.8	946.86	44
1020.	135.0	31.5	994.90	45
1050.	138.0	32.2	1039.61	46
1080.	141.5	33.1	1093.01	47
1110.	144.0	33.6	1131.98	48
1140.	147.0	34.3	1179.63	49
1170.	151.0	35.3	1244.70	50
1200.	154.5	36.1	1303.08	5

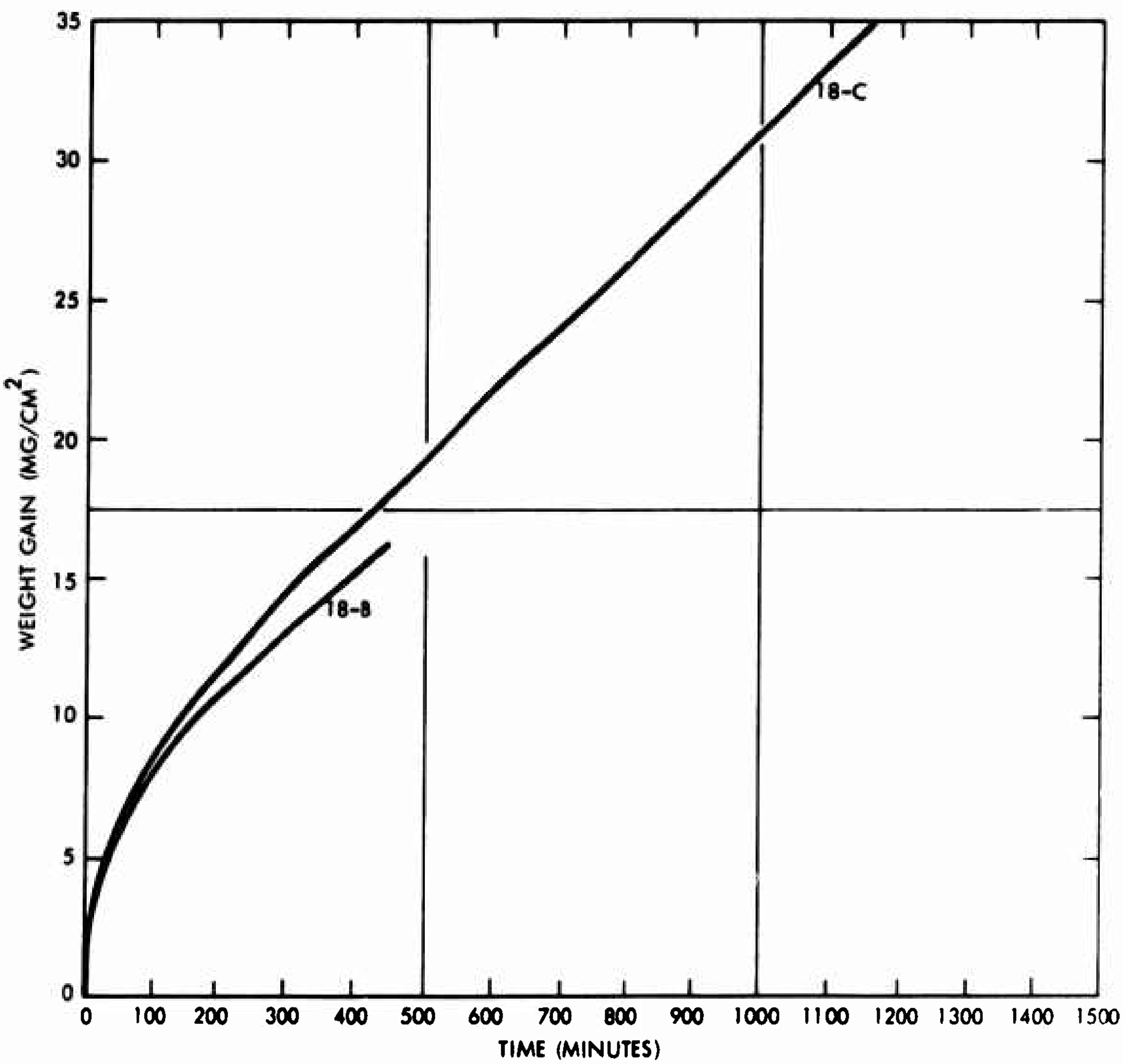

Figure A-2. Oxidation Behavior of Experimental Niobium Alloys at 1200°C

19-B

TIME-MIN	WT-LOSS	WT-LOSS/AREA	(WT-LOSS/AREA)*SQR
1.	1.5	.4	.13
2.	5.0	1.2	1.40
3.	8.5	2.0	4.06
4.	9.0	2.1	4.55
5.	10.0	2.4	5.62
10.	12.5	3.0	8.77
15.	14.0	3.3	11.01
20.	16.7	4.0	15.66
25.	18.5	4.4	19.22
30.	19.5	4.6	21.35
40.	22.0	5.2	27.18
50.	24.5	5.8	33.71
60.	26.0	6.2	37.96
90.	31.5	7.5	55.72
120.	35.5	8.4	70.77
150.	39.5	9.4	87.61
180.	42.5	10.1	101.43
210.	45.5	10.8	116.25
240.	48.5	11.5	132.09
270.	51.5	12.2	148.93
300.	54.0	12.8	163.74
330.	56.5	13.4	179.26
360.	59.5	14.1	198.80
390.	61.5	14.6	212.39
420.	63.5	15.0	226.42

19-C

TIME-MIN	WT-LOSS	WT-LOSS/AREA	(WT-LOSS/AREA)-SQR	
1.	1.0	.2	.04	1
2.	3.5	.7	.53	2
3.	6.5	1.3	1.81	3
4.	7.3	1.5	2.28	4
5.	7.5	1.6	2.41	5
10.	10.5	2.2	4.73	6
15.	12.2	2.5	6.38	7
20.	15.7	3.3	10.57	8
25.	17.5	3.6	13.13	9
30.	19.0	3.9	15.47	10
40.	21.5	4.5	19.81	11
50.	23.7	4.9	24.08	12
60.	26.2	5.4	29.42	13
90.	31.5	6.5	42.53	14
120.	36.0	7.5	55.55	15
150.	39.7	8.2	67.56	16
180.	43.5	9.0	81.11	17
210.	46.5	9.6	92.69	18
240.	49.5	10.2	105.03	19
270.	52.5	10.9	118.15	20
300.	55.5	11.5	132.04	21
330.	58.3	12.1	145.69	22
360.	60.7	12.6	157.94	23
390.	63.0	13.0	170.13	24
420.	65.5	13.6	183.90	25
450.	68.3	14.1	199.96	26
480.	70.5	14.6	213.05	27
510.	73.0	15.1	228.43	28
540.	75.5	15.6	244.34	29
570.	77.5	16.0	257.46	30
600.	79.5	16.5	270.92	31
630.	82.0	17.0	288.23	32
660.	83.7	17.3	300.30	33
690.	86.0	17.8	317.03	34
720.	88.0	18.2	331.95	35
750.	90.0	18.6	347.21	36
780.	92.0	19.0	362.81	37
810.	93.7	19.4	376.34	38
840.	95.5	19.8	390.94	39
870.	97.3	20.1	405.82	40
900.	99.3	20.6	422.67	41
930.	101.0	20.9	437.27	42
960.	103.0	21.3	454.76	43
990.	104.5	21.6	468.10	44
1020.	106.5	22.0	486.19	45
1050.	108.5	22.5	504.62	46
1080.	110.5	22.9	523.40	47
1110.	112.0	23.2	537.70	48
1140.	114.0	23.6	557.08	49
1170.	115.7	24.0	573.82	50
1200.	117.5	24.3	591.81	51
1230.	119.5	24.7	612.13	52
1260.	121.0	25.1	627.59	53

20-A

TIME-MIN	WT-LOSS	WT-LOSS/AREA	(WT-LOSS/AREA)-SQR
1.	2.5	.5	.30
2.	6.0	1.3	1.70
3.	9.0	2.0	3.83
4.	9.5	2.1	4.27
5.	10.5	2.3	5.21
10.	13.5	2.9	8.61
15.	15.0	3.3	10.63
20.	18.7	4.1	16.53
25.	20.5	4.5	19.86
30.	21.5	4.7	21.85
40.	24.5	5.3	28.37
50.	27.5	6.0	35.74
60.	29.5	6.4	41.13
90.	36.0	7.8	61.25
120.	42.5	9.2	85.36
150.	47.5	10.3	106.63
180.	52.5	11.4	130.26
210.	57.5	12.5	156.25
240.	62.5	13.6	184.61
270.	67.0	14.6	212.15
300.	71.5	15.5	241.60
330.	76.5	16.6	276.57
360.	81.0	17.6	310.07
390.	85.5	18.6	345.47

21-A

TIME-MIN	WT-LOSS	WT-LOSS/AREA	(WT-LOSS/AREA)-SQR
1.	6.5	1.4	1.92
2.	10.0	2.1	4.55
3.	14.0	3.0	8.91
4.	15.5	3.3	10.92
5.	18.0	3.8	14.73
10.	26.5	5.7	31.93
15.	34.0	7.2	52.55
20.	40.7	8.7	75.31
25.	46.5	9.9	98.30
30.	53.5	11.4	130.13
40.	65.5	14.0	195.05
50.	78.5	16.7	280.15
60.	91.5	19.5	380.62
90.	130.5	27.8	774.24
120.	174.5	37.2	1384.35
150.	221.5	47.2	2230.50
180.	269.5	57.5	3301.96
210.	319.5	68.1	4640.83

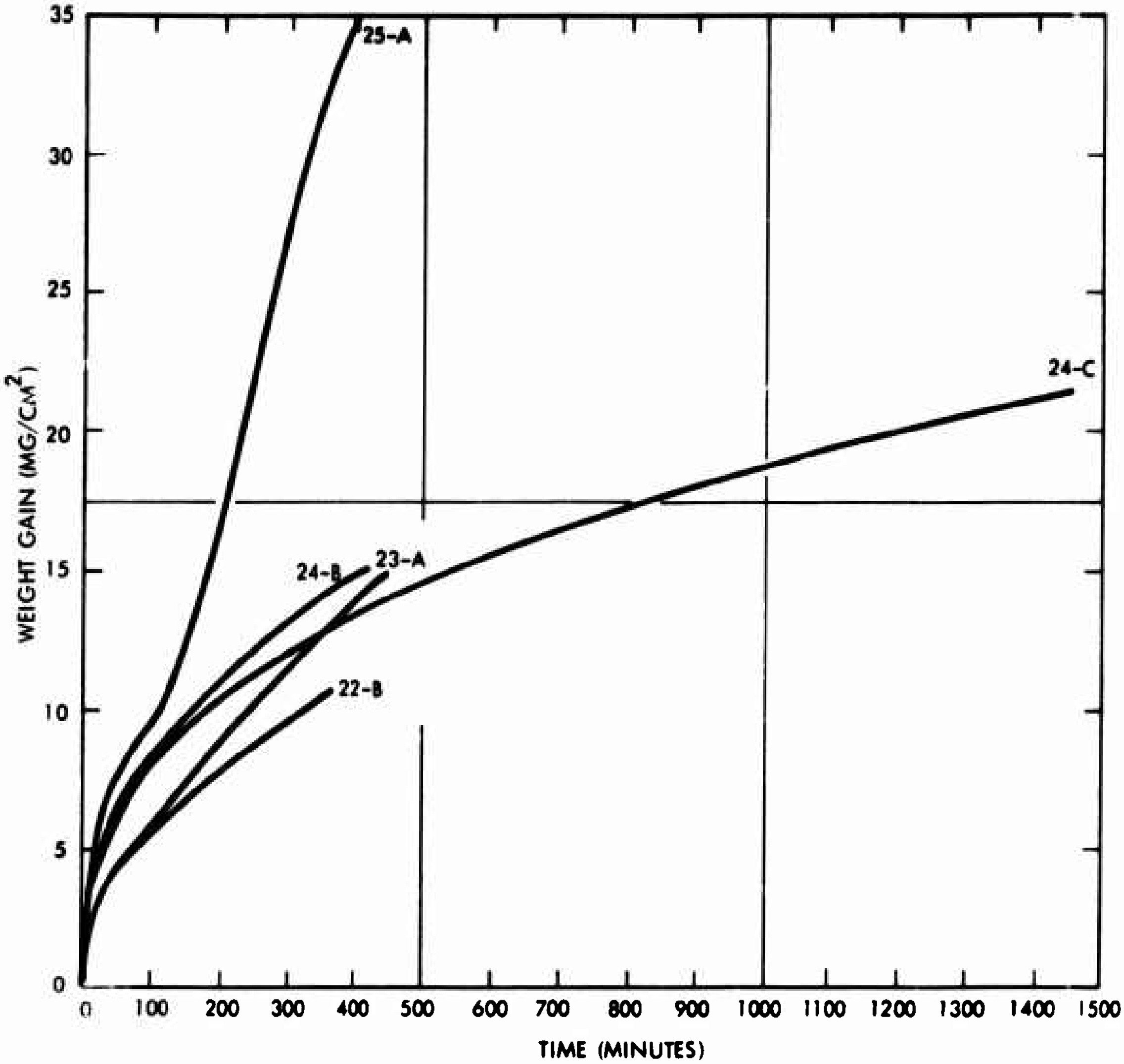

Figure A-3. Oxidation Behavior of Experimental Niobium Alloys at 1200°C

22-B

TIME-MIN	WT-LOSS	WT-LOSS/AREA	(WT-LOSS/AREA)-SQR
1.	-.5	-.1	.01
2.	3.0	.6	.39
3.	10.0	2.1	4.30
4.	10.5	2.2	4.75
5.	11.0	2.3	5.21
10.	13.5	2.8	7.84
15.	13.0	2.7	7.27
20.	15.2	3.2	9.94
25.	15.5	3.2	10.34
30.	16.5	3.4	11.72
40.	18.5	3.8	14.73
50.	19.5	4.0	16.37
60.	21.5	4.5	19.90
90.	25.5	5.3	27.99
120.	28.5	5.9	34.96
150.	32.5	6.7	45.46
180.	35.5	7.4	54.25
210.	38.5	8.0	63.80
240.	41.5	8.6	74.13
270.	39.0	8.1	65.47
300.	46.5	9.6	93.07
330.	49.5	10.3	105.47
360.	51.5	10.7	114.16

23-A

TIME-MIN	WT-LOSS	WT-LOSS/AREA	(WT-LOSS/AREA)-SQR
1.	.5	.1	.01
2.	3.0	.7	.50
3.	5.5	1.3	1.67
4.	5.7	1.3	1.80
5.	6.2	1.5	2.13
10.	7.5	1.8	3.11
15.	9.0	2.1	4.48
20.	11.7	2.8	7.58
25.	12.5	2.9	8.65
30.	13.5	3.2	10.09
40.	15.5	3.6	13.30
50.	17.5	4.1	16.96
60.	19.5	4.6	21.05
90.	23.5	5.5	30.57
120.	27.5	6.5	41.87
150.	31.5	7.4	54.93
180.	34.5	8.1	65.90
210.	38.5	9.1	82.06
240.	41.5	9.8	95.35
270.	45.5	10.7	114.62
300.	48.5	11.4	130.23
330.	52.0	12.2	149.70
360.	54.5	12.8	164.44
390.	57.5	13.5	183.04
420.	60.5	14.2	202.64

24-B

TIME-MIN	WT-LOSS	WT-LOSS/AREA	(WT-LOSS/AREA)-SQR
1.	2.5	.6	.34
2.	5.5	1.3	1.64
3.	8.0	1.9	3.48
4.	7.5	1.7	3.06
5.	7.0	1.6	2.66
10.	10.5	2.4	5.99
15.	14.0	3.3	10.65
20.	17.7	4.1	17.02
25.	20.5	4.8	22.83
30.	22.5	5.2	27.51
40.	25.0	5.8	33.96
50.	27.5	6.4	41.09
60.	29.5	6.9	47.29
90.	34.5	8.0	64.67
120.	38.5	9.0	80.54
150.	42.5	9.9	98.14
180.	45.5	10.6	112.49
210.	48.5	11.3	127.81
240.	50.5	11.8	138.57
270.	53.5	12.5	155.52
300.	56.5	13.2	173.45
330.	58.5	13.6	185.95
360.	60.5	14.1	198.68
390.	62.5	14.6	212.25
420.	64.5	15.0	226.05

24-C

TIME-MIN	WT-LOSS	WT-LOSS/AREA	(WT-LOSS/AREA)-SQR	
1.	3.5	.7	.50	1
2.	4.0	.8	.66	2
3.	10.0	2.0	4.10	3
4.	10.5	2.1	4.52	4
5.	12.8	2.6	6.71	5
10.	16.7	3.4	11.43	6
15.	19.5	3.9	15.58	7
20.	22.7	4.6	21.12	8
25.	24.7	5.0	25.00	9
30.	26.5	5.4	28.78	10
40.	29.3	5.9	35.18	11
50.	31.7	6.4	41.18	12
60.	34.5	7.0	48.77	13
90.	38.6	7.8	61.05	14
120.	43.0	8.7	75.77	15
150.	46.7	9.5	89.37	16
180.	49.5	10.0	100.41	17
210.	52.5	10.6	112.94	18
240.	55.0	11.1	123.96	19
270.	57.5	11.6	135.48	20
300.	59.5	12.0	145.07	21
330.	61.7	12.5	156.00	22
360.	64.2	13.0	168.89	23
390.	66.0	13.4	178.50	24
420.	67.5	13.7	186.70	25
450.	69.2	14.0	196.23	26
480.	71.0	14.4	206.57	27
510.	72.0	14.6	212.43	28
540.	73.7	14.9	222.58	29
570.	75.3	15.2	232.35	30
600.	76.5	15.5	239.81	31
630.	77.5	15.7	246.12	32
660.	78.6	15.9	253.16	33
690.	80.0	16.2	262.26	34
720.	81.3	16.5	270.85	35
750.	82.5	16.7	278.90	36
780.	83.5	16.9	285.71	37
810.	84.5	17.1	292.59	38
840.	86.0	17.4	303.07	39
870.	87.3	17.7	312.30	40
900.	87.8	17.8	315.89	41
930.	89.3	18.1	326.78	42
960.	90.3	18.3	334.13	43
990.	91.5	18.5	343.07	44
1020.	92.5	18.7	350.61	45
1050.	93.5	18.9	358.24	46
1080.	94.0	19.0	362.08	47
1110.	95.3	19.3	372.16	48
1140.	96.3	19.5	380.01	49
1170.	96.7	19.6	383.18	50
1200.	97.7	19.8	391.14	51
1230.	98.7	20.0	399.19	52
1260.	99.5	20.1	405.69	53
1290.	100.5	20.3	413.88	54
1320.	101.5	20.5	422.16	55
1350.	103.5	21.0	438.96	56
1380.	104.0	21.1	443.21	57
1410.	104.2	21.1	444.92	58

25-A

TIME-MIN	WT-LOSS	WT-LOSS/AREA	(WT-LOSS/AREA)-SQR
1.	-.5	-.1	.01
2.	12.0	2.6	6.66
3.	17.0	3.7	13.37
4.	18.5	4.0	15.83
5.	19.0	4.1	16.70
10.	17.5	3.8	14.16
15.	16.5	3.5	12.59
20.	17.7	3.8	14.49
25.	18.5	4.0	15.83
30.	18.5	4.0	15.83
40.	22.5	4.8	23.41
50.	26.5	5.7	32.48
60.	29.5	6.3	40.25
90.	39.5	8.5	72.16
120.	48.5	10.4	108.79
150.	59.5	12.8	163.73
180.	70.5	15.2	229.86
210.	83.5	18.0	322.45
240.	96.5	20.8	430.67
270.	114.5	24.6	606.32
300.	128.0	27.5	757.73
330.	141.5	30.4	925.99
360.	152.5	32.8	1075.56
390.	165.5	35.6	1266.75
420.	177.5	38.2	1457.10

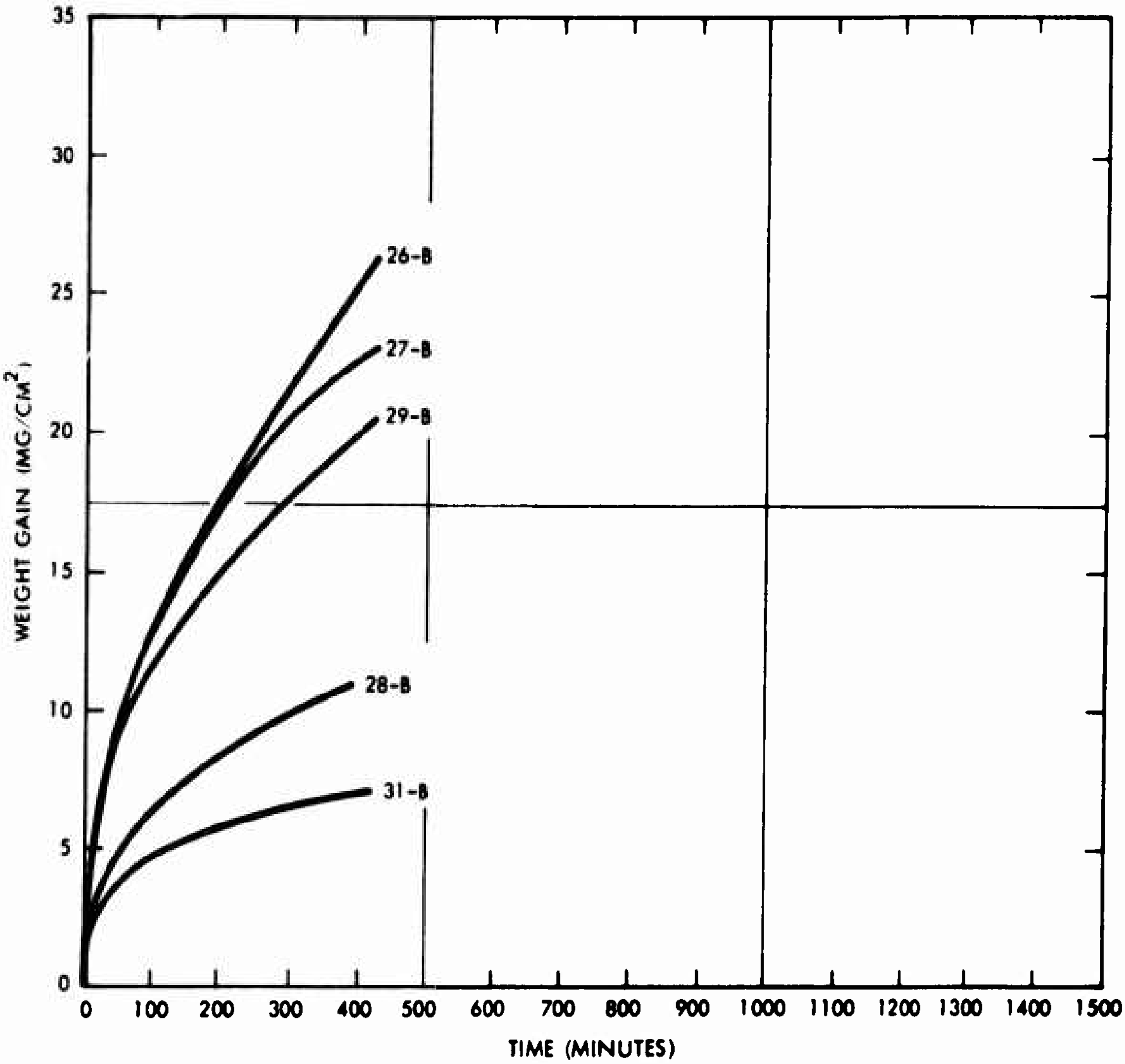

Figure A-4. Oxidation Behavior of Experimental Niobium Alloys at 1200°C

26-B

TIME-MIN	WT-LOSS	WT-LOSS/AREA	(WT-LOSS/AREA)-SQR	
1.	1.0	.5	.20	1
2.	3.0	1.4	1.83	2
3.	6.5	2.9	8.60	3
4.	7.0	3.2	9.97	4
5.	7.5	3.4	11.44	5
10.	10.0	4.5	20.35	6
15.	11.5	5.2	26.91	7
20.	14.2	6.4	41.02	8
25.	15.0	6.8	45.78	9
30.	16.0	7.2	52.08	10
40.	18.5	8.3	69.63	11
50.	20.8	9.4	88.02	12
60.	23.0	10.4	107.63	13
90.	27.5	12.4	153.86	14
120.	31.0	14.0	195.52	15
150.	34.5	15.6	242.16	16
180.	38.0	17.1	293.79	17
210.	41.0	18.5	342.01	18
240.	44.0	19.8	393.89	19
270.	46.0	20.7	430.51	20
300.	49.0	22.1	488.50	21
330.	51.0	23.0	529.19	22
360.	53.0	23.9	571.51	23
390.	56.0	25.3	638.04	24
420.	58.0	26.2	684.42	25

27-B

TIME-MIN	WT-LOSS	WT-LOSS/AREA	(WT-LOSS/AREA)-SQR	
1.	.2	.1	.01	1
2.	3.2	1.4	1.89	2
3.	6.2	2.7	7.08	3
4.	6.7	2.9	8.27	4
5.	7.2	3.1	9.55	5
10.	9.7	4.2	17.33	6
15.	12.0	5.2	26.52	7
20.	14.9	6.4	40.89	8
25.	16.7	7.2	51.37	9
30.	17.7	7.6	57.71	10
40.	19.9	8.5	72.94	11
50.	22.5	9.7	93.25	12
60.	23.7	10.2	103.46	13
90.	28.7	12.3	151.72	14
120.	32.2	13.8	190.99	15
150.	35.5	15.2	232.14	16
180.	37.7	16.2	261.60	17
210.	40.7	17.5	305.12	18
240.	42.5	18.2	332.71	19
270.	44.7	19.2	368.05	20
300.	46.7	20.0	401.72	21
330.	48.7	20.9	436.86	22
360.	50.7	21.8	473.48	23
390.	52.2	22.4	501.91	24
420.	53.7	23.0	531.17	25

28-B

TIME-MIN	WT-LOSS	WT-LOSS/AREA	(WT-LOSS/AREA)-SQR	
1.	.3	.2	.02	1
2.	1.3	.7	.42	2
3.	3.8	1.9	3.61	3
4.	4.3	2.2	4.62	4
5.	4.3	2.2	4.62	5
10.	7.3	3.7	13.32	6
15.	8.6	4.3	18.49	7
20.	10.5	5.2	27.56	8
25.	12.0	6.0	36.00	9
30.	12.3	6.2	37.82	10
40.	14.3	7.2	51.12	11
50.	15.3	7.7	58.52	12
60.	16.3	8.2	66.42	13
90.	19.5	9.7	95.06	14
120.	21.3	10.7	113.42	15
150.	23.5	11.7	138.06	16
180.	25.1	12.5	157.50	17
210.	27.3	13.7	186.32	18
240.	28.3	14.2	200.22	19
270.	30.3	15.2	229.52	20
300.	31.3	15.7	244.92	21
330.	32.3	16.2	260.82	22
360.	33.3	16.7	277.22	23
390.	34.5	17.2	297.56	24

28-B

TIME-MIN	WT-LOSS	WT-LOSS/AREA	(WT-LOSS/AREA)-SQR	
1.	.3	.1	.01	1
2.	1.3	.4	.17	2
3.	3.8	1.2	1.45	3
4.	4.3	1.4	1.85	4
5.	4.3	1.4	1.85	5
10.	7.3	2.3	5.34	6
15.	8.6	2.7	7.42	7
20.	10.5	3.3	11.05	8
25.	12.0	3.8	14.44	9
30.	12.3	3.9	15.17	10
40.	14.3	4.5	20.50	11
50.	15.3	4.8	23.47	12
60.	16.3	5.2	26.64	13
90.	19.5	6.2	38.13	14
120.	21.3	6.7	45.49	15
150.	23.5	7.4	55.37	16
180.	25.1	7.9	63.17	17
210.	27.3	8.6	74.73	18
240.	28.3	9.0	80.31	19
270.	30.3	9.6	92.06	20
300.	31.3	9.9	98.23	21
330.	32.3	10.2	104.61	22
360.	33.3	10.5	111.19	23
390.	34.5	10.9	119.35	24

29-B

TIME-MIN	WT-LOSS	WT-LOSS/AREA	(WT-LOSS/AREA)-SQR	
1.	-.2	-.1	.01	1
2.	1.8	.8	.65	2
3.	4.8	2.2	4.84	3
4.	5.3	2.4	5.65	4
5.	6.3	2.8	7.99	5
10.	9.5	4.3	18.16	6
15.	10.8	4.8	23.48	7
20.	14.0	6.3	39.45	8
25.	15.3	6.9	47.12	9
30.	16.3	7.3	53.48	10
40.	17.8	8.0	63.77	11
50.	19.8	8.9	78.91	12
60.	21.3	9.6	91.31	13
90.	24.3	10.9	118.85	14
120.	27.3	12.2	150.00	15
150.	29.5	13.2	175.16	16
180.	32.3	14.5	209.98	17
210.	34.3	15.4	236.79	18
240.	36.3	16.3	265.21	19
270.	38.1	17.1	292.17	20
300.	39.5	17.7	314.03	21
330.	41.3	18.5	343.30	22
360.	42.8	19.2	368.70	23
390.	44.3	19.9	394.99	24
420.	45.8	20.5	422.19	25

31-B

TIME-MIN	WT-LOSS	WT-LOSS/AREA	(WT-LOSS/AREA)-SQR	
1.	.0	.0	.00	1
2.	.5	.2	.04	2
3.	2.5	1.0	1.07	3
4.	2.5	1.0	1.07	4
5.	2.5	1.0	1.07	5
10.	3.0	1.2	1.54	6
15.	4.5	1.9	3.47	7
20.	6.2	2.6	6.60	8
25.	6.8	2.8	7.93	9
30.	7.2	3.0	8.90	10
40.	8.5	3.5	12.40	11
50.	8.5	3.5	12.40	12
60.	9.0	3.7	13.90	13
90.	11.0	4.6	20.76	14
120.	11.5	4.8	22.69	15
150.	12.5	5.2	26.81	16
180.	13.0	5.4	29.00	17
210.	14.0	5.8	33.63	18
240.	14.8	6.1	37.59	19
270.	15.0	6.2	38.61	20
300.	15.5	6.4	41.23	21
330.	16.0	6.6	43.93	22
360.	16.0	6.6	43.93	23
390.	17.0	7.0	49.59	24
420.	17.2	7.1	50.77	25

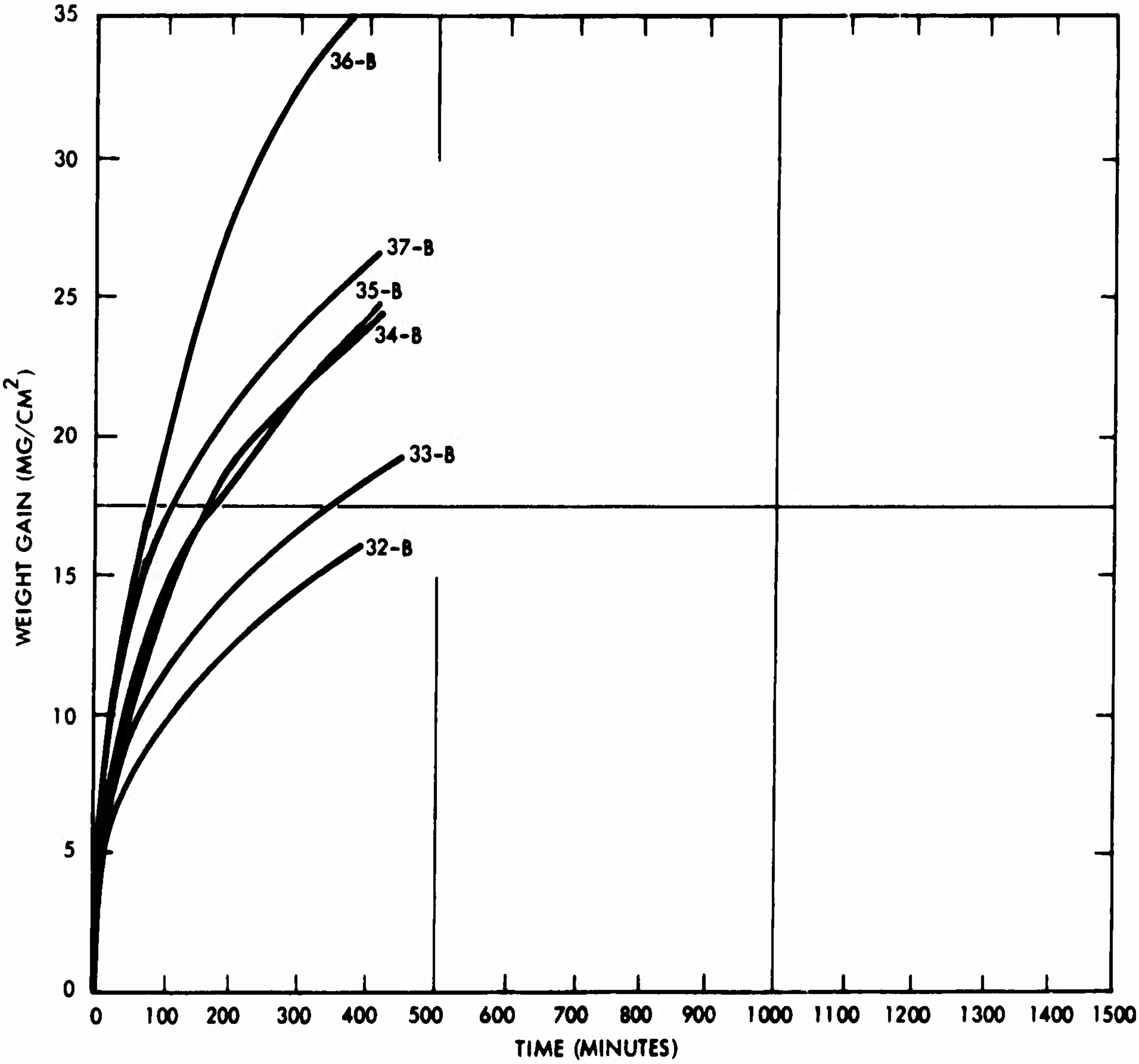

Figure A-5. Oxidation Behavior of Experimental Niobium Alloys at 1200°C

32-B

TIME-MIN	WT-LOSS	WT-LOSS/AREA	(WT-LOSS/AREA)-SQR	
1.	4.5	1.8	3.07	1
2.	6.5	2.5	6.40	2
3.	9.0	3.5	12.27	3
4.	9.5	3.7	13.67	4
5.	10.0	3.9	15.15	5
10.	12.0	4.7	21.82	6
15.	13.5	5.3	27.61	7
20.	16.2	6.3	39.77	8
25.	16.5	6.4	41.25	9
30.	17.7	6.9	47.47	10
40.	18.7	7.3	52.99	11
50.	20.3	7.9	62.44	12
60.	21.3	8.3	68.74	13
90.	24.3	9.5	89.47	14
120.	26.8	10.4	108.83	15
150.	29.3	11.4	130.08	16
180.	30.8	12.0	143.74	17
210.	32.5	12.7	160.04	18
240.	34.5	13.4	180.35	19
270.	36.0	14.0	196.37	20
300.	37.5	14.6	213.08	21
330.	38.5	15.0	224.59	22
360.	40.0	15.6	242.43	23
390.	41.3	16.1	258.45	24

33-B

TIME-MIN	WT-LOSS	WT-LOSS/AREA	(WT-LOSS/AREA)-SQR	
1.	3.7	1.9	3.66	1
2.	5.8	3.0	8.99	2
3.	8.0	4.1	17.11	3
4.	8.0	4.1	17.11	4
5.	8.0	4.1	17.11	5
10.	9.7	5.0	25.16	6
15.	11.2	5.8	33.54	7
20.	13.7	7.1	50.18	8
25.	14.5	7.5	56.21	9
30.	15.5	8.0	64.23	10
40.	16.7	8.6	74.56	11
50.	18.2	9.4	88.56	12
60.	19.5	10.1	101.66	13
90.	21.5	11.1	123.58	14
120.	23.5	12.2	147.65	15
150.	25.3	13.1	171.13	16
180.	27.0	14.0	194.90	17
210.	28.5	14.7	217.16	18
240.	29.5	15.3	232.67	19
270.	30.5	15.8	248.71	20
300.	32.3	16.7	278.93	21
330.	32.7	16.9	285.88	22
360.	34.1	17.6	310.88	23
390.	35.2	18.2	331.26	24
420.	36.3	18.8	352.29	25
450.	37.3	19.3	371.97	26

34-B

TIME-MIN	WT-LOSS	WT-LOSS/AREA	(WT-LOSS/AREA)-SQR	
1.	4.2	1.7	2.94	1
2.	6.5	2.7	7.05	2
3.	8.8	3.6	12.92	3
4.	9.0	3.7	13.52	4
5.	9.5	3.9	15.06	5
10.	12.0	4.9	24.03	6
15.	14.3	5.8	34.12	7
20.	17.2	7.0	49.37	8
25.	19.0	7.8	60.24	9
30.	20.5	8.4	70.13	10
40.	23.0	9.4	88.27	11
50.	25.2	10.3	105.97	12
60.	27.5	11.2	126.20	13
90.	33.0	13.5	181.72	14
120.	37.5	15.3	234.66	15
150.	41.5	17.0	287.39	16
180.	44.2	18.1	326.00	17
210.	47.0	19.2	368.61	18
240.	49.0	20.0	400.65	19
270.	51.2	20.9	437.44	20
300.	53.2	21.7	472.28	21
330.	55.0	22.5	504.78	22
360.	56.0	22.9	523.30	23
390.	58.0	23.7	561.35	24
420.	59.5	24.3	590.76	25

35-B

TIME-MIN	WT-LOSS	WT-LOSS/AREA	(WT-LOSS/AREA)-SQR	
1.	3.0	1.3	1.64	1
2.	6.0	2.6	6.57	2
3.	9.0	3.8	14.78	3
4.	9.5	4.1	16.47	4
5.	10.0	4.3	18.25	5
10.	12.5	5.3	28.51	6
15.	15.2	6.5	42.16	7
20.	18.7	8.0	63.81	8
25.	20.0	8.5	72.99	9
30.	21.3	9.1	82.79	10
40.	23.5	10.0	100.77	11
50.	25.5	10.9	118.65	12
60.	27.5	11.7	137.99	13
90.	31.5	13.5	181.06	14
120.	35.3	15.1	227.38	15
150.	38.5	16.4	270.47	16
180.	41.3	17.6	311.24	17
210.	43.5	18.6	345.28	18
240.	46.3	19.8	391.16	19
270.	48.5	20.7	429.22	20
300.	50.5	21.6	465.35	21
330.	52.5	22.4	502.94	22
360.	54.0	23.1	532.09	23
390.	56.0	23.9	572.23	24
420.	58.0	24.8	613.84	25

36-B

TIME-MIN	WT-LOSS	WT-LOSS/AREA	(WT-LOSS/AREA)-SQR	
1.	6.5	2.6	6.75	1
2.	10.5	4.2	17.63	2
3.	14.5	5.8	33.61	3
4.	15.0	6.0	35.97	4
5.	15.5	6.2	38.41	5
10.	19.5	7.8	60.79	6
15.	22.7	9.1	82.38	7
20.	26.1	10.4	108.91	8
25.	27.7	11.1	122.67	9
30.	29.5	11.8	139.13	10
40.	33.5	13.4	179.42	11
50.	36.5	14.6	212.99	12
60.	39.5	15.8	249.44	13
90.	48.3	19.3	372.96	14
120.	55.5	22.2	492.45	15
150.	61.3	24.5	600.75	16
180.	66.3	26.5	702.75	17
210.	70.7	28.3	799.12	18
240.	74.7	29.9	892.10	19
270.	78.3	31.3	980.16	20
300.	81.4	32.5	1059.31	21
330.	83.5	33.4	1114.67	22
360.	86.5	34.6	1196.20	23
390.	88.5	35.4	1252.16	24
420.	91.0	36.4	1323.90	25

37-B

TIME-MIN	WT-LOSS	WT-LOSS/AREA	(WT-LOSS/AREA)-SQR	
1.	5.0	2.3	5.33	1
2.	9.5	4.4	19.24	2
3.	13.5	6.2	38.85	3
4.	13.5	6.2	38.85	4
5.	14.0	6.5	41.78	5
10.	16.8	7.8	60.16	6
15.	18.5	8.5	72.95	7
20.	22.2	10.2	105.05	8
25.	23.7	10.9	119.72	9
30.	24.5	11.3	127.94	10
40.	27.0	12.5	155.39	11
50.	28.8	13.3	176.79	12
60.	30.8	14.2	202.20	13
90.	34.8	16.1	258.13	14
120.	38.8	17.9	320.88	15
150.	41.0	18.9	358.30	16
180.	43.5	20.1	403.33	17
210.	45.8	21.1	447.11	18
240.	48.0	22.2	491.10	19
270.	50.0	23.1	532.67	20
300.	52.0	24.0	576.35	21
330.	53.0	24.5	598.74	22
360.	54.7	25.3	637.76	23
390.	56.0	25.9	668.43	24
420.	57.3	26.5	699.83	25

APPENDIX B
OXIDE DIFFUSION RESULTS

(Table and Figure numbers correspond to the run numbers on Table 1 in the text.
For several conditions, numbers exceeding the plotting routine's capabilities were generated and graphs were not plotted.)

TABLE B-1

800C-1/20 CONB

TIME-MIN	WT-LOSS	LOG(1-M(T)/Q)	M(T)/A-SQR	M(T)/Q
4.	-.0020	-.2905E-02	.2173E-06	.0067
9.	.1380	.1644E 00	.1035E-02	-.4600
14.	.2260	.2439E 00	.2775E-02	-.7533
31.	.2880	.2923E 00	.4507E-02	-.9600
41.	.2740	.2816E 00	.4079E-02	-.9133
42.	.2660	.2757E 00	.3845E-02	-.8867
44.	.2980	.2996E 00	.4825E-02	-.9933
52.	.2400	.2553E 00	.3130E-02	-.8000
62.	.2240	.2422E 00	.2726E-02	-.7467
72.	.1160	.1420E 00	.7311E-03	-.3867
82.	.1400	.1663E 00	.1065E-02	-.4667
92.	.1260	.1523E 00	.8626E-03	-.4200
102.	.1420	.1683E 00	.1096E-02	-.4733
112.	.1080	.1335E 00	.6338E-03	-.3600
122.	.1040	.1293E 00	.5877E-03	-.3467
132.	.1000	.1249E 00	.5434E-03	-.3333
142.	.1160	.1420E 00	.7311E-03	-.3867
152.	.1100	.1357E 00	.6575E-03	-.3667
161.	.0960	.1226E 00	.5218E-03	-.3267
171.	.1120	.1378E 00	.6816E-03	-.3733
181.	.1120	.1376E 00	.6816E-03	-.3733
191.	.1040	.1293E 00	.5877E-03	-.3467
211.	.1100	.1357E 00	.6575E-03	-.3667
231.	.1460	.1722E 00	.1158E-02	-.4867
251.	.1400	.1663E 00	.1065E-02	-.4667
281.	.1000	.1249E 00	.5434E-03	-.3333
295.	.1240	.1502E 00	.8355E-03	-.4133
315.	.1260	.1523E 00	.8626E-03	-.4200
355.	.0940	.1184E 00	.4801E-03	-.3133
433.	.0900	.1139E 00	.4401E-03	-.3000
446.	.1060	.1314E 00	.6105E-03	-.3533
481.	.1120	.1378E 00	.6816E-03	-.3733
500.	.1080	.1335E 00	.6338E-03	-.3600
536.	.0900	.1139E 00	.4401E-03	-.3000
596.	.0940	.1184E 00	.4801E-03	-.3133
655.	.0800	.1027E 00	.3477E-03	-.2667
707.	.0920	.1162E 00	.4599E-03	-.3067
774.	.0860	.1095E 00	.4019E-03	-.2867
834.	.0720	.9342E-01	.2817E-03	-.2400
893.	.0580	.7676E-01	.1826E-03	-.1933
953.	.0820	.1049E 00	.3654E-03	-.2733
1009.	.0900	.1139E 00	.4401E-03	-.3000
1069.	.0560	.7433E-01	.1704E-03	-.1867
1128.	.0760	.9867E-01	.3138E-03	-.2533
1188.	.0640	.8398E-01	.2226E-03	-.2133
1247.	.0700	.9108E-01	.2662E-03	-.2333
1307.	.0640	.8398E-01	.2226E-03	-.2133
1366.	.0600	.7918E-01	.1956E-03	-.2000
1425.	.0640	.8398E-01	.2226E-03	-.2133
1485.	.1000	.1249E 00	.5434E-03	-.3333

TABLE B-2

800C-1/1 CONB-1

TIME-MIN	WT-LOSS	LOG(1-M(T)/Q)	M(T)/A-SQR	M(T)/Q
7.	-.5980	-.3962E-02	.1943E-01	.0091
11.	-.7360	-.4920E-02	.2959E-01	.0113
16.	-.9960	-.6653E-02	.5390E-01	.0152
46.	-5.5920	-.3875E-01	.1699E 01	.0854
66.	-7.0840	-.4970E-01	.2727E 01	.1081
113.	-10.3200	-.7444E-01	.5787E 01	.1575
173.	-13.3560	-.9902E-01	.9693E 01	.2039
232.	-15.6840	-.1188E 00	.1337E 02	.2394
292.	-17.6100	-.1360E 00	.1685E 02	.2688
361.	-19.3460	-.1520E 00	.2034E 02	.2953
436.	-21.3360	-.1711E 00	.2473E 02	.3257
510.	-23.2300	-.1902E 00	.2932E 02	.3546
584.	-25.0780	-.2096E 00	.3417E 02	.3828
644.	-26.5420	-.2256E 00	.3828E 02	.4051
718.	-28.3460	-.2462E 00	.4366E 02	.4327
792.	-30.1320	-.2676E 00	.4933E 02	.4599
852.	-31.5340	-.2851E 00	.5403E 02	.4813
911.	-32.9420	-.3035E 00	.5896E 02	.5028
971.	-34.3260	-.3224E 00	.6402E 02	.5240
1015.	-35.3400	-.3367E 00	.6786E 02	.5394
1056.	-36.4740	-.3534E 00	.7229E 02	.5568
1116.	-37.8060	-.3737E 00	.7768E 02	.5771
1185.	-39.6700	-.4040E 00	.8551E 02	.6055
1265.	-41.2380	-.4312E 00	.9240E 02	.6295
1345.	-42.9000	-.4620E 00	.1000E 03	.6548
1414.	-44.3020	-.4898E 00	.1068E 03	.6762
1485.	-45.9760	-.5255E 00	.1149E 03	.7018
1604.	-48.1740	-.5773E 00	.1261E 03	.7353
1723.	-50.2160	-.6317E 00	.1370E 03	.7665
1842.	-52.0600	-.6875E 00	.1473E 03	.7947
1962.	-53.7260	-.7450E 00	.1565E 03	.8201
2081.	-55.2140	-.8036E 00	.1656E 03	.8428
2199.	-56.5840	-.8656E 00	.1740E 03	.8637
2318.	-57.7940	-.9268E 00	.1815E 03	.8822
2415.	-58.6280	-.9785E 00	.1868E 03	.8949
2471.	-59.0880	-.1009E 01	.1897E 03	.9019
2545.	-59.6980	-.1052E 01	.1936E 03	.9113
2605.	-60.1660	-.1088E 01	.1967E 03	.9184
2665.	-60.6000	-.1125E 01	.1995E 03	.9250
2725.	-61.0400	-.1166E 01	.2024E 03	.9317
2784.	-61.4120	-.1204E 01	.2049E 03	.9374
2854.	-61.7780	-.1244E 01	.2074E 03	.9430
2918.	-62.3080	-.1311E 01	.2109E 03	.9511
3037.	-62.9380	-.1406E 01	.2152E 03	.9607
3157.	-63.4940	-.1511E 01	.2191E 03	.9692
3366.	-64.2580	-.1718E 01	.2244E 03	.9809
3574.	-64.7980	-.1963E 01	.2261E 03	.9891
3782.	-65.1620	-.2272E 01	.2307E 03	.9947
3991.	-65.3880	-.2723E 01	.2323E 03	.9981
4288.	-65.5100	-.4515E 01	.2332E 03	1.0000

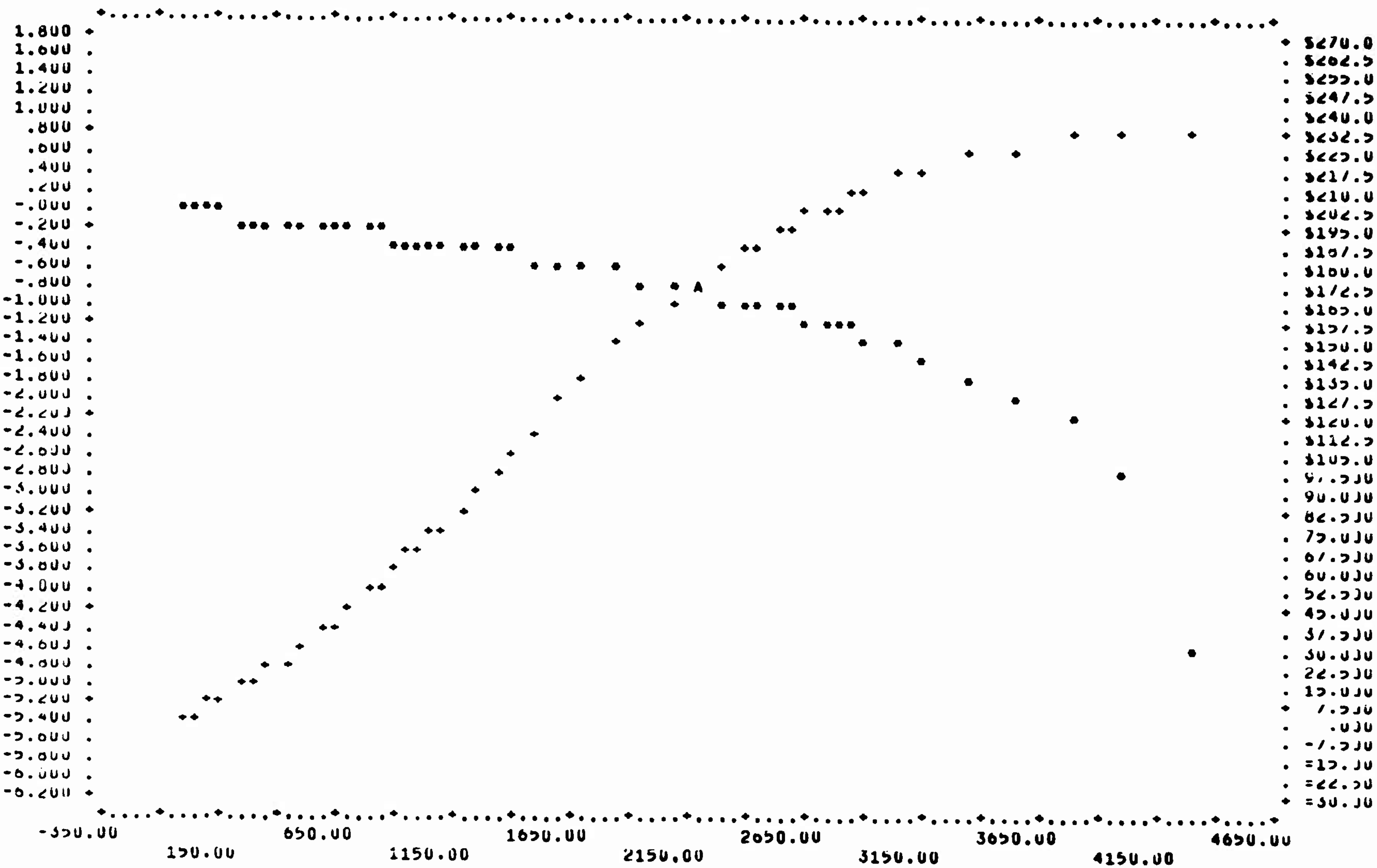

Figure B-2. 800C-1/1 CONB-1

TABLE B-3

800C-1/1 CONB-2

TIME-MIN	WT-LOSS	LOG(1-M(T)/Q)	M(T)/A-SUR	M(T)/Q
4.	-.0000	.0000E 00	.1105E-20	.0000
9.	-1.2920	-.1252E-01	.9070E-01	.0284
14.	-1.8020	-.1757E-01	.1764E 00	.0396
19.	-2.2160	-.2171E-01	.2668E 00	.0488
24.	-2.6420	-.2601E-01	.3793E 00	.0581
28.	-2.9480	-.2912E-01	.4722E 00	.0649
33.	-3.2900	-.3263E-01	.5881E 00	.0724
38.	-3.6200	-.3605E-01	.7120E 00	.0796
41.	-3.9560	-.3955E-01	.8504E 00	.0870
46.	-4.3160	-.4333E-01	.1012E 01	.0950
51.	-4.6560	-.4694E-01	.1176E 01	.1024
56.	-5.0400	-.5105E-01	.1380E 01	.1109
61.	-5.4400	-.5537E-01	.1606E 01	.1197
66.	-5.8440	-.5977E-01	.1856E 01	.1286
71.	-6.3060	-.6489E-01	.2162E 01	.1388
76.	-6.7960	-.7034E-01	.2510E 01	.1495
81.	-7.2800	-.7581E-01	.2880E 01	.1602
86.	-7.7820	-.8156E-01	.3291E 01	.1712
91.	-8.3320	-.8795E-01	.3772E 01	.1833
96.	-8.9080	-.9474E-01	.4312E 01	.1960
101.	-9.4840	-.1016E 00	.4887E 01	.2087
131.	-13.3180	-.1506E 00	.9637E 01	.2930
161.	-17.4420	-.2103E 00	.1653E 02	.3838
190.	-21.6500	-.2811E 00	.2549E 02	.4766
220.	-25.7960	-.3641E 00	.3616E 02	.5676
250.	-29.7120	-.4606E 00	.4797E 02	.6537
280.	-33.2480	-.5711E 00	.6006E 02	.7315
309.	-36.2880	-.6955E 00	.7155E 02	.7984
339.	-38.7980	-.8346E 00	.8179E 02	.8536
369.	-40.8060	-.9906E 00	.9048E 02	.8978
399.	-42.3360	-.1164E 01	.9739E 02	.9315
429.	-43.4280	-.1352E 01	.1025E 03	.9555
458.	-44.1500	-.1544E 01	.1059E 03	.9714
488.	-44.6180	-.1737E 01	.1082E 03	.9817
518.	-44.8920	-.1911E 01	.1095E 03	.9877
548.	-45.0680	-.2075E 01	.1104E 03	.9916
578.	-45.1820	-.2229E 01	.1109E 03	.9941
607.	-45.2520	-.2361E 01	.1113E 03	.9956
637.	-45.2980	-.2476E 01	.1115E 03	.9967
697.	-45.3740	-.2777E 01	.1119E 03	.9983
756.	-45.4220	-.3210E 01	.1121E 03	.9994
816.	-45.4360	-.3511E 01	.1122E 03	.9997
875.	-45.4480	-.4357E 01	.1122E 03	1.0000
935.	-45.4600	-.3656E 01	.1123E 03	1.0002
994.	-45.4580	-.3754E 01	.1123E 03	1.0002
1054.	-45.4320	-.3402E 01	.1122E 03	.9996
1113.	-45.4540	~~-.4025E 01~~	.1123E 03	1.0001
1173.	-45.4500	.1701E 39	.1122E 03	1.0000
1233.	-45.4500	.1701E 39	.1122E 03	1.0000

TABLE B-4

800C-20/1 CONB

TIME-MIN	WT-LOSS	LOG(1-M(T)/Q)	M(T)/A-SQR	M(T)/Q
6.	-.0040	-.2612E-04	.8694E-06	.0001
21.	-1.3640	-.8999E-02	.1011E 00	.0205
41.	-3.1840	-.2130E-01	.5508E 00	.0479
56.	-4.6000	-.3113E-01	.1150E 01	.0692
76.	-6.4820	-.4453E-01	.2283E 01	.0975
91.	-7.8920	-.5466E-01	.3384E 01	.1187
111.	-9.6920	-.6840E-01	.5104E 01	.1457
146.	-12.6400	-.9154E-01	.8681E 01	.1900
205.	-17.1440	-.1295E 00	.1597E 02	.2578
265.	-20.9960	-.1647E 00	.2395E 02	.3157
384.	-27.0320	-.2265E 00	.3970E 02	.4064
474.	-30.5560	-.2671E 00	.5073E 02	.4594
593.	-34.3760	-.3159E 00	.6421E 02	.5169
682.	-36.7780	-.3497E 00	.7350E 02	.5530
801.	-39.5380	-.3920E 00	.8494E 02	.5945
890.	-41.3680	-.4225E 00	.9299E 02	.6220
1010.	-43.5680	-.4623E 00	.1031E 03	.6551
1099.	-45.0560	-.4914E 00	.1103E 03	.6774
1218.	-46.8260	-.5288E 00	.1191E 03	.7040
1307.	-48.0160	-.5559E 00	.1253E 03	.7219
1427.	-49.4960	-.5921E 00	.1331E 03	.7442
1516.	-50.5340	-.6194E 00	.1388E 03	.7596
1636.	-51.8380	-.6564E 00	.1460E 03	.7794
1725.	-52.7700	-.6849E 00	.1513E 03	.7934
1844.	-53.9180	-.7228E 00	.1580E 03	.8107
1933.	-54.7040	-.7508E 00	.1626E 03	.8225
2042.	-55.6420	-.7867E 00	.1682E 03	.8366
2132.	-56.2940	-.8136E 00	.1722E 03	.8464
2251.	-57.1260	-.8505E 00	.1773E 03	.8589
2340.	-57.6780	-.8768E 00	.1808E 03	.8672
2459.	-58.3600	-.9117E 00	.1851E 03	.8775
2548.	-58.8520	-.9388E 00	.1882E 03	.8849
2667.	-59.4520	-.9742E 00	.1921E 03	.8939
2756.	-59.8780	-.1001E 01	.1948E 03	.9003
2875.	-60.4380	-.1037E 01	.1983E 03	.9083
3024.	-61.0400	-.1085E 01	.2024E 03	.9178
3262.	-61.9300	-.1162E 01	.2084E 03	.9311
2740.	-62.5040	-.1220E 01	.2123E 03	.9398
2978.	-63.1660	-.1299E 01	.2168E 03	.9497
3156.	-63.6340	-.1364E 01	.2200E 03	.9568
3494.	-64.1760	-.1455E 01	.2238E 03	.9649
3672.	-64.5380	-.1528E 01	.2263E 03	.9704
3910.	-64.9660	-.1635E 01	.2293E 03	.9768
4069.	-65.2460	-.1721E 01	.2313E 03	.9810
4327.	-65.5760	-.1853E 01	.2337E 03	.9860
4499.	-65.8040	-.1974E 01	.2353E 03	.9894
4637.	-66.1000	-.2210E 01	.2374E 03	.9938
4816.	-66.2840	-.2469E 01	.2387E 03	.9966
4990.	-66.3840	-.2723E 01	.2394E 03	.9981
5219.	-66.5120	-.4522E 01	.2404E 03	1.0000

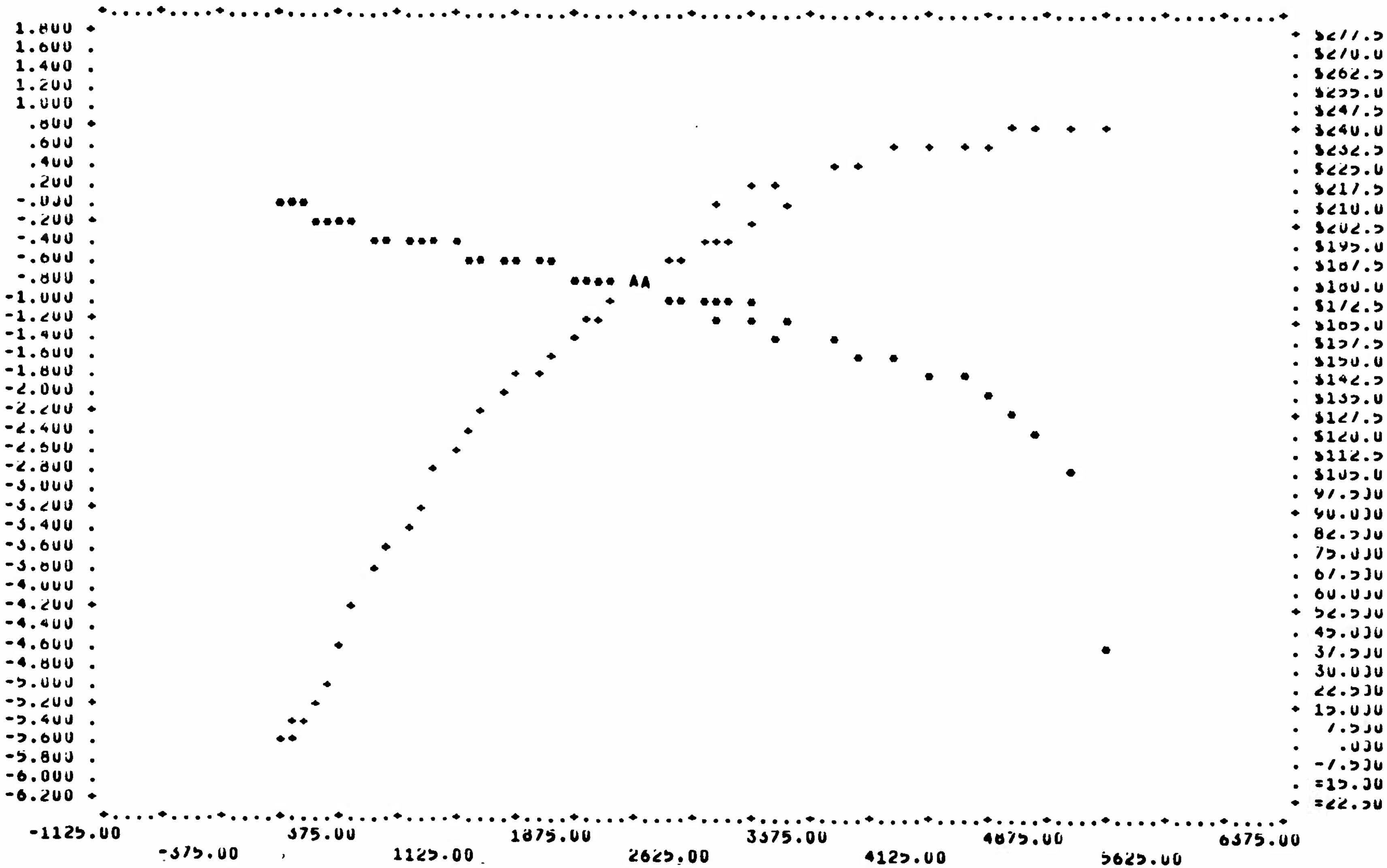

Figure B-4. 800C-20/1 CONB

TABLE B-5

1000C-1/20 CONB

TIME-MIN	WT-LOSS	LOG(1-M(T)/Q)	M(T)/A-SUR	M(T)/Q
5.	-.7140	-.3677E 00	.2770E-01	.5712
10.	-.9600	-.6345E 00	.5006E-01	.7680
15.	-.9200	-.5784E 00	.4599E-01	.7360
20.	-.9520	-.6227E 00	.4924E-01	.7616
79.	-1.0000	-.6990E 00	.5434E-01	.8000
139.	-1.0260	-.7467E 00	.5720E-01	.8208
199.	-1.0840	-.8768E 00	.6365E-01	.8672
258.	-1.0440	-.7830E 00	.5922E-01	.8352
318.	-1.0780	-.8614E 00	.6314E-01	.8624
377.	-1.0640	-.8274E 00	.6151E-01	.8512
437.	-1.0980	-.9151E 00	.6551E-01	.8784
496.	-1.1240	-.9965E 00	.6865E-01	.8992
556.	-1.1060	-.9385E 00	.6647E-01	.8848
615.	-1.1180	-.9763E 00	.6792E-01	.8944
677.	-1.1260	-.1003E 01	.6689E-01	.9008
734.	-1.1260	-.1003E 01	.6689E-01	.9008
794.	-1.1360	-.1040E 01	.7012E-01	.9088
857.	-1.1480	-.1088E 01	.7161E-01	.9184
913.	-1.1640	-.1162E 01	.7362E-01	.9312
972.	-1.1660	-.1173E 01	.7387E-01	.9328
973.	-1.2480	-.2796E 01	.8463E-01	.9984
974.	-1.1520	-.1106E 01	.7211E-01	.9216
984.	-1.1440	-.1072E 01	.7111E-01	.9152
991.	-.6280	-.3031E 00	.2143E-01	.5024

TABLE B-6

1000C-1/1 CONB-1

TIME-MIN	WT-LOSS	LOG(1-M(T)/Q)	M(T)/A-SQR	M(T)/Q
3.	.0000	.0000E 00	.1106E-21	-.0000
4.	-4.7600	-.3543E-01	.1231E 01	.0783
6.	-20.2540	-.1761E 00	.2229E 02	.3333
7.	-23.2660	-.2097E 00	.2941E 02	.3829
9.	-25.3140	-.2341E 00	.3482E 02	.4166
18.	-28.0920	-.2695E 00	.4288E 02	.4623
19.	-28.3580	-.2730E 00	.4370E 02	.4667
21.	-28.7680	-.2786E 00	.4497E 02	.4735
25.	-30.0360	-.2961E 00	.4902E 02	.4943
30.	-31.1120	-.3116E 00	.5259E 02	.5120
35.	-31.9400	-.3239E 00	.5543E 02	.5257
40.	-32.8340	-.3376E 00	.5858E 02	.5404
50.	-34.8040	-.3694E 00	.6582E 02	.5728
55.	-35.9460	-.3869E 00	.7021E 02	.5916
60.	-37.2300	-.4120E 00	.7531E 02	.6127
65.	-38.6000	-.4380E 00	.8096E 02	.6353
70.	-40.0320	-.4671E 00	.8708E 02	.6589
75.	-41.5440	-.5000E 00	.9378E 02	.6837
80.	-43.0720	-.5359E 00	.1008E 03	.7089
85.	-44.6240	-.5758E 00	.1082E 03	.7344
90.	-46.1480	-.6189E 00	.1157E 03	.7595
95.	-47.6700	-.6607E 00	.1235E 03	.7846
100.	-49.1640	-.7193E 00	.1313E 03	.8092
105.	-50.5560	-.7748E 00	.1389E 03	.8321
110.	-51.9700	-.8396E 00	.1468E 03	.8553
115.	-53.2240	-.9065E 00	.1539E 03	.8760
120.	-54.5560	-.9909E 00	.1617E 03	.8979
135.	-57.4620	-.1265E 01	.1794E 03	.9457
150.	-59.2680	-.1610E 01	.1909E 03	.9754
165.	-60.1920	-.2029E 01	.1969E 03	.9907
180.	-60.6280	-.2603E 01	.1997E 03	.9978
195.	-60.7660	-.4005E 01	.2006E 03	1.0001
210.	-60.7840	-.3403E 01	.2008E 03	1.0004
224.	-60.8000	-.3182E 01	.2009E 03	1.0007
238.	-60.7940	-.3252E 01	.2008E 03	1.0006
252.	-60.7660	-.4005E 01	.2006E 03	1.0001
267.	-60.7980	-.3204E 01	.2008E 03	1.0006
282.	-60.7820	-.3441E 01	.2007E 03	1.0004
297.	-60.7860	-.3369E 01	.2008E 03	1.0004
312.	-60.7680	-.3861E 01	.2006E 03	1.0001

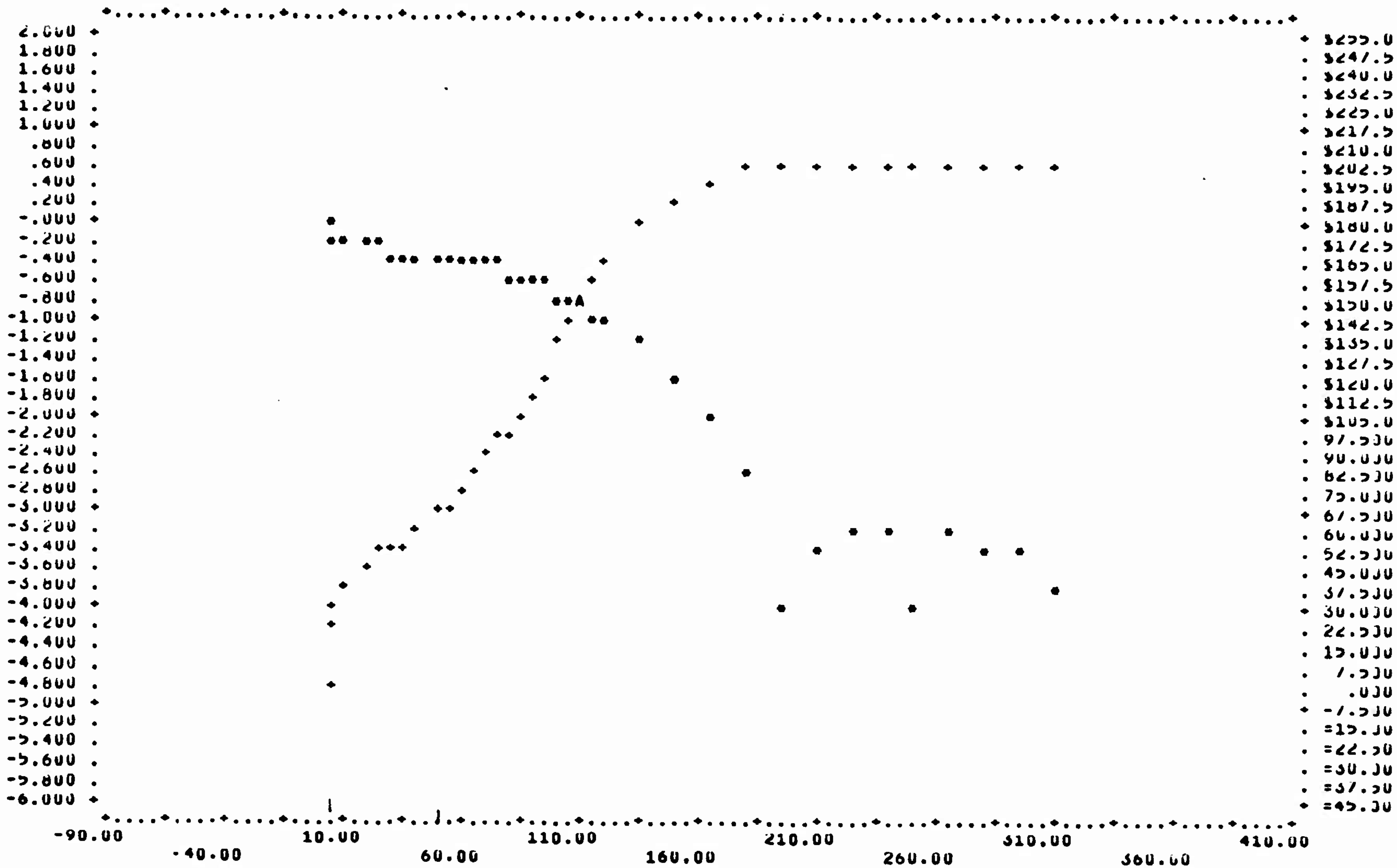

Figure B-6. 1000C-1/1 CONB-1

TABLE B-7

1000C-1/1 CONB-2

TIME-MIN	WT-LOSS	LOG(1-M(T)/Q)	M(T)/A-SUR	M(T)/Q
2.	13.9620	.1276E 00	.1059E 02	-.3416
4.	-.1700	-.1810E-02	.1570E-02	.0042
7.	-2.3380	-.2558E-01	.2970E 00	.0572
11.	-3.2900	-.3645E-01	.5881E 00	.0805
15.	-4.4080	-.4956E-01	.1056E 01	.1079
20.	-5.5960	-.6395E-01	.1702E 01	.1369
25.	-6.5660	-.7606E-01	.2343E 01	.1607
30.	-7.6260	-.8969E-01	.3160E 01	.1866
35.	-8.4120	-.1001E 00	.3845E 01	.2058
40.	-9.2760	-.1118E 00	.4675E 01	.2270
45.	-10.2260	-.1251E 00	.5682E 01	.2502
50.	-11.2140	-.1393E 00	.6833E 01	.2744
55.	-12.3200	-.1558E 00	.8247E 01	.3014
60.	-13.5360	-.1747E 00	.9956E 01	.3312
65.	-14.8160	-.1955E 00	.1193E 02	.3625
70.	-16.2080	-.2194E 00	.1427E 02	.3966
75.	-17.6100	-.2448E 00	.1685E 02	.4309
80.	-19.0860	-.2733E 00	.1979E 02	.4670
85.	-20.6080	-.3047E 00	.2308E 02	.5042
90.	-22.1180	-.3384E 00	.2658E 02	.5412
93.	-22.9700	-.3586E 00	.2867E 02	.5620
97.	-24.4980	-.3973E 00	.3261E 02	.5994
102.	-26.0080	-.4393E 00	.3675E 02	.6364
107.	-27.5300	-.4862E 00	.4118E 02	.6736
111.	-28.9840	-.5364E 00	.4565E 02	.7092
116.	-30.4020	-.5915E 00	.5022E 02	.7439
121.	-31.7500	-.6514E 00	.5477E 02	.7769
126.	-32.9580	-.7131E 00	.5902E 02	.8064
130.	-33.7980	-.7619E 00	.6207E 02	.8270
135.	-34.8460	-.8315E 00	.6598E 02	.8526
140.	-35.7760	-.9043E 00	.6955E 02	.8754
145.	-36.6040	-.9814E 00	.7280E 02	.8956
150.	-37.3300	-.1062E 01	.7572E 02	.9134
155.	-37.9520	-.1146E 01	.7826E 02	.9286
157.	-38.2000	-.1185E 01	.7929E 02	.9347
162.	-38.6640	-.1268E 01	.8123E 02	.9460
167.	-39.0920	-.1361E 01	.8304E 02	.9565
187.	-40.1800	-.1773E 01	.8772E 02	.9831
207.	-40.5760	-.2143E 01	.8946E 02	.9928
227.	-40.7560	-.2554E 01	.9025E 02	.9972
247.	-40.7960	-.2742E 01	.9043E 02	.9982
267.	-40.8160	-.2879E 01	.9052E 02	.9987
287.	-40.8480	-.3269E 01	.9066E 02	.9995
302.	-40.8120	-.2846E 01	.9050E 02	.9986
322.	-40.8480	-.3269E 01	.9066E 02	.9995
342.	-40.8060	-.2805E 01	.9048E 02	.9984
362.	-40.8380	-.3106E 01	.9062E 02	.9992
422.	-40.8040	-.2792E 01	.9047E 02	.9984
453.	-40.9940	-.2518E 01	.9131E 02	1.0030
454.	-40.8720	-.4310E 01	.9077E 02	1.0000

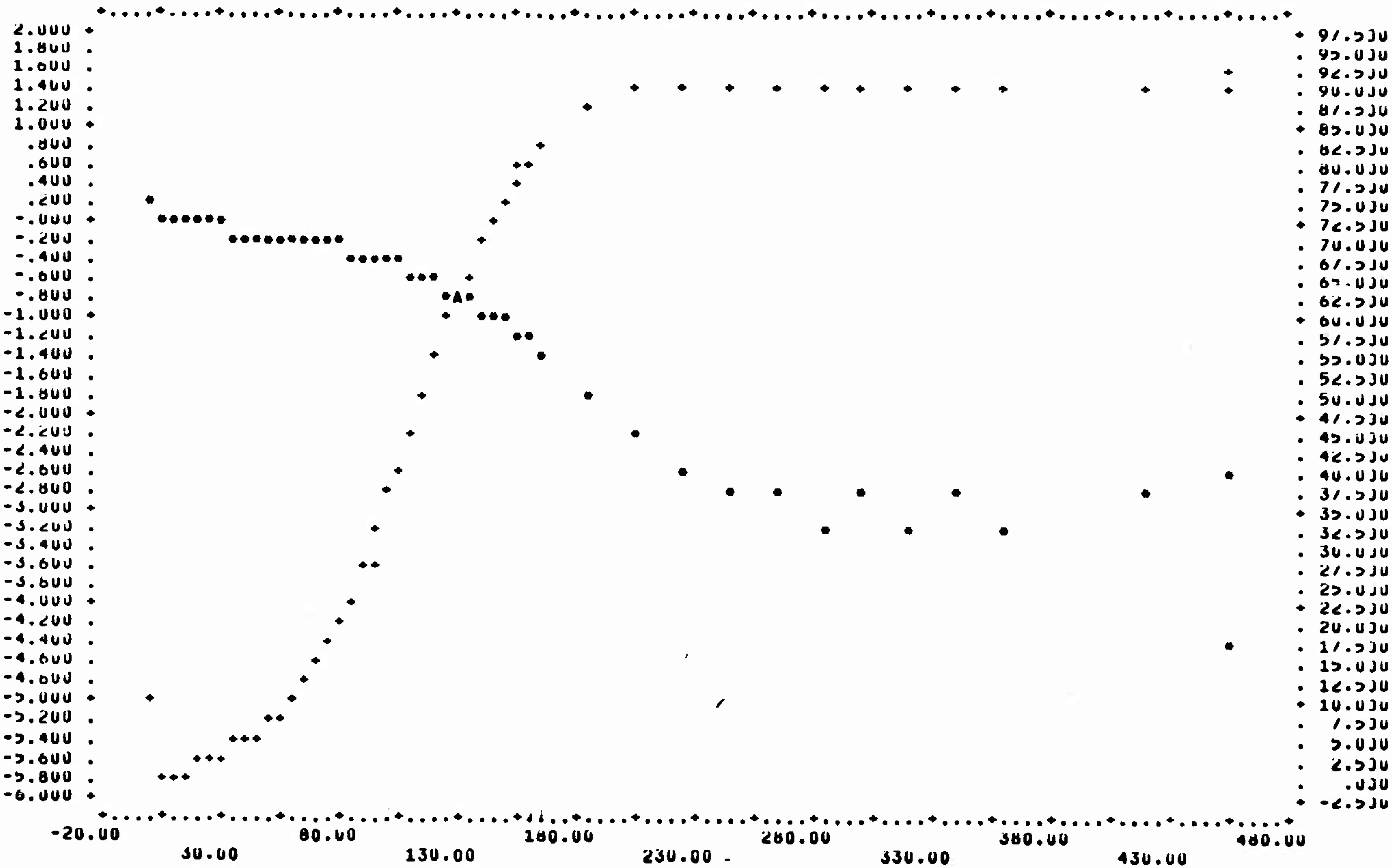

Figure B-7. 1000C-1/1 CONB-2

TABLE B-8

1000C 20/1 CONB

TIME-MIN	WT-LOSS	LOG(1-M(T)/Q)	M(T)/A-SQR	M(T)/Q
1.	-.3660	-.1413E-02	.7279E-02	.0032
4.	-.6900	-.2668E-02	.2587E-01	.0061
5.	-1.7360	-.6745E-02	.1638E 00	.0154
6.	-2.0860	-.8117E-02	.2364E 00	.0185
11.	-5.6530	-.2236E-01	.1736E 01	.0502
16.	-9.2060	-.3703E-01	.4605E 01	.0817
21.	-12.6180	-.5159E-01	.8651E 01	.1120
26.	-15.9760	-.6642E-01	.1387E 02	.1418
31.	-19.3000	-.8162E-01	.2024E 02	.1713
36.	-22.6160	-.9732E-01	.2779E 02	.2008
41.	-25.8920	-.1134E 00	.3643E 02	.2298
46.	-29.1360	-.1300E 00	.4613E 02	.2586
51.	-32.3320	-.1469E 00	.5680E 02	.2870
56.	-35.6080	-.1650E 00	.6889E 02	.3161
61.	-38.6490	-.1825E 00	.8116E 02	.3431
65.	-41.6026	-.2002E 00	.9404E 02	.3693
70.	-44.4706	-.2181E 00	.1075E 03	.3948
75.	-47.2406	-.2361E 00	.1213E 03	.4194
80.	-49.9146	-.2542E 00	.1354E 03	.4431
148.	-84.7886	-.6067E 00	.3906E 03	.7527
150.	-84.6286	-.6042E 00	.3892E 03	.7513
152.	-85.1686	-.6127E 00	.3941E 03	.7560
172.	-90.3086	-.7026E 00	.4431E 03	.8017
191.	-94.5086	-.7931E 00	.4853E 03	.8390
211.	-97.9686	-.8850E 00	.5215E 03	.8697
251.	-103.0286	-.1068E 01	.5766E 03	.9146
291.	-106.2886	-.1246E 01	.6136E 03	.9435
330.	-108.3886	-.1422E 01	.6383E 03	.9622
370.	-109.7486	-.1569E 01	.6545E 03	.9742
420.	-110.6486	-.1750E 01	.6652E 03	.9822
460.	-111.2286	-.1899E 01	.6722E 03	.9874
500.	-111.5886	-.2026E 01	.6766E 03	.9906
540.	-111.8286	-.2137E 01	.6795E 03	.9927
579.	-112.0486	-.2273E 01	.6822E 03	.9947
619.	-112.1686	-.2369E 01	.6836E 03	.9957
659.	-112.2486	-.2448E 01	.6846E 03	.9964
699.	-112.3086	-.2518E 01	.6853E 03	.9970
738.	-112.3886	-.2634E 01	.6863E 03	.9977
778.	-112.4486	-.2748E 01	.6871E 03	.9982
818.	-112.4686	-.2793E 01	.6873E 03	.9984
858.	-112.5486	-.3046E 01	.6883E 03	.9991
897.	-112.5886	-.3264E 01	.6888E 03	.9995
937.	-112.6086	-.3435E 01	.6890E 03	.9996
997.	-112.6486	-.4906E 01	.6895E 03	1.0000
1036.	-112.6486	-.4906E 01	.6895E 03	1.0000
1076.	-112.6086	-.3435E 01	.6890E 03	.9996
1095.	-112.4886	-.2844E 01	.6875E 03	.9986
1113.	-112.4686	-.2793E 01	.6873E 03	.9984
1177.	-112.4686	-.2793E 01	.6873E 03	.9984

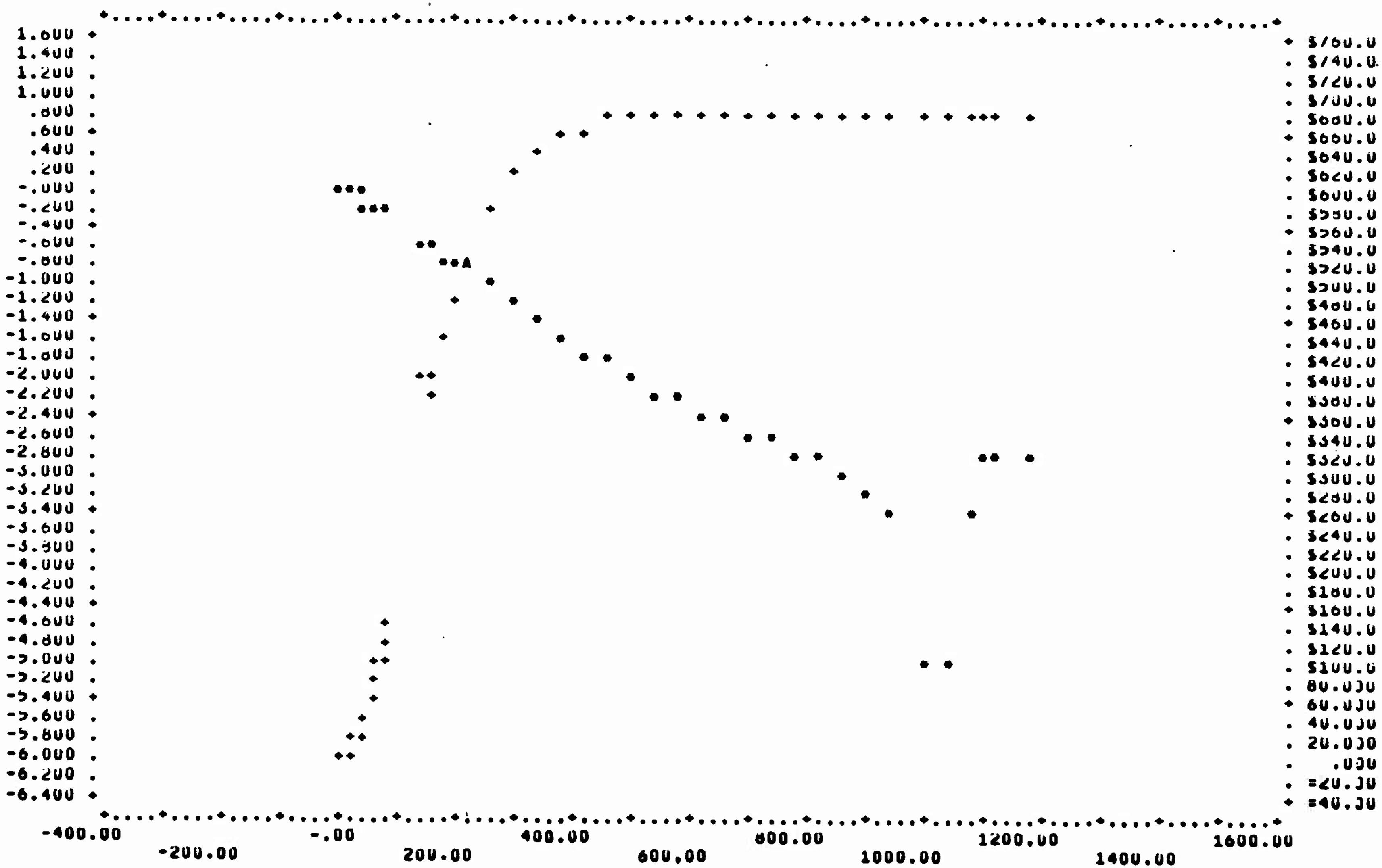

Figure B-8. 1000C 20/1 CONB

TABLE B-9

1175C-1/20 CONB

TIME-MIN	WT-LOSS	LOG(1-M(T)/Q)	M(T)/A-SQR	M(T)/Q
13.	.0000	.0000E 00	.1088E-21	-.0000
23.	-3.3400	-.3972E-01	.6061E 00	.0874
33.	-5.4940	-.6741E-01	.1640E 01	.1438
43.	-7.7750	-.9879E-01	.3285E 01	.2034
53.	-9.8980	-.1302E 00	.5323E 01	.2590
63.	-11.7740	-.1600E 00	.7532E 01	.3081
73.	-13.5120	-.1895E 00	.9920E 01	.3536
83.	-15.2140	-.2205E 00	.1258E 02	.3981
93.	-16.6720	-.2489E 00	.1510E 02	.4363
103.	-17.9900	-.2763E 00	.1759E 02	.4707
113.	-19.0960	-.3008E 00	.1981E 02	.4997
122.	-20.0320	-.3226E 00	.2180E 02	.5242
132.	-20.8460	-.3424E 00	.2361E 02	.5455
142.	-21.4720	-.3584E 00	.2505E 02	.5619
152.	-22.0460	-.3735E 00	.2641E 02	.5769
182.	-23.3520	-.4101E 00	.2963E 02	.6111
242.	-25.1600	-.4664E 00	.3440E 02	.6584
302.	-26.5400	-.5150E 00	.3827E 02	.6945
361.	-27.6980	-.5603E 00	.4169E 02	.7248
422.	-28.6060	-.5995E 00	.4446E 02	.7485
480.	-29.4540	-.6396E 00	.4714E 02	.7707
540.	-30.1940	-.6780E 00	.4954E 02	.7901
599.	-30.8940	-.7176E 00	.5186E 02	.8084
659.	-31.4500	-.7519E 00	.5374E 02	.8230
718.	-32.0240	-.7904E 00	.5572E 02	.8380
778.	-32.5380	-.8260E 00	.5753E 02	.8514
837.	-32.8380	-.8516E 00	.5859E 02	.8593
897.	-33.2960	-.8903E 00	.6024E 02	.8713
956.	-33.5660	-.9148E 00	.6122E 02	.8783
1016.	-34.1140	-.9692E 00	.6323E 02	.8927
1076.	-34.3500	-.9950E 00	.6411E 02	.8988
1136.	-34.6580	-.1031E 01	.6527E 02	.9069
1195.	-34.8780	-.1059E 01	.6610E 02	.9127
1254.	-35.1760	-.1099E 01	.6723E 02	.9205
1314.	-35.5120	-.1150E 01	.6852E 02	.9292
1373.	-35.6380	-.1171E 01	.6901E 02	.9325
1394.	-35.7180	-.1185E 01	.6932E 02	.9346
1442.	-35.9340	-.1224E 01	.7016E 02	.9403
1501.	-36.0940	-.1255E 01	.7079E 02	.9445
1561.	-36.2740	-.1294E 01	.7150E 02	.9492
1621.	-36.4780	-.1342E 01	.7230E 02	.9545
1680.	-36.6220	-.1380E 01	.7287E 02	.9583
1740.	-36.8120	-.1435E 01	.7363E 02	.9633
1800.	-36.9180	-.1469E 01	.7406E 02	.9660
1909.	-37.0840	-.1528E 01	.7472E 02	.9704
1988.	-37.5140	-.1736E 01	.7647E 02	.9816
2166.	-37.7980	-.1961E 01	.7763E 02	.9891
2345.	-37.9780	-.2206E 01	.7837E 02	.9938
2523.	-38.2040	-.3503E 01	.7931E 02	.9997
2730.	-38.3200	-.2565E 01	.7979E 02	1.0027

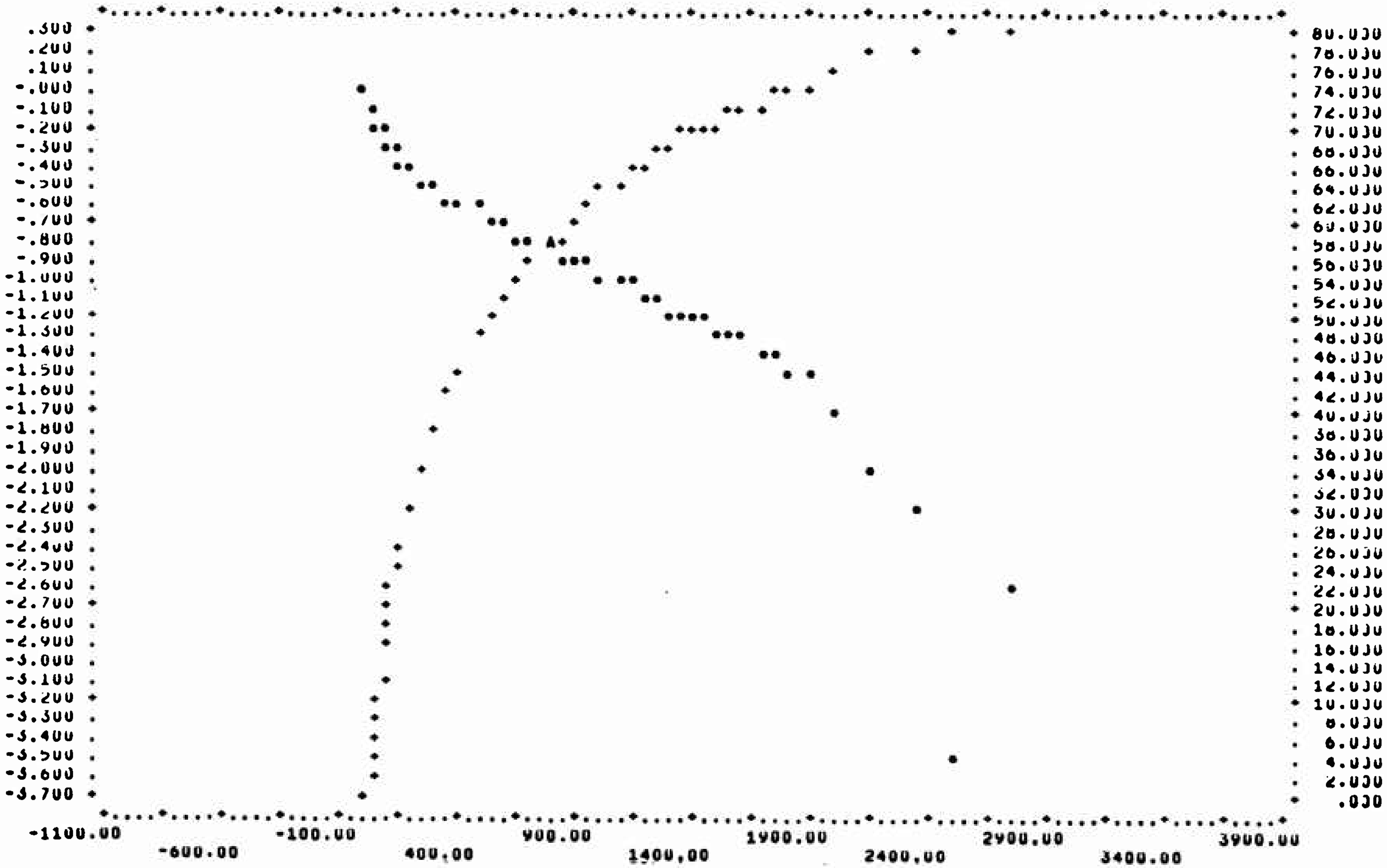

Figure B-9. 1175C-1/20 CONB

TABLE B-10

1175C-1/1 CONB

TIME-MIN	WT-LOSS	LOG(1-M(T)/Q)	M(T)/A-SQR	M(T)/Q
5.	.0000	.0000E 00	.0000E 00	.0000
10.	-7.6340	-.8571E-01	.3167E 01	.1791
15.	-9.6160	-.1110E 00	.5024E 01	.2256
20.	-11.1640	-.1319E 00	.6772E 01	.2619
25.	-12.6760	-.1533E 00	.8731E 01	.2974
30.	-14.3080	-.1776E 00	.1112E 02	.3357
35.	-15.9780	-.2040E 00	.1387E 02	.3749
39.	-17.7540	-.2340E 00	.1713E 02	.4165
44.	-20.8240	-.2912E 00	.2356E 02	.4886
49.	-21.5820	-.3066E 00	.2531E 02	.5063
54.	-23.6040	-.3504E 00	.3027E 02	.5538
59.	-25.6340	-.3995E 00	.3570E 02	.6014
64.	-27.6660	-.4548E 00	.4159E 02	.6491
69.	-29.5900	-.5146E 00	.4757E 02	.6942
74.	-31.3860	-.5790E 00	.5353E 02	.7363
79.	-33.0510	-.6486E 00	.5935E 02	.7754
84.	-34.5180	-.7208E 00	.6474E 02	.8098
89.	-35.8410	-.7982E 00	.6980E 02	.8409
94.	-36.9700	-.8773E 00	.7427E 02	.8674
99.	-37.9360	-.9587E 00	.7820E 02	.8900
104.	-38.5620	-.1021E 01	.8080E 02	.9047
163.	-42.1040	-.1914E 01	.9632E 02	.9878
223.	-42.3500	-.2192E 01	.9745E 02	.9936
283.	-42.4340	-.2351E 01	.9784E 02	.9955
342.	-42.4580	-.2410E 01	.9795E 02	.9961
402.	-42.4940	-.2516E 01	.9812E 02	.9970
461.	-42.5320	-.2666E 01	.9829E 02	.9978
521.	-42.5480	-.2749E 01	.9837E 02	.9982
580.	-42.5660	-.2866E 01	.9845E 02	.9986
640.	-42.5760	-.2948E 01	.9850E 02	.9989
669.	-42.5940	-.3153E 01	.9858E 02	.9993
760.	-42.6100	-.3484E 01	.9865E 02	.9997
820.	-42.6020	-.3287E 01	.9862E 02	.9995
880.	-42.6000	-.3249E 01	.9861E 02	.9994
940.	-42.6020	-.3287E 01	.9862E 02	.9995
1000.	-42.6120	-.3550E 01	.9866E 02	.9997
1060.	-42.6040	-.3329E 01	.9862E 02	.9995
1120.	-42.6080	-.3426E 01	.9864E 02	.9996
1179.	-42.6140	-.3630E 01	.9867E 02	.9998
1239.	-42.6060	-.3374E 01	.9863E 02	.9996
1299.	-42.5980	-.3215E 01	.9860E 02	.9994
1359.	-42.5840	-.3026E 01	.9853E 02	.9991
1441.	-42.6240	.1701E 39	.9872E 02	1.0000
1452.	-42.2180	-.2021E 01	.9685E 02	.9905

TABLE B-11

1175C-20/1 CONB

TIME-MIN	WT-LOSS	LOG(1-M(T)/Q)	M(T)/A-SQR	M(T)/Q
2.	.0000	.0000E 00	.1176E-21	-.0000
17.	.0040	.3004E-04	.8694E-06	-.0001
32.	-.0840	-.6314E-03	.3834E-03	.0015
47.	-.3300	-.2486E-02	.5917E-02	.0057
62.	-.7200	-.5442E-02	.2817E-01	.0125
77.	-1.2280	-.9323E-02	.8194E-01	.0212
92.	-1.8160	-.1386E-01	.1792E 00	.0314
107.	-2.3810	-.1826E-01	.3080E 00	.0412
196.	-6.2340	-.4955E-01	.2112E 01	.1078
286.	-9.8280	-.8091E-01	.5248E 01	.1700
375.	-13.1880	-.1124E 00	.9450E 01	.2281
465.	-16.2720	-.1435E 00	.1439E 02	.2814
554.	-19.2520	-.1759E 00	.2014E 02	.3330
643.	-21.9980	-.2079E 00	.2629E 02	.3805
732.	-24.5700	-.2403E 00	.3280E 02	.4249
822.	-26.9760	-.2729E 00	.3954E 02	.4666
911.	-29.2020	-.3054E 00	.4634E 02	.5051
1000.	-31.3220	-.3389E 00	.5331E 02	.5417
1149.	-34.6140	-.3965E 00	.6510E 02	.5987
1238.	-36.4220	-.4317E 00	.7208E 02	.6299
1328.	-38.1020	-.4672E 00	.7888E 02	.6590
1389.	-39.4320	-.4975E 00	.8449E 02	.6820
1478.	-40.8440	-.5322E 00	.9064E 02	.7064
1573.	-42.0160	-.5633E 00	.9592E 02	.7267
1635.	-43.1440	-.5955E 00	.1011E 03	.7462
1725.	-44.3760	-.6335E 00	.1070E 03	.7675
1762.	-45.3460	-.6661E 00	.1117E 03	.7843
1845.	-45.8440	-.6838E 00	.1142E 03	.7929
1965.	-47.2080	-.7363E 00	.1211E 03	.8165
2084.	-48.3920	-.7877E 00	.1272E 03	.8369
2262.	-49.8950	-.8631E 00	.1353E 03	.8630
2438.	-50.9240	-.9235E 00	.1409E 03	.8807
2587.	-52.1520	-.1009E 01	.1478E 03	.9020
2765.	-52.9640	-.1076E 01	.1524E 03	.9160
2943.	-53.6080	-.1138E 01	.1562E 03	.9272
3122.	-54.1360	-.1196E 01	.1592E 03	.9363
3300.	-54.5440	-.1247E 01	.1617E 03	.9433
3428.	-54.8680	-.1292E 01	.1636E 03	.9489
3656.	-55.1400	-.1334E 01	.1652E 03	.9536
3834.	-55.3680	-.1373E 01	.1666E 03	.9576
4013.	-55.5500	-.1408E 01	.1677E 03	.9609
4191.	-55.7120	-.1438E 01	.1686E 03	.9635
4369.	-57.8120	-.3859E 01	.1816E 03	.9999
4547.	-55.9040	-.1480E 01	.1698E 03	.9669
4725.	-55.9840	-.1498E 01	.1703E 03	.9682
4903.	-56.0760	-.1521E 01	.1709E 03	.9698
5141.	-56.1240	-.1533E 01	.1712E 03	.9707
5320.	-56.6240	-.1664E 01	.1742E 03	.9793
5498.	-57.2800	-.2030E 01	.1783E 03	.9907
5666.	-56.3920	-.1607E 01	.1726E 03	.9753

Astronuclear Laboratory

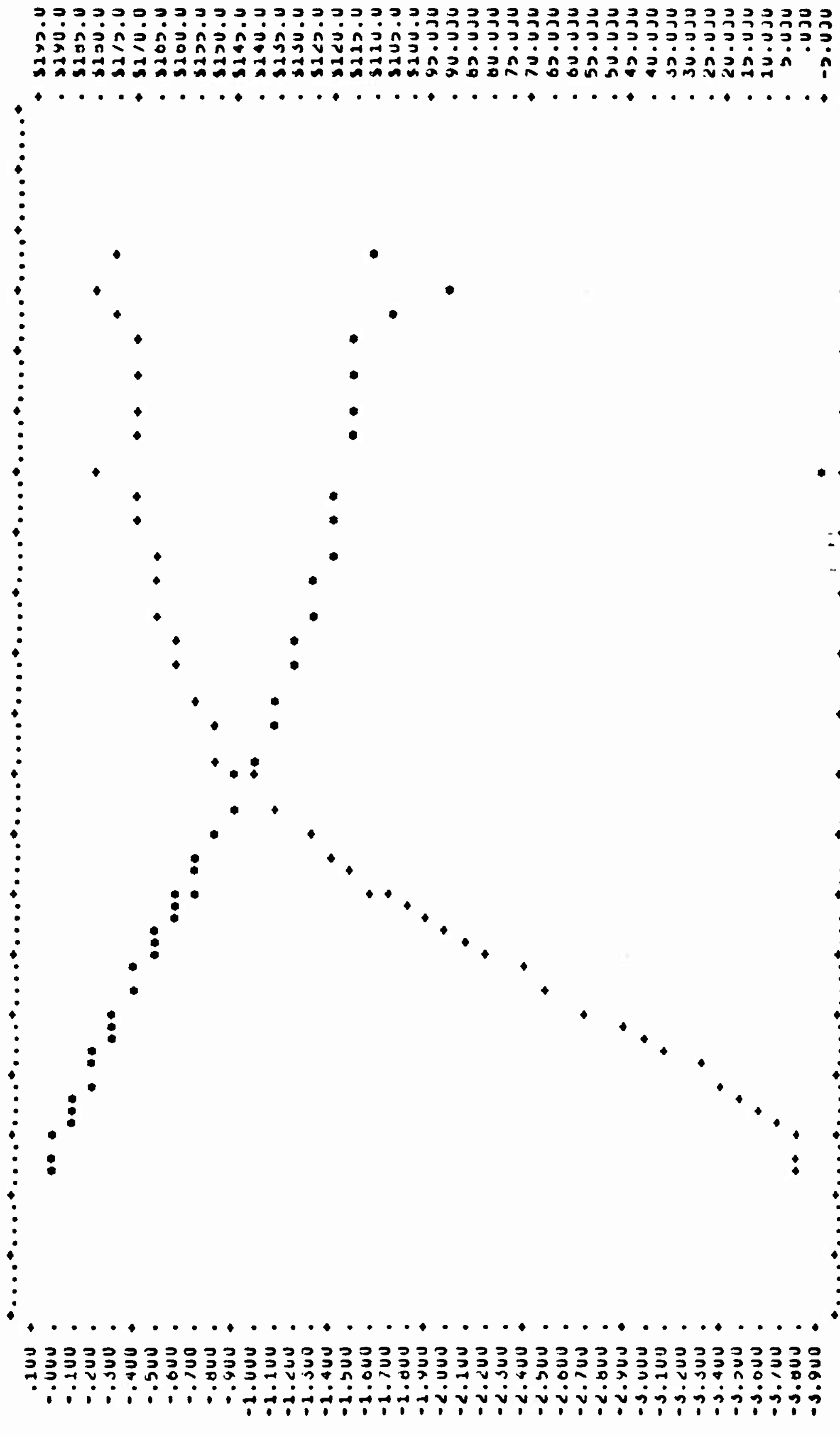

Figure B-11. 1176C-20/1 CONB

APPENDIX C

X-RAY DIFFRACTION d SPACINGS AND RELATIVE INTENSITIES

Table C-1. X-ray Diffraction Lines and Relative Intensities for the Oxide Formed on a Nb-Cr Alloy at 1200°C

1-A (Pressed and Sintered) and 1-B (Arc Welded)		
d, Å	I/I_o	Comments
5.1	vw	o
4.8	vw	o
3.75	s	o
3.57	s	o
3.44	mw	o
3.29	s	*
2.79	m	o
2.70	vw	o
2.53	ms	*
2.32	m	*
2.23	vw	*
2.05	m	o
1.91	mw	o
1.785	vw	-
1.571	mw	-
1.568	mw	-
1.548	v	o
1.58	v	o
1.47	vw	*
1.40	w	*
1.375	w(B)	*

o NbO_2 - (19-859) (monoclinic)

* $CrNbO_4$ - (20-311) Tetragonal)

(B) Broad Peak

- No match found

Table C-2. X-ray Diffraction Lines and Relative Intensities for the Oxide Formed on a Nb-Cr Alloy at 1200°C

5-A (Pressed and Sintered)			5-B (Arc Melted)		
d, Å	I/I_o	Comments	d, Å	I/I_o	Comments
-			5.1	w	o
-			4.75	w	o
3.75	m	o	3.75	s	o
3.58	m	o	3.67	s	+
3.43	w	o	3.42-3	m	o
3.28	s	Δ	3.28	s	Δ
2.78	mw	-	2.78	m	-
2.69	w	o	2.69	w	o
-			2.55	mw(B)	-
2.52-3	ms	*Δ	2.52-3	ms	*Δ
2.32	mw	o*Δ	2.32	mw	o*Δ
2.23	vw	*	2.23	vw	*
2.05	w	o	2.085	m	-
1.91	w	o	2.05	m	o
1.79	vw	o	1.91	mw	o
1.71	ms	*Δ	1.785	w	o
1.68	m(B)	oΔ	1.71	ms	*Δ
1.64	w	*	1.68	m(B)	oΔ+
			1.64	w	*
1.575	w	-	1.60	w	-
1.505	w	-	1.57	mw	·
1.47	vw	Δ	1.505	vw	-
1.40	w	o	1.47	vw	Δ
1.37-8	w(B)	+	1.415	vw	
			1.40	w	o
			1.37-8	w(B)	*

* $CrNbO_4$ (20-311)　　+ Cr_2O_3 (6-0504)

o NbO_2 (19-859)　　Δ $NbCr_2$ (50-0701)

Table C-3. X-ray Diffraction Lines and Relative Intensities for the Oxide Formed on a Nb-Fe-Al Alloy at 1200°C

11-A (Pressed and Sintered)			11-B (Arc Melted)		
d, Å	I/I_o	Comments	d, Å	I/I_o	Comments
6.4	w		-		
6.1	w		-		
4.72	w		-		
3.8	mw		3.79	w	
3.7	mw	*	3.72	mw	*
3.6	mw		3.60	ms	
3.54	s	*	3.52	ms	
3.40	m		-		
3.09	mw	*	3.13	w	
2.88	m	*	2.92	m	
2.77	w		2.87	m	
2.68	mw	*	2.80	vw	
2.30	w		2.69	m(B)	*
2.07	w(B)	*	2.04	m(B)	*
2.04	m	*	-		
1.90	w		-		
1.87	w	*	1.88	mw(B)	*
1.78	w		1.79	mw(B)	
1.625	m				
1.625	m		-		
1.58	m	*	1.58	mw(B)	*
-			1.50	mw(B)	
-			1.425	mw(B)	
-			1.39	mw(B)	

* $NbAlO_4$ (14-494)

Table C-4. X-Ray Diffraction Lines and Relative Intensities for the Oxide Formed on a Nb-Cr Alloy at 1200°C

12-A (Pressed and Sintered)			12-B (Arc Melted)		
d, Å	I/I_o	Comments	d, Å	I/I_o	Comments
5.1	w	o	-		
4.75	w	o	-		
3.75	s	o	-		
3.67	s	-	-		
3.42-3	m	o	3.3	w	-
3.28	s	*	3.25	s	*
2.78	m	o	-		
2.69	w	-	-		
2.52-3	ms	*	2.51	s	*
2.32	mw	*	2.31	mw	*
2.23	vw	*	2.21	mw	*
2.05	m	o	-		
1.91	mw	o	-		
1.785	w	-	-		
1.71	ms	*	1.70	s	*
1.68	m(B)	o	-		
1.64	w	*	1.632	mw	*
1.57	mw	-	-		
1.505	vw	*	1.50	w	*
1.47	vw	*	1.465	w	*
1.40	w	*	-		
1.37-8	w(B)	*	1.37	m(B)	*

o NbO_2 (19-859)
* $NbCrO_4$ (20-311)

Table C-5. X-ray Diffraction Lines and Relative Intensities for the Oxide Formed on a Nb-Co-Al Alloy at 1200°C

13-A (Pressed and Sintered)			13-B (Arc Melted)		
d, Å	I/I_o	Comments	d, Å	I/I_o	Comments
--	-	-	7.1	w	-
6.4	w	-	--	-	-
6.1	w	o	--	-	
--	-		5.1	w	o*
4.72	w	*	--	-	
3.80	mw	*	--	-	
3.70	mw	o	--	-	
3.60	mw	*	3.62	m	*
3.54	s	o	3.54	s	o
3.40	m	*	3.40	m	*
--	-	-	3.30	m	-
3.09	mw	o	3.09	w	o
--	-	-	2.93	ms	-
2.88	m		--	-	
2.77	w	*	2.78	mw	-
2.68	mw	o	2.68	mw	o
--	-		2.55	w	-
--	-		2.35	vw	-
2.30	vw	*	2.30	vw	*
2.07	w (B)		--	-	
2.04	m	*	2.05	w (B)	*
1.90	w	*	1.91	w	*
1.87	w		1.87	w	-
1.78	w	*	--	-	
--	-		1.72	w (B)	*
--	-		1.67	w (B)	*
1.625	m	*	--	-	
1.58	m	*	1.57	mw	*
1.445	mw		1.45	mw	-

* Al_2O_3-Nb_2O_5 (16-545)
o $NbAlO_4$ (14-494)

Table C-6. X-ray Diffraction Lines and Relative Intensities for the Oxides Formed on an Arc Melted Nb-Fe-Al Alloy at 1200°C

14 (Arc Melted)			14 (As-Oxidized)			14 (After Grinding)		
d, Å	I/I_o*	Comments	d, Å	I/I_o**	Comments	d, Å	I/I_o**	Comments
5.6	vw							
5.5	vw							
			3.98	(8)				
3.70	m	o				3.75	(50)	Δ
			3.59	(30)	Δ			
3.51	s	o						
3.40	w	-						
						3.37	(56)	Δ
3.32	w	o						
3.09	m	o						
			2.92	(42)	Δ			
2.89	m	o						
			2.81	(13)				
			2.69	(100)				
2.68	m	o						
						2.56	(100)	-
						2.20	(33)	
2.04	mw(B)	o						
						2.03	(33)	Δ
						1.91	(56)	Δ
						1.87	(67)	-
			1.78	(17)				
						1.74	(44)	Δ
1.68	m		1.69	(29)	Δ			
			1.60	(33)				
1.57	m							
						1.34	(33)	
			1.31	(33)				

* Powder Pattern

** Oxide still on the metal (Defractometer)

o $NbAlO_4$ (14-494)

Δ $FeNbO_4$ (16-358)

Table C-7. X-ray Diffraction Lines and Relative Intensities for the Oxides Formed on a Nb-Fe-Al Alloy at 1200°C

15 (Arc Melted)			15 (Arc Melted)			15 (Arc Melted)		
d, Å	I/I_o*	Comments	d, Å	I/I_o*	Comments	d, Å	I/I_o**	Comments
5.60	w		5.60	w(B)				
5.00	mw		5.00	w				
3.70	mw		3.69	m				
3.60	mw		3.60	m				
3.52	s		3.51	s		3.55	(17)	Δ
3.32	m		3.30	w				
3.08	mw		3.07	w				
2.95	ms		2.92	s		2.97	(12)	
2.89	vs		2.87	s		2.89	(47)	
2.67	ms		2.65	ms		2.67	(100)	Δ
2.54	m		2.53	w				
2.49	m		2.47	mw		2.49	(15)	Δ
2.43	mw		2.43	mw		2.43	(18)	
2.36	vw							
2.19	w		2.18	mw				
2.15	vw		2.14	mw				
1.86	mw		2.03	w				
1.81	w		1.85	mw				
1.78	vw		1.82	mw				
1.76	vw		1.77	vw				
1.73	ms		1.72	m				
1.71	w							
1.695	w		1.68	mw				
1.679	ms		1.665	m		1.68	(41)	Δ
1.565 - 1.595	mw		1.595	vw		1.59	(18)	Δ
1.525	w		1.56	vw				
1.502	mw							
1.475	w							
1.440	m							
1.425	m(B)					1.43	(18)	Δ
1.40	w							

* Powder Pattern

** Oxide still on metal (Diffractometer)

Δ $FeNbO_4$ (16-358)

Table C-8. X-ray Diffraction Lines and Relative Intensities for the Oxides Formed on a Nb-Fe-Al Alloy at 1200°C

16-A- Pressed and Sintered			16-B (Arc Melted)			16-C (Arc-Melted)		
d, Å	I/I_o	Comments	d, Å	I/I_o	Comments	d, Å	I/I_o	Comments
			5.55	vw		5.55	w	
			5.00	w		5.01	mw	
3.7	vw		3.68	m		3.70	m	
3.6	vw		3.51	s		3.52	s	
3.13	vw		3.39	vw		3.07	m	
2.92	vw		3.30	vw		2.88	ms	
2.66	w		3.06	mw		2.75	w	
2.53	m		2.96	m		2.53	vw	
-	-		2.91	m		2.48	vw	
2.33-4	s		2.86	m		2.42	vw	
2.23	ms		2.75	w		2.29	vw	
2.19	ms		2.65	m		2.18	vw	
2.03	w(B)		-	-		2.15	vw	
2.01	w(B)		-	-		2.07	vw	
1.82	w		2.03	vw(B)		2.03	vw	
			1.885	vw		1.87	mw	
			1.85	mw		1.78	mw	
			1.815	w		1.725	w	
			1.77	w		1.685	wv	
			1.72	w		1.67	m	
			1.565	mv		1.58	mw(B)	
						1.50	vw	
						1.44	vw	
						1.42	w	

Table C-9. X-ray Diffraction Lines and Relative Intensities for the Oxides Formed on a Nb-Co-Al Alloy at 1200°C

17-A (Pressed and Sintered)			17-B (Arc Melted)			17-C (Arc-Melted)		
d, Å	I/I$_o$	Comments	d, Å	I/I$_o$	Comments	d, Å	I/I$_o$	Comments
-	-		5.55	w		-	-	
5.1	w	o	5.00	mw		-	-	
4.8	w	o	-	-		-	-	
3.75	m	o	-	-		-	-	
-	-		3.70	mw	*	3.7	mw	*
-	-		-	-		3.59	s	
3.57	m	o	-	-		-	-	
-	-		3.52	s		3.51	s	
3.43	m	o	-	-		-	-	
-	-		3.40	vw		3.40	vw	
-	-		3.07	m	*	3.10	m	*
-	-		2.87	vw		-	-	
2.855	mw		-	-		-	-	
2.800	mw	o	-	-		-	-	
-	-		2.75	vw		2.76	vw	
2.70	-		-	-		-	-	
-	-		2.66	m	*	2.67	m	*
2.52	m	o	2.50	mw		-	-	
2.48	m		-	-		-	-	
-	-		2.43	w		-	-	
2.36	w		-	-		-	-	
2.31	w	o	-	-		-	-	
2.23	w		-	-		-	-	
2.205	w	o	-	-		-	-	
2.07	mw		2.05	mw	*	2.06	w	*
-	-		2.01	mw		-	-	
1.915	mw		-	-		-	-	
1.890	mw		-	-		-	-	
-	-		1.86	m	*	1.86	m	*
1.820	mw		-	-		-	-	
1.79	w		-	-		-	-	
1.765	mw		1.77	w		-	-	
1.725	m		-	-		-	-	
1.71	mw		1.70	vw		-	-	
1.69	w		1.68	vw		-	-	
1.67	w	o	1.66	vw		-	-	
1.58	w	o	1.593	vw		-	-	
-	-		1.568	ms	*	1.57	m	*
1.53	m		1.52	w		-	-	
-	-		1.486	w		-	-	
1.475	w		-	-		-	-	
1.45	ms		1.442	mw		1.45	mw	

o Al_2O_3-$9Nb_2O_5$ (16-545)
* $NbAlO_4$ (14-494)

Table C-10. X-ray Diffraction Lines and Relative Intensities for the Oxide Formed on a Nb-Co-Al Alloy at 1200°C

18-A (Pressed and Sintered)		
d, Å	I/I_o	Comments
3.75	vw	
3.55	w	
3.11	w	
2.95	w	
2.80	vw	
2.67	mw	
2.39	s	
2.32	ms	
2.28	ms	
2.23	ms	
2.17	s	
2.12	mw	
1.98	mw	
1.492	mw	
1.425	m	
1.397	mw	
1.357	m	
1.355	m	
1.290	w	
1.198	w	
1.166		

Table C-11. X-ray Diffraction Lines and Relative Intensities for the Oxides Formed on a Nb-Co-Al Alloy at 1200°C

19-A (Pressed and Sintered)			19-B (Arc Melted)			19-C (Arc Melted)		
d, Å	I/I_o	Comments	d, Å	I/I_o	Comments	d, Å	I/I_o	Comments
6.40	w	-	5.60	w		5.6	w	
6.10	w	*	5.02	w		5.02	mw	
4.72	w	-	3.70	m		3.70	ms	
3.80	mw	-	3.58	mw		3.51	s	
3.70	mw	*	3.51	s		3.39	m	
3.60	mw	-	3.39	w		3.07	mw	
3.54	s	*	3.07	w		2.97	mw	
3.40	m	-	2.97	mw		2.92	mw	
3.09	mw	*	2.92	m		2.77	mw	
2.93	s	-	2.75	w		2.67	m	
2.88	m	*	2.66	mw		2.50	w(B)	
2.77	w	-	-	-		2.30	w (B)	
2.68	mw	*	2.03	mw		2.05	mw	
2.30	w	*	1.895	mw		1.895	mw	
2.22	m	*	1.85	vw		1.858	w	
2.16	m	*	-	-		1.775	w	
2.07	w	-	1.70	vw(B)		1.710	w	
2.04	m	-	-	-		1.67	mw	
1.90	w	*	1.66	vw(B)		1.66	mw	
1.87	w	*	1.565	mw		1.568	m	
1.78	w	-	1.441	w		1.392	vw	
1.675	m	-	-	-		1.365	vw	
1.58	m	*	-	-		-	-	

* $AlNbO_4$ (14-494)

Table C-12. X-ray Diffraction Lines and Relative Intensities for the Oxide Formed on a Nb-Co-Al Alloy at 1200°C

20-A (Pressed and Sintered)			21-A (Pressed and Sintered)		
d, Å	I/I_o	Comments	d, Å	I/I_o	Comments
5.1	m	o	-		
4.8	m	o			
3.75	s	o	3.75	s	o
3.57	s	o	3.57	s	o
3.43	s	o	3.43	m	o
			-		
2.95	m	-	2.95	s	-
2.79	m	o	2.79	mw	o
2.68	m	-	2.79	mw	-
			2.65-2.70	mw	-
2.40	m		2.40	m	-
2.295	mw		2.295	mw	-
2.03-6	ms	(o)	2.03-6	ms	(o)
1.91	m	(o)	1.91	m	(o)
1.72	m	(o)	1.72	m	(o)
1.68	m	(o)	1.68	m	(o)
1.58	m	o	1.58	w	o
1.55	w	-	1.55	w	-
1.53	w	o	1.53	w	o
1.45	m	o	1.45	mw	o
1.41	mw	-	1.41	mw	-
1.33	w	-	-		
1.305	w	-	1.305	w	-
1.28	w	-	1.28	w	-

o Al_2O_3-$9Nb_2O_5$ (16-545)
( ) Indicates card intensities are weaker than those found on the films

Table C-13. X-ray Diffraction Lines and Relative Intensities of the Oxides Formed on a Nb-Co-Al Alloy at 1200°C

22-A (Pressed and Sintered)			22-B (Arc Melted)		
d, Å	I/I_o	Comments	d, Å	I/I_o	Comments
5.1	m	o *	--	-	
4.8	m	o *	--	-	
3.75	s	o *	--	-	
--	-		3.67	s	
3.57	s	o *	3.55	s	
3.43	s	o *	--	-	
--	-		3.29	m	
2.95	m		--	-	
2.79	m	o *	2.79	m	
2.68	m		2.69	m	
--	-		2.53	m	
2.40	m		--	-	
--	-		2.31	w	
2.295	mw		--	-	
2.03 - 2.06	ms	o *	2.05	w	
1.91	m	o *	1.90	w	
1.72	m	o -	--	-	
1.68	m	o *	1.69	w	
1.58	mw	*	1.58	w	
1.55	w	*	--	-	
1.53	w	*	--	-	
1.45	m	o -	--	-	
1.41	mw	-	--	-	
1.33	w	-	--	-	
1.305	w	-	--	-	
1.28	w	*	--	-	

o Al_2O_3-$9Nb_2O_5$ (16-545)
* NbO_2 (19-859)

Table C-14. X-ray Diffraction Lines and Relative Intensities for the Oxides Formed on a Nb-Co-Al Alloy at 1200°C

24-A (Pressed and Sintered)			24-B (Arc-Melted)			24-C (Arc-Melted)		
d, Å	I/I$_o$	Comment	d, Å	I/I$_o$	Comment	d, Å	I/I$_o$	Comment
						6.2	w	*
5.1	w	o	5.0	w	*	5.05	mw	*
4.8	vw	o	-	-		4.78	w	
3.75	ms	o	-	-		-	-	
-	-		3.71	m	*	3.72	m	*
-	-		3.65	m	-	-	-	
3.57	ms	o	-	-		3.56	s	*
-	-		3.53	s	-	-	-	
3.43	m	o	3.41	m	-	3.43	w	
3.10	vw		3.08	m	*	3.09	m	*
-	-		2.99	w	-	3.00	w	*
2.95	mw		2.95	w	*	2.95	w	
2.79	m	o	-	-		2.78	w	*
2.65 - 2.70	m	o	-	-		2.68	m	*
2.49 - 2.54	m	o	2.52	vw		2.50	w	
2.41	m	o	-	-		2.45	vw	*
2.34	s		-	-		-	-	
2.295	mw		-	-		2.3	vw	
2.22 - 2.23	m		-	-		-	-	
2.185	m		-	-		2.16	vw	
2.135	mw		-	-		-	-	
2.03 - 2.06	mw	o	2.06	mw	*	2.06	mw	*
-	-		-	-		2.03	w	*
1.91	mw	o	1.90	mw	-	1.91	mw	
1.82	w		1.86	mw	*	1.87	mw	*
-	-		1.78	w	-	1.79	mw	
1.72	w	o	-	-		-	-	
1.68	w	o	-	-		1.68	mw	
-	-		-	-		1.67	w	
1.58	mw	o	1.57	m	*	1.58	ms	*
1.53	vw		-	-		-	-	
1.50	w	o	-	-		-	-	
1.45	w	o	-	-		1.45	w	
1.41	mw		-	-		-	-	
1.33	w		-	-		-	-	
1.305	w		-	-		-	-	
1.28	w		-	-		-	-	

* 14 - 494 - $AlNbO_4$

o 16 - 545 - Al_2O_3-$9Nb_2O_5$

Table C-15. X-ray Diffraction Lines and Relative Intensities for the Oxide Formed on Nb-Co-Al Alloys at 1200°C

23-A (Pressed and Sintered)			25-A (Pressed and Sintered)		
d, Å	I/I_o	Comments	d, Å	I/I_o	Comments
5.1	w	o	5.1	vw	o
4.8	vw	o	4.75	vw	o
3.75	s	o	3.75	m	o
3.57	s	o	3.65	m	-
3.43	m	o	3.57	m	o
-			3.43	mw	o
2.95	s	o	2.95	s	-
2.79	m	o	2.85	vw	-
2.65-			2.79	vw	o
2.70	mw	o	2.70	vw	o
2.49-			2.53	w	o
2.54	mw	o			
2.295	mw	-	2.48	w	-
			2.36	vw	-
2.03-6	ms	o	2.23	vw	-
1.91	m	o	2.20	vw	-
1.72	w	o	2.06	w(B)	o
-			1.91-2	w	o
1.58	w	o	1.89	w	-
			1.87	w	-
			1.77	mw	-
1.45	mw	o	1.725	m	-
1.41	mw	-	1.705	m	-
			1.69	vw	o
1.305	w	-	1.67	vw	o
1.28	w	-	1.58	w	-
			1.53	mw	-
			1.45	m	-
			1.37	vw	-

o Al_2O_3-Nb_2O_5 (16-545)

Table C-16. X-ray Diffraction Lines and Relative Intensities for the Oxides Formed on a Nb-Co-Al Alloy at 1200°C

26 (Arc Melted)			26 (Arc Melted)			27 (Arc Melted)		
d, Å	I/I_o*	Comments	d, Å	I/I_o**	Comments	d, Å	I/I_o*	Comments
			4.483	36		5.55	w(B)	
			4.270	27		5.00	w(B)	
3.60	mw	-	4.058	18		4.70	vw	
3.55	s	Δ	3.969	27		3.70	ms	
3.35	mw	-	3.786	32		3.51	s	
3.04	mw	Δ	3.663	27		3.39	m	
3.00	mw	Δ	3.562	36		3.07	m	
2.90	mw	Δ	2.959	91		2.96	mw	
2.75	mw	-	2.876	64		2.91	m	
2.64	mw	Δ	2.788	54		2.76	mw	
2.03	mw	Δ	2.592	71		2.66	mw	
1.89	mw	-	2.563	91		2.50	w	
1.85	s	Δ	2.458	64		2.29	w	
1.765	mw	Δ	2.270	27		2.21	vw	
1.70	mw	Δ	1.892	64		2.04	mw(B)	
1.66	w	Δ	1.873	86		2.01	w	
1.587	m	Δ	1.765	54		1.891	mw	
1.560	s	Δ	1.717	45		1.85	mw	
			1.528	86		1.77	mw	
			1.451	100		1.70	mw	
						1.67	w	
						1.65	w	
						1.565	ms	
						1.441	m	
						1.391	w	

* Powder pattern

** Oxide still on the metal (Diffractometer)

Δ $NbAlO_4$ (14-494) slight shift

Table C-17. X-ray Diffraction and Relative Intensities for the Oxide Formed on a Nb-Fe-Al Alloy at 1200°C

28 (Arc Melted)			28 (Arc Melted)		
d, Å	I/I_o	Comments	d, Å	I/I_o	Comments
3.641	20		3.66	12	
3.198	7				
2.959	10		2.969	3	
2.894	11		2.884	6	
2.671	100		2.683	100	
			2.501	13.0	
			2.353	3	
			2.196	18	
2.188	19				
2.129	25		2,136	12	
1.862	16				
1.827	38		1.831	17	
1.799	6				
1.728	4		1.686	49	
1.682	100				
1.588	13		1.480	21	
1.475	18		1.449	12	
1.424	12		1.342	8	
1.341	16				

Table C-18. X-ray Diffraction Lines and Relative Intensities for the Oxides Formed on Nb-Cr-Al-Co (31) and Nb-Co-Al (32, 33) Alloys at 1200°C

31 (Arc Melted)			32 (Arc Melted)			33 (Arc Melted)		
d, Å	I/I_o	Comments	d, Å	I/I_o	Comments	d, Å	I/I_o	Comments
3.376	20		4.332	5		3.647	32	
3.278	96		3.969	5		3.562	11	
2.912	8		3.754	11		-	-	
2.585	16		3.648	26		-	-	
2.525	100		3.576	33		-	-	
2.475	26		3.446	9		2.954	100	
2.315	16		3.132	11		2.862	26	
2.222	2		3.069	18		2.776	11	
2.171	32		2.954	100		-	-	
1.998	8		2.867	14		2.585	22	
1.743	17		-	-		2.522	26	
1.710	80		2.525	23		2.488	26	
1.642	18		2.488	16		2.499	22	
1.580	8		2.449	14		2.227	11	
1.469	24		2.227	4		2.201	16	
1.379	24		2.201	9		2.071	16	
1.371	32		-	-		-	-	
-	-		2.071	18		1.888	27	
-	-		-	-		1.870	47	
-	-		1.907	23		1.845	32	
-	-		-	-		1.821	11	
-	-		1.871	79		1.765	26	
-	-		1.822	7		1.741	5	
-	-		1.789	7		1.722	16	
-	-		1.762	18		1.710	32	
-	-		1.725	23		-	-	
-	-		1.713	21		-	-	
-	-		1.686	9		-	-	
-	-		1.669	12		1.558	11	
-	-		-	-		1.527	37	
-	-		1.603	28		-	-	
-	-		-	-		1.475	11	
-	-		1.528	21		-	-	
-	-		-	-		1.448	47	
-	-		1.477	9		1.435	16	
-	-		-	-		1.374	22	
-	-		1.447	30		-	-	
-	-		1.375	11		-	-	
-	-		1.238	17				
-	-		1.187	21				

Table C-19. X-ray Diffraction Lines and Relative Intensities for the Oxide Formed on a Nb-Co-Al Alloy at 1200°C

36 (Arc Melted)			37 (Arc Melted)		
d, Å	I/I_o	Comments	d, Å	I/I_o	Comments
3.95	10	- -			
3.75	20	- *	5.438	7	
3.67	32	o -	3.648	21	
3.58	84	o *	3.562	32	o
3.44	14	- -			
3.10	40	- -			
3.07	30	o -			
2.97	100	- -	2.95	100	
2.87	18	o -	2.858	21	o
2.69	24	o *	2.69	7	o
2.54	24	o *	2.515	36	o
2.49	22	- *	2.485	36	-
2.46	12	- -	2.449	21	-
2.36	8	- -			
2.23	8	- -	2.22	14	-
2.21	8	- -	2.196	21	-
2.11	10	- -			
2.08	24	o -	2.071	21	o
2.04	12	- *			
2.03	12	- *			
2.00	8	- -			
1.99	6	- -			
1.91	28	- *	1.91	14	-
1.87	90	o *	1.89	21	-
1.83	18	- -	1.87	50	o
1.82	18	- -	1.817	7	-
1.77	28	o -	1.765	21	o
1.73	28	- -	1.725	14	-
1.72	34	- *	1.713	21	-
1.67	16	- *			
			1.526	28	-
			1.447	40	-
			1.371	14	-

Table C-20. X-ray Diffraction Lines and Relative Intensities for Arc Melted Niobates for Which no ASTM Data Card was Found

Nb_2CoO_6 (Arc Melted)			$NbCoO_4$ (Arc Melted)		
d, Å	I/I_o	Comments	d, Å	I/I_o	Comments
3.6	m		4.4	vw	
3.31	ms		3.69	w	
2.92	s		3.59	w	
2.82	vw		3.39	m	
2.73	w		3.29	m	
2.54	ms		2.95	ms	
2.50	vw		2.90	s	
2.46	w		2.79	m	
2.34	w		2.72	s	
2.24	w		2.60	m	
2.06	w		2.54	s	
1.87	mw		2.49	vw	
1.81	w		2.45	vw	
1.73	m		2.37	vw	
1.70	mw		2.33	vw	
1.515	m		2.05	w	
1.490	w		1.895	w	
1.44	m		1.865	m	
1.395	vw		1.746	m	
.919	m		1.722	ms	
.917	mw		1.690	w	
.906	m		1.510	w	
.9035	w		1.478	m	
.9025	w		1.435	m	
			1.390	vw	
			1.335	w	
			1.29	vw	
			1.28	vw	
			1.25	vw	
			1.212	vw	
			1.200	vw	
			1.185	vw	
			1.176	vw	
			1.162	mw	
			1.123	mw	